Høgskulen på Vestlandet

Master Thesis

ING5002D

Predefinert informasjon

Startdato:	09-05-2020 09:00	**Termin:**	2020 VÅR
Sluttdato:	02-06-2020 14:00	**Vurderingsform:**	Norsk 6-trinns skala (A-F)
Eksamensform:	Masteroppgave		
SIS-kode:	203 ING5002D 1 MOPPG 2020 VÅR HAUGESUND		
Intern sensor:	(Anonymisert)		

Deltaker

Kandidatnr.: 307

Informasjon fra deltaker

Tittel *: Numerisk studie av kriteriet for luftstrøm til trykksettingssystemer med bruk av Fire Dynamics Simulator

Engelsk tittel *: Numerical study of the airflow criterion of pressurization systems using Fire Dynamics Simulator

Egenerklæring *:	Ja	**Inneholder besvarelsen konfidensielt materiale?:**	Nei
Jeg bekrefter at jeg har registrert oppgavetittelen på norsk og engelsk i StudentWeb og vet at denne vil stå på vitnemålet mitt *:	Ja		

Jeg godkjenner avtalen om publisering av masteroppgaven min *

Ja

Er masteroppgaven skrevet som del av et større forskningsprosjekt ved HVL? *

Nei

Er masteroppgaven skrevet ved bedrift/virksomhet i næringsliv eller offentlig sektor? *

Nei

Numerical study of the airflow criterion of pressurization systems using Fire Dynamics Simulator

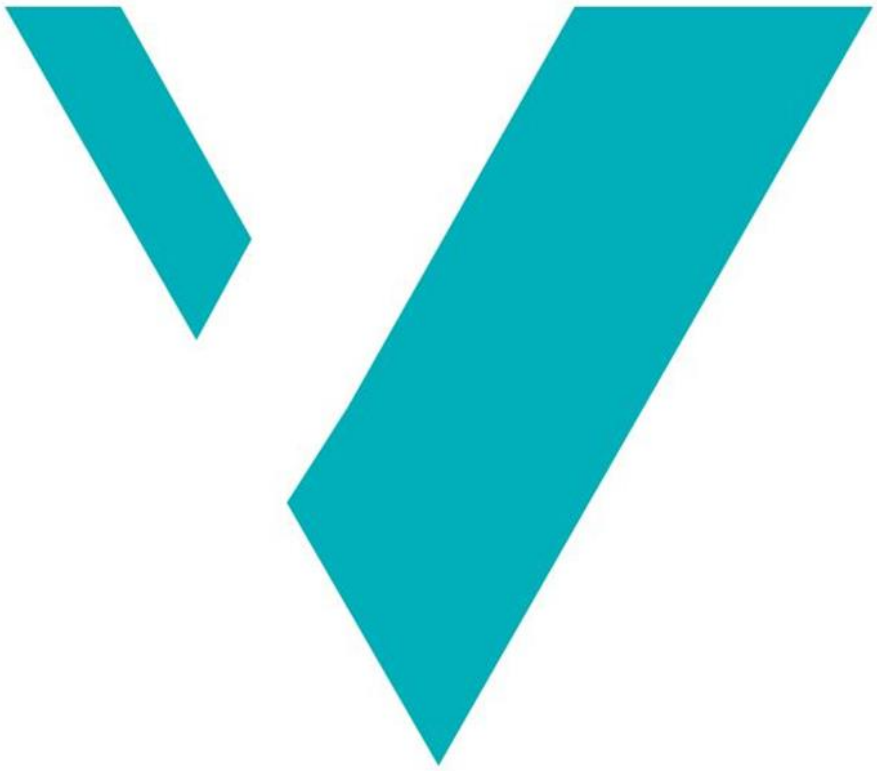

Marco Ribaric

WESTERN NORWAY UNIVERSITY OF APPLIED SCIENCES

Master Thesis in Fire Safety Engineering

Tønsberg
June, 2020

Subject code: ING5002D | Candidate number: 307 | Submission deadline: 02.06.2020

Western Norway University of Applied Sciences

Numerical study of the airflow criterion of pressurization systems using Fire Dynamics Simulator

Master thesis in Fire Safety Engineering

Author: Marco Ribaric	Author sign. 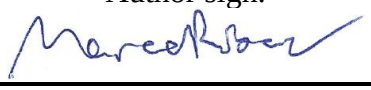

Thesis submitted: Spring 2020	Open thesis

Tutor:
Professor Sanjay K. Khattri

Keywords:
- Pressurization
- Airflow
- Air supply
- Smoke-spread
- CFD
- FDS

Number of pages: 82
+
Appendix: 32

Tønsberg, 01. June 2020

Preface

This thesis is the final stage of the Fire Safety Engineering, Master of Science, program at the Western Norway University of Applied Sciences in Haugesund.

My time at the university has been challenging but highly educational. The idea of this thesis is based on topics learned from the subjects Advanced Fire and Egress Modelling, and Building Fire Safety, and discussions with my tutor, Professor Sanjay K. Khattri. A combination of literature review and simulations was an approach I was aiming for.

The topic around smoke control systems was investigated during pre-studies, and several approaches were simulated to see how to address this task. It became obvious to me that a pressurization system consists of many parameters. This can generate a great number of scenarios to investigate. Therefore, it became necessary to limit the number of parameters to be analysed.

All models are wrong, but some models are useful.
George E.P. Box, 1976

Tønsberg, 1. June 2020.

Marco Ribaric

Western Norway University of Applied Sciences

Acknowledgements

I would like to thank my tutor, Professor Sanjay K. Khattri. With his help, I managed to limit the investigation which made my research more specific and focused on single factors.

Thanks to Thunderhead Engineering, which supported me with a Pyrosim license during the time of this thesis.

Additionally, I would like to thank my employer Norconsult AS, which has shown me great support during the whole study. The amount of flexibility I had during these years has been essential to me being able to do this study parallel with a near fulltime job.

Finally, I want to thank my wife Anastasiia. It has been three intensive but great years. I managed to combine my studies with a nearly fulltime job, moved twice, and became a father for the first time to my son Magnus. She also contributed to discussions and proofreading. All of this would not have been possible without her support.

Western Norway University of Applied Sciences

Abstract

Smoke control systems are used to prevent the spread of fire and smoke within buildings. Typical areas to be protected are the egress routes, atriums, and areas with larger fire loads. Smoke control systems prevent excessive financial and material losses. However, larger fire sections within buildings can be allowed by improving the fire safety with a smoke control system.

Extraction systems and pressurization systems are commonly used principles. The extraction system prevents the spread by extracting the smoke from the fire compartment. The pressurization system prevents the spread by pressurizing the compartments to be protected.

The pressurization system must safeguard the pressure criterion and the airflow criterion. The pressure criterion prevents the spread of smoke through gaps and cracks (a closed but leaky door), by creating an overpressure in the adjacent compartment to the fire compartment. The airflow criterion prevents the spread of smoke through larger openings like open doors, by creating an airflow from the adjacent compartment to the fire compartment.

The airflow criterion is investigated with Fire Dynamics Simulator (FDS). FDS is a Computational Fluid Dynamics (CFD) code for fire-driven fluid flows designed for fire applications. FDS allows the user to simulate the outcome of a defined fire scenario. For example, it is possible to assess how long tenable conditions can be safeguarded in a certain area. The outcome of a fire scenario can be simulated many times, which is an advantage when the goal is to study the outcome of minor parameter changes. The use of CFD codes is an alternative to full-scale experiments, which are often limited to cost.

Density, mass fraction and volume fraction of various gas species, pressure difference, temperature and visibility of defined areas, is an example of data possible to collect from full-scale experiments. However, such measurements in high quantities are limited to the number and types of devices. Old devices (and perhaps new) could as well be affected by decreased accuracy. FDS conducts precise mathematical calculations in large quantities. The disadvantage of CFD models is the high demand for computational power. A 10-minute scenario can take days to simulate, and in most cases, it is necessary to perform multiple simulations to address all uncertainties.

Six model geometries are used to study the airflow criterion between two compartments: the fire room compartment and the pressurized compartment. Factors such as compartment sizes and opening areas are altered between the model geometries. Model geometries with a lobby compartment implemented between the two main compartments are also used to assess the impact of this. For each model geometries, scenarios are conducted where the HRR (heat release rate, or fire size) and the air supply rate (the rate of the pressurization system) is altered.

Results from the conducted simulations show that as the HRR increases, the density of the fire products increases in the pressurized compartment. As the air supply increases the density of the fire products decreases. Altered compartment sizes, ventilation opening areas (openings to the outside which supplies the fire with oxygen) and ventilation opening locations, has an impact on the product density development in each compartment. For the case with a lobby compartment implemented between the two main compartments, the product density is decreased in the pressurized compartment, compared to the equivalent case without a lobby compartment.

Sammendrag

Røykkontrollsystemer brukes til å forhindre spredning av brann og røyk i bygninger. Typiske områder som beskyttes er rømningsveier, glassgårder, og områder med større brannbelastning. Røykkontrollsystemer forhindrer store økonomiske og materielle tap. Imidlertid kan større brannseksjoner i bygninger tillates ved å forbedre brannsikkerheten med et røykkontrollsystem.

Røykventilasjon og trykksetting er ofte brukte prinsipper for røykkontrollsystemer. Røykventilasjon forhindrer røykspredning ved å trekke ut røyken fra brannrommet. Trykksetting forhindrer røykspredning ved å trykksette rommet som skal beskyttes.

Trykksetting må ivareta kriteriet for overtrykk og luftstrøm. Et overtrykk forhindrer spredning av røyk gjennom mindre åpninger som utette dører, ved å skape et overtrykk i det tilstøtende rommet til brannrommet. En luftstrøm forhindrer spredning av røyk gjennom større åpninger som åpne dører, ved å danne en luftstrøm fra det tilstøtende rommet til brannrommet.

Kriteriet for luftstrøm er undersøkt med Fire Dynamics Simulator (FDS). FDS er en numerisk fluiddynamikk kode (Computational Fluid Dynamics, CFD) for branndrevne fluidstrømmer designet for brann applikasjoner. FDS lar brukeren simulere utfallet av et definert brannscenario. For eksempel er det mulig å vurdere hvor lenge sikre forhold kan ivaretas i et bestemt område. Utfallet av et brannscenario kan simuleres mange ganger, noe som er en fordel når målet er å studere utfallet av mindre parameterendringer. Bruken av CFD-koder er et alternativ til fullskala eksperimenter, som ofte er begrenset til kostnader.

Tetthet, massefraksjon og volumfraksjon av forskjellige gassarter, trykkforskjell, temperatur og sikt i definerte områder, er et eksempel på data som er mulig å samle inn fra fullskala eksperimenter. Målinger i store mengder er imidlertid begrenset til antall og typer av måleutstyr. Gamle utstyr (og eventuell nye) kan påvirkes av redusert nøyaktighet. FDS utfører presise matematiske beregninger i store mengder. Ulempen med CFD-modeller er det høye kravet til datakraft. Et 10-minutters scenario kan ta dager å simulere, og i de fleste fall er det nødvendig å utføre flere simuleringer for å ivareta alle usikkerheter.

Seks modellgeometrier brukes til å studere kriteriet for luftstrøm mellom to enheter: brannrommet og det trykksatte rommet. Faktorer som rom-størrelser og åpningsarealer varierer mellom modellgeometriene. Modellgeometrier, der et mellomliggende rom er plassert mellom de to hovedenhetene, brukes til å vurdere effekten av dette. For hver modellgeometri blir scenarier utført der varmeproduksjonen til brannen og lufttilførselsraten (raten til trykksettingssystemet) endres.

Resultater fra de utførte simuleringene viser at ved økt varmeproduksjonen, øker branngassenes tetthet i det trykksatte rommet. Når raten til lufttilførselen øker, reduseres branngassenes tetthet. Endrede romstørrelser, areal til ventilasjonsåpninger (åpninger til utsiden som forsyner brannen med oksygen) og ventilasjonsåpningenes plassering, har innvirkning på utviklingen til branngassenes tetthet i hvert rom. For scenariet der et mellomliggende rom er plassert mellom de to hovedrommene, reduseres branngassenes tetthet i det trykksatte rommet, sammenlignet med tilsvarende scenario uten mellomliggende rom.

Table of contents

List of figures

List of tables

Definitions

Air supply	The mechanical fans of a pressurization system, which supplies a compartment with air
Airflow	The generated flow of air through an opening
C	Carbon atom
CFD	Computational Fluid Dynamics
CO	Carbon monoxide
CO_2	Carbon dioxide
DNS	Direct Numerical Simulation
Eddy	Swirling turbulent flows
FDS	Fire Dynamics Simulator
F	Fuel
Fire Room Compartment	The compartment where the fire is located
Fuel load	The type and amount of fuel in a compartment
H	Hydrogen atom
HRR	Heat release rate, the fire size
HRRPUA	Heat release rate per unit area
LES	Large Eddy Simulation
Lobby Compartment	The compartment which is located between the fire room compartment and the pressurized compartment
Mesh Sensitivity Analysis	The process of where the resolution of a mesh is determined
N	Nitrogen atom
N_2	Molecular nitrogen, composed of two nitrogen atoms
NSZ	Non-smoke zone
O	Oxygen atom
O_2	Molecular oxygen, composed of two oxygen atoms
Overpressure	The pressure in a compartment, which is higher than the pressure in the adjacent compartment
Pressurized Compartment	The compartment which is to be protected. The air supply points are located in this compartment
Products	Gases produced from a fire
Product density	The density of the gases produced from a fire
RANS	Reynolds-Averaged Navier-Stokes
S	Soot
SSZ	Surrounding smoke-zone
Steady-state conditions	The condition of where the state of the current process is constant
SVLES	Simple Large Eddy Simulation
SZ	Smoke-zone
VLES	Very Large Eddy Simulation

Nomenclature

A_f	Fire source area	$[m^2]$
A_o	Ventilation opening area	$[m^2]$
c_p	Specific heat at constant pressure	$[J/(g \times K)]$
d	Thickness	$[m]$
D	Fire source diameter	$[m]$
D_α	Material diffusivity of species α	$[m^2/s]$
D^*	Characteristic fire source diameter	$[m]$
f	External body force	$[N]$
Fr	Froude number	$[–]$
g	Gravity constant	$[m/s^2]$
h	Sensible enthalpy	$[J]$
H_o	Ventilation opening height	$[m]$
ΔH_c	Heat of Combustion per unit mass of consumed fuel	$[MJ/kg]$
k	Conductivity	$[W/(m \times K)]$
L	Flame height	$[m]$
Ma	Mach number	$[–]$
$\dot{m}_\alpha$	Mass flow rate of species α	$[kg/s]$
$\dot{m}_\alpha$	Mass flow rate of species α per unit area	$[kg/(s \times m^2)]$
$\dot{m}_\alpha'''$	Mass production (destruction) rate of species α per unit volume	$[kg/(s \times m^3)]$
P	Pressure	$[Pa]$
Δp	Pressure difference	$[Pa]$
Q	Energy	$[kJ]$
$\dot{Q}$	Heat release rate	$[kW]$
$\dot{Q}''$	Heat release rate per unit area	$[kW/m^2]$
$\dot{Q}'''$	Heat release rate per unit volume	$[kW/m^3]$
$\dot{Q}^*$	Nondimensional heat release rate	$[–]$
R	Universal gas constant	$[J/(K \times mol)]$
T	Temperature	$[K]$
T_{in}	Temperature of species flowing into a compartment	$[K]$
T_o	Temperature, outside	$[K]$
T_{out}	Temperature of species flowing out of a compartment	$[K]$
T_s	Temperature, inside shafts	$[K]$
T_∞	Temperature, ambient conditions	$[K]$
t	Time	$[s]$
u	Velocity vector	$[m/s]$
V_{in}	Volume of species flowing into a compartment	$[m^3]$
V_{out}	Volume of species flowing out of a compartment	$[m^3]$
W	Average molecular weight	$[g/mol]$
W_α	Molecular weight of species α	$[g/mol]$
X_α	Volume fraction of species α in soot	$[m^3/m^3]$
Y_α	Mass fraction of species α in fuel	$[g/g]$
z	Height	$[m]$

Greek symbols

α	Fire growth rate	$[kW/s^2]$
γ	Yield of species α by chemical reaction	$[g/g]$
δx	Cell size	$[m]$
ε	Rate of dissipation of turbulent kinetic energy	$[W/g]$
υ	Number of molecules	$[–]$
ρ	Density	$[g/m^3]$
ρ_∞	Density, ambient conditions	$[g/m^3]$
τ	Viscous stress tensor	$[N/m^2]$
∇p	Pressure gradient	$[Pa]$

Subscripts

∞	Ambient conditions
a	Air
C	Per unit mass of fuel
f	Flame
f	Fuel
F	Fuel
in	Flow into a compartment
m	Mass
o	Opening
o	Outside
out	Flow out of a compartment
p	Pressure
s	Inside, shaft
v	Number of nitrogen atoms
x	Number of carbon atoms
y	Number of hydrogen atoms
z	Number of oxygen atoms
α	Species

1. Introduction

A fire can produce a significant amount of smoke which can harm people and material values. Smoke control systems are used to prevent the spread of fire and smoke to adjacent spaces. A pressurization system prevents the spread by pressurizing the compartments to be protected. Modern standards require stairwells which stretch above a certain height to be pressurized, and the pressurization system must safeguard two criteria, the pressure criterion and the airflow criterion.

The pressure criterion safeguards the spread of fire products through gaps and cracks (a closed but leaky door), by creating an overpressure between the pressurized compartment and adjacent spaces. The airflow criterion safeguards the spread of smoke through larger openings, like open doors, by generating an airflow through the opening and preventing the spread of smoke in the opposite direction. To balance these two criteria is a complicated task, due to the pressurization system being depended upon leaks, openings, air supply rates and relief vents.

The objective of this study is to investigate the airflow criterion of a pressurization system between two compartments connected with an opening. The investigation is conducted with FDS (Fire Dynamics Simulator). Several model geometries are investigated where the compartment sizes and ventilation opening areas are altered. Model geometries with a lobby compartment implemented between the two main compartments are also investigated. Simulations of various HRRs contra altered air supply rates are conducted for each model geometry. The product density development in each compartment is assessed through various HRRs and air supply rates.

The thesis starts with a presentation of the theoretical background for smoke control systems, fire scenarios, validated full-scale experiments, and computational fluid dynamics.

The methods regarding the simulation setup, assessment of parameters, mesh sensitivity analysis and evaluation procedures are described in chapter 3.

Results from the simulations are presented in chapter 4.

The results and findings, the impact of the pressurization system, tenable conditions and the airflow through openings are discussed in chapter 5.

The results and finding are concluded in chapter 6.

2. Theory

The theoretical background around smoke control systems, fire scenarios and CFD codes is presented in this section. It includes a description of the physical mechanisms of smoke control systems and a description of various smoke control systems. The driving forces of smoke movement are essential to understand when designing a smoke control system. Past validated full-scale experiments of smoke control systems are described. The section ends with a description of design fires, and how these can be specified in CFD codes like FDS.

2.1. Physical Mechanisms of Smoke Control

The physical mechanisms of smoke control are briefly described in this section. These mechanisms are compartmentation, dilution, pressurization, airflow, and buoyancy, and they are recognized as a way of controlling the spread of fire and smoke.

Compartmentation

Compartmentation, a passive fire barrier, is the simplest way of controlling the spread of smoke by limiting it to a defined boundary. Closing a door is a form of a barrier to prevent the spread of smoke, a door without a self-closing mechanism rely on the fact that the door is closed by a person. Another example is fire dampers closing at activation. Compartmentation prevents the supply of air to the fire [1].

Dilution

Smoke moving away from the fire mixes with other gas species, which is air in normal conditions, resulting in a reduced concentration of smoke. This effect is called dilution. Dilution can be improved with a mechanical system. A compartment containing an extinguished fire can be supplied with air to dilute the smoke. If the fire is still active and the fire room compartment is sealed off from adjacent spaces, the adjacent spaces can be supplied with air to dilute the smoke from these areas. Mechanical dilution systems should not be used in a fire room compartment with an active fire. There is a great risk that the supplied oxygen causes the HRR to increase [1].

Smoke consists of components such as soot, CO, and CO_2. The human body tolerates them up to a certain level. As the smoke concentration decreases, tenable conditions is eventually achieved regarding these factors. By decreasing the smoke concentration, the air concentration increases. The human body tolerates a decreased concentration of oxygen down to a certain level.

Pressurization

By creating an overpressure in an adjacent compartment to the fire room compartment, the flow of smoke through gaps and cracks (a closed but leaky door) towards the pressurized area is prohibited [1]. More details on pressurization are given in chapter 2.2.

In comparison to smoke control through pressurization, the spread of smoke through much larger openings or paths is prohibited by creating an airflow through these openings in the opposite direction.

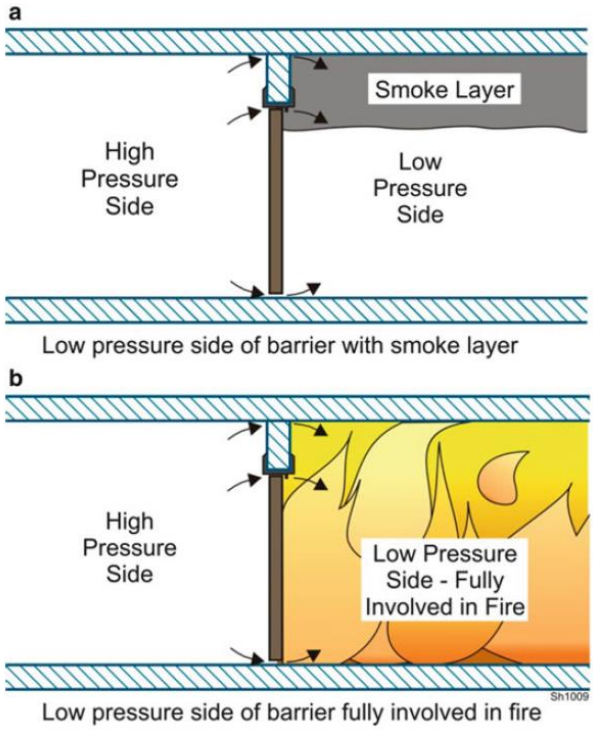

Figure 2.1 – The pressure difference across a barrier controls the smoke-flow. Image extracted from [1].

Airflow

By supplying air towards the smoke, the smoke is prevented to move towards a certain area. Depending upon the airflow velocity, the smoke can be kept stable or forced to move in the desired direction. This feature must be used with caution, the supply of oxygen can increase the HRR [1].

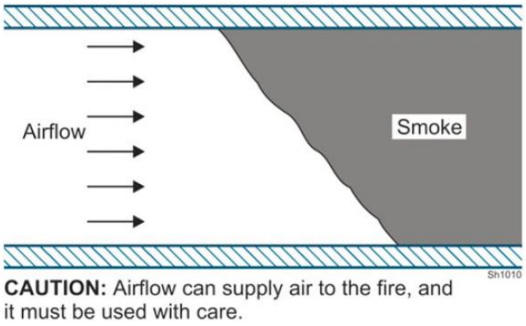

Figure 2.2 – Airflow can control the flow of smoke. Image extracted from [1].

Buoyancy

The system is depended upon the upward smoke-flow, the smoke is depended upon the buoyancy force. As the smoke spreads upwards, it expands and cools down due to mixing with cooler air. Hotter gases are less dense than cooler gases (for example air at normal temperatures). Smoke naturally spreads upwards due to buoyancy. A less dense gas specie always flows upwards to above the denser gas specie. The density of the gas specie (for example smoke or air) is depended upon its current temperature. As the temperature increases, the density decreases [1].

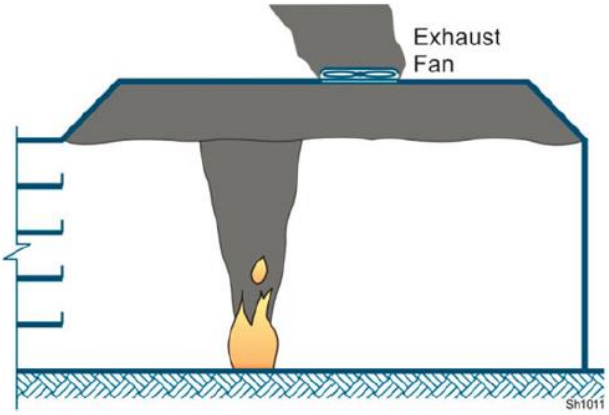

Figure 2.3 – Upward flow of smoke due to buoyancy, where the excess smoke is controlled by a mechanical smoke extraction system. Image extracted from [1].

The ideal gas law is stated as:

$$PW = \rho RT \tag{2.1}$$

where P is the pressure, W is the molecular weight of the gas specie, ρ is the density, R is the ideal gas constant, and T is the temperature. By implementing the standard atmospheric pressure, 101325 Pa, the molecular weight of air, 0,0289 kg/mol (approximately), and the ideal gas constant, 8,3145 J/(K mol) into eq. 2.1, a new equation is stated:

$$\rho = \frac{353}{T} \tag{2.2}$$

At 20 °C, the density of air is approximately 1,20 kg/m^3. This equation can also be used for smoke even though it is a different gas species since smoke mostly consists of air. Smoke at 300 °C has a density of approximately 0,62 kg/m^3 [2]. This difference initiates the buoyancy effect.

2.2. Smoke control systems

Commonly used smoke control systems are pressurization systems and extraction systems. Both topics are described in this section, though this study focuses on the pressurization system.

2.2.1. Pressurization systems

Pressurization systems maintain tenable conditions in for example a stairwell or a corridor. These systems control the smoke movement between the fire room compartment and adjacent spaces. A pressurization system can also be used to control and prevent the spread of smoke in elevator shafts and in defined smoke zones.

Stairwell pressurization

The function of the stairwell pressurization system depends upon (1) the dimensions of the stairwell and enclosure compartments, (2) the initial wind and temperature conditions, (3) the fire scenario, and (4) the pressure difference and the volume flow between the fire room compartment and the stairwell.

- The dimensions of the stairwell and enclosure compartments

Factors that can affect a pressurization system are the building height, the stairwell height, cross-sectional areas, number of floors and floor plans, objects and shapes of the stairwell, leaks and flow areas of the building compartments (both internal and external), and others.

For example, to pressurize larger volumes, extended time is demanded to reach the desired pressure difference between the pressurized and unpressurized volumes. The bigger the area of leaks is, the larger fraction of supplied air escapes the pressurized volume, which results in a larger demand of air supply to keep the desired overpressure [3].

A lobby compartment between the stairwell and the fire room compartment can be a benefit to the system. The lobby compartment reduces the probability of an open-door connection between the stairwell and the fire room compartment. A lobby compartment can be designed as an unpressurized, pressurized or ventilated compartment [1].

- The initial temperature and wind conditions

Temperature differences between the compartments and the stairwell, and between the stairwell and the outdoor, can initiate the stack effect (chapter 2.3). Both winter and summer conditions must be considered during the design of the stairwell pressurization systems. The worst case of typical outdoor winter and summer temperatures for the current location is analysed against typical indoor temperatures. The temperature variation over height must be considered in the design process. The temperature is typically lower in the top of a high building and higher on the ground level. The wind condition can affect any overpressure relief vent or the mechanical features of the pressurization fan [3].

– The fire scenario

The amount of smoke entering the stairwell depends upon the fire scenario. The size of the fire is the leading determinant factor of the amount of produced smoke and the soot concentration. Smoke escapes the fire room compartment through any opening, and larger fires will most likely break windows (without fire resistance), leading to smoke flowing out through the windows. Smoke also enters the stairwell through doors which have not been closed (by human force or a self-closing mechanism) during the evacuation. However, the smoke might not escape the fire room compartment through the stairwell door if the stairwell is pressurized [3].

– The pressure difference and the volume flow between the fire room compartment and the stairwell

A pressurization system must safeguard two criteria, (1) the pressure criterion and (2) the airflow criterion, as described in standard NS-EN 12101-6:2005 [4]. The pressure criterion is valid for small gaps and cracks (a closed but leaky door), and the airflow criterion is valid for larger openings (an open door). Smoke is prevented to spread from the fire room compartment to the pressurized compartment by creating an overpressure in the pressurized compartment.

If the door between the fire room compartment and the stairwell is open, the smoke will escape the fire room compartment and enter the stairwell. A pressurization system keeps the stairwell smoke-free by creating a flow of air through the opening in the direction from the stairwell to the fire room compartment. The flow of air can be designed so that no smoke enters the stairwell, but it can also be designed at a lower level so that some smoke is allowed to enter the stairwell, but little enough to still safeguard the tenable conditions. Naturally, smoke does not flow from low-pressure areas to high-pressure areas [3].

The pressure difference between the stairwell and the compartment should not be too high, this can affect the self-closing mechanism or restrict the possibility to open and close doors. The pressure difference must be kept within a defined pressure interval to keep the stairwell smoke-free, and doors functional.

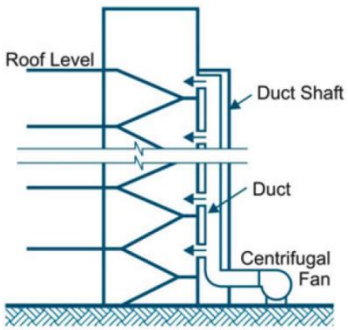

Figure 2.4 – Stairwell pressurization with multiple air supply injection. Image extracted and cropped from [1].

A door suddenly opening causes the pressure in the stairwell to decrease. An airflow is created through the opening preventing the spread of smoke in the opposite direction. If another door opens, the total airflow distributes across the two openings. If the airflow becomes too low, the air supply rate must increase to achieve the minimum demanded airflow. When all the doors suddenly

close, the pressure increases in the stairwell. If this pressure is too high the relief vent must release excess air and the air supply rate must decrease.

The air supply points can impact the effectivity of the pressurization system. A system with a single injection point can have air supplied in the bottom, the top, or the middle of the stairwell. For taller stairwells, multiple injection points are recommended to prohibit the pressurization system to fail [1].

Smoke zones

The concept of smoke zones is used within buildings to surround the fire area with overpressure. This prevents the smoke to spread to other parts of the building [1].

The following three terms are used in the further description:

- Smoke-zone (SZ) – The fire room compartment
- Surrounding smoke-zone (SSZ) – Surrounding area to the fire room compartment
- Non smoke-zone (NSZ) – The rest of the building

By pressurizing the SSZ, smoke can not spread from the SZ to the SSZ and the NSZ. The zone separation is depended upon the current situation, and the desired and required level of safety due to regulations. Too many zones can be difficult to design properly. It can be more effective to separate whole floors of tall buildings into single zones. Large floors in lower buildings can with advantage be separated into smaller zones.

When a fire occurs, the fire floor and the floor above is defined as the SZ. Connecting floors above and below the SZ is then defined as the SSZ. It must be considered that no tenable conditions can be achieved in the SZ. The SZ must be evacuated. Tenable conditions are kept in the SSZ and the NSZ. The system can fail if the SZ is not airtight or if leaks are not considered.

It is important to consider that if the wrong floors are defined as the SZ by an error, smoke can spread much more rapidly through the whole building. For example, if the floors above or below the fire floors are defined as SZ, the fire floors will automatically become the SSZ, and therefore be pressurized. This forces the smoke away to the NSZ and allows the smoke to spread easier to other parts of the building through stairwells and shafts [1].

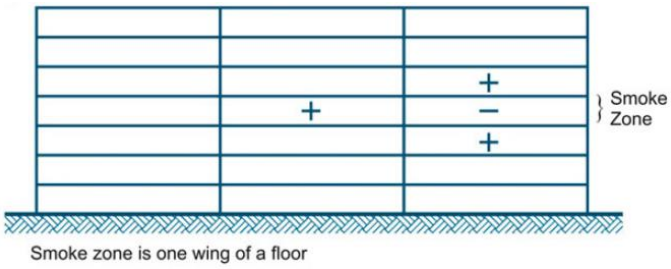

Figure 2.5 – A smoke-zone (negative) surrounded by several surrounding smoke-zones (positive). Image extracted and cropped from [1].

2.2.2. Extraction system

A smoke extraction system extracts smoke from a defined area, like an atrium or a large hall, and prevent the spread of smoke to adjacent areas, or to create a smoke-free layer height with tenable conditions at the occupant level in the same compartment. The extraction system can be designed as a natural smoke ventilation system, or as a mechanical smoke extraction system, with lids or vents located on the roof or high up on the walls [1].

Mechanical smoke extraction systems

Mechanical smoke extraction systems consist of vents (extraction fans) which extracts smoke at a rate high enough to prevent the spread of smoke to adjacent areas or to control the smoke-free layer [1].

Advantages:

- When the vents have reached its maximum extraction rate, smoke can be extracted quite fast.
- The system is not depended upon the buoyancy of the smoke.

Disadvantages:

- The system is designed for a certain HRR. If the HRR and the smoke production become larger than the system is designed for, the smoke control system can fail.
- There is a risk that air is extracted instead of smoke if the vents have a too large extract rate. This scenario is called the plugholding effect.
- It takes some time before the vents reach its maximum extraction rate. If the fire grows more rapidly than accounted for, or if the fire detection system fails (leading to delayed activation of the smoke control system), the smoke extraction system can fail due to the fire being bigger than what the current vent effectivity can handle.

Some ways to improve the effectiveness of the mechanical smoke extraction system are:

- Adding more vents with smaller extraction rates can improve the smoke control system if designed properly. The total volume extraction rate of five vents can be better than one vent with the same total volume extraction rate. Plugholding can be avoided.
- Smoke barriers in the ceiling prevent the spread of smoke across larger ceiling areas. In this way, the smoke is limited to "smoke-cells" in the ceiling.
- Smoke detectors with shorter detection time activate the system earlier, making the vents reach its maximum extraction rate earlier in the fire phase.

Natural smoke ventilation systems

Natural smoke ventilation systems consist of lids located on the roof or high up on walls. Smoke spreads upwards due to the buoyancy force and escapes through open lids. A large enough lid area prevents the spread of smoke to adjacent areas or controls the smoke-free layer.

A natural system is best suited in high-ceiling compartments (for example an atrium in a shopping mall). It is difficult to safeguard the smoke-free zone in a low-ceiling compartment without a mechanical system [1].

Advantages:

- If the fire becomes larger and produces more smoke, more lids can be opened to ventilate the excess smoke. The lids can be opened one and one as the fire develops.

Disadvantages:

- The system is depended upon the upward smoke-flow, the smoke is depended upon the buoyancy force. As the smoke spreads upwards, it expands and cools down due to mixing with cooler air. Hotter gases are less dense than cooler gases (for example air at normal temperatures).
- During warm days a hotter layer of air can be created below the ceiling and the lids, for example in an atrium with a glass ceiling. As the smoke spreads upwards and cools down to a temperature lower than the layer of hot air below the ceiling, the smoke can be prevented to pass by and escape the building, due to the buoyancy force. This problem can be avoided with mechanical vents.

2.3. The driving forces of smoke movement

The driving forces of smoke movement are buoyancy of combustion gases, expansion of combustion gases, fan-powered ventilation systems, elevator piston effect, stack effect, and wind. All except the first two (buoyancy and expansion of combustion gases) are also driving forces of air movement under nonfire conditions.

The driving forces, which cause the movement of smoke, can overpower the smoke control systems if the smoke control system is not properly designed. The smoke movement is in general affected by a combination of these factors. Any factor, which can affect the smoke control system, must be known and understood. How these driving forces act in the absence of any other driving force is briefly described in this section [5].

Buoyancy of combustion gases

The smoke produced during a fire flows upwards due to buoyancy. Smoke is hotter than the surrounding gas specie (air) and is less dense (buoyancy, chapter 2.1) [5].

Expansion of combustion gases

The energy released a fire causes the combustion gases to expand. In a fire room compartment with one opening to the adjacent space, smoke flows out in the top of the opening, and air enters the fire room compartment through the bottom of the opening. As the fire becomes fully developed and steady-state conditions are ruling, the mass flux of smoke out of the compartment equals the mass flux of air entering the compartment (with the fuel mass flux neglected) [5].

Assuming that the thermal properties of smoke and air are equal, the ratio of the volume flux flowing in and out of the compartment equals to the ratio of absolute temperature (K) of the gases (smoke and air) flowing in and out of the compartment. It is assumed that no pressure difference is established across the opening due to large flow areas (large openings) [5]. By rewriting eq. 2.1 and implementing the assumptions, the following equation is stated:

$$\frac{V_{out}}{V_{in}} = \frac{T_{out}}{T_{in}} \tag{2.3}$$

According to eq. 2.3, the volume of smoke at 300 °C is 1,96 times larger than the volume of air at 20 °C.

Fan-Powered Ventilation Systems

Modern HVAC systems (heating, ventilating, and air-cooling systems) can affect the smoke movement within a building. HVAC systems can extract smoke from compartments, and it can make smoke spread to other compartments connected to the same HVAC channel. Modern standards demand that the risk of fire-spread and smoke-spread to other compartments through the HVAC system are minimal or none.

In 1939 the National Board of Fire Underwriters (NBFU) released a report of analysed fires documented by the National Fire Protection Association (NFPA). Out of 25 fires recorder between January 1936 and April 1938, 19 of them involved combustion in the HVAC system. In five cases with no combustion in the HVAC system smoke was distributed through the channels. As a result, modern HVAC systems are designed in non-combustible materials and shuts down when smoke is detected in the system to avoid spread [5].

Elevator Piston Effect

Elevators moving in a shaft can cause the elevator piston effect. An elevator moving upwards in the shaft causes the volume of air above the elevator to compress and become denser. The volume below the same elevator expands and become less dense. This creates a flow of air through gaps and cracks from the denser to the less dense side, until (in theory) equal densities are achieved. Not only air from the shaft flows from one side to the other, but also air from other parts of the building. The opposite occurs when the elevator moves downwards.

During a fire, the elevator piston effect can cause a quicker spread of smoke from one part of the building to another through the elevator shafts [5].

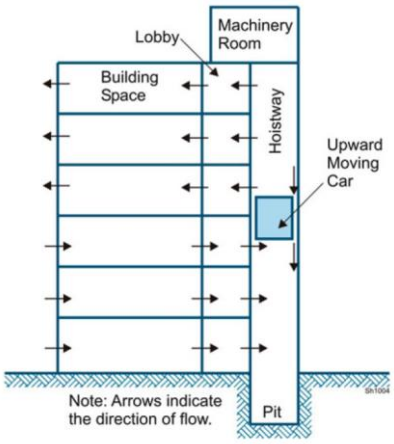

Figure 2.6 – Airflow due to the elevator piston effect. An elevator car moves downward causing an upward movement of air. Image extracted from [1].

Stack effect

In nonfire conditions, the movement of air causes the stack effect. When it is cold outside and warm inside, there is an upward movement of air inside the building shafts (for example stairwells, elevator shafts and ducts, this is referred to as the normal stack effect. The stack effect is greater as the temperature difference between the shafts and the outside is greater [5].

Hot air moves upwards in shafts in relative to the cold outdoor air (buoyancy, chapter 2.1). Due to the stack effect, a pressure difference is created between the shaft and the outside, which is directly affected by the temperature difference and the distance from the neutral plane.

A neutral plane forms between two spaces, for example, the inside of a compartment (or a shaft) and the outside, as illustrated in Figure 2.7 [5]. The pressure is equal on the same plane in both spaces. This is valid as there is no horizontal flow at this plane.

Hot air escapes the building above the neutral plane, and cold air enters the building below the neutral plane. As the HVAC system is initiated, continuous production of warm air upholds the stack effect. In a building with several shafts and temperature differences, several neutral planes can appear.

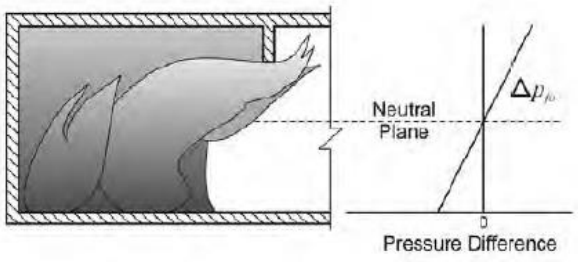

Figure 2.7 – The neutral plane. The pressure is equal in both spaces at the same plane. Image extracted from [5].

When it is hotter outside than inside, the reverse stack effect is initiated. A downward flow of air is governing within the building. Hot air enters the building above the neutral plane and cold air escapes the building below the neutral plane.

During a fire, the stack effect contributes to quicker smoke-spread in shafts. During a fire below the neutral plane, smoke tends to enter the shafts and flow upwards. When the smoke has spread to above the neutral plane, the smoke flows from the shaft to other compartments.

During a fire above the neutral plane, the smoke might through gaps and cracks spread to the floor above the fire plane, but the smoke is prevented to spread to the shafts due to the resistance from the stack effect. In situations where the smoke has enough buoyancy to overcome the stack effect, the smoke enters the shafts, flow upwards and spread to other compartments. The pressure difference between the shaft and the outside above a height can be estimated with the following expression:

$$\Delta p = 3460 \left(\frac{1}{T_o} - \frac{1}{T_s}\right) \times z \tag{2.4}$$

where Δp is the pressure difference between a shaft and the outside, T_o is the outside temperature, T_s is the shaft-inside temperature, and z is the height above or below (negative value) the neutral

plane. This equation can also be used for calculations between a compartment and the outside, as illustrated in Figure 2.7.

No neutral plane can be created in a pressurized stairwell, the flows are different from those in Figure 2.8 and Figure 2.9. No stack effect can be established in a properly designed pressurized stairwell since the temperature differences that causes the stack effect is accounted for [5].

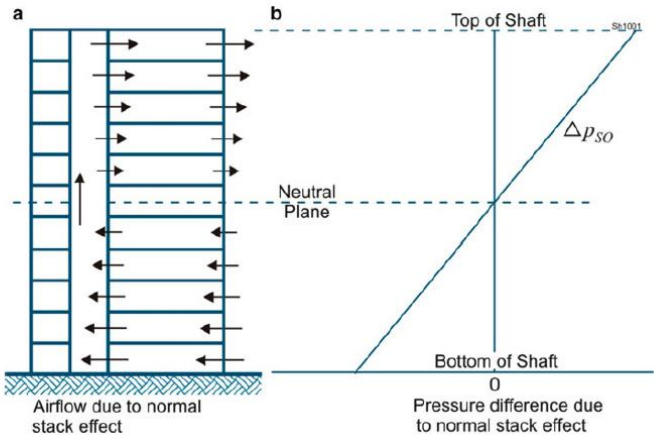

Figure 2.8 – Airflow and pressure difference of normal stack effect. Image extracted from [1].

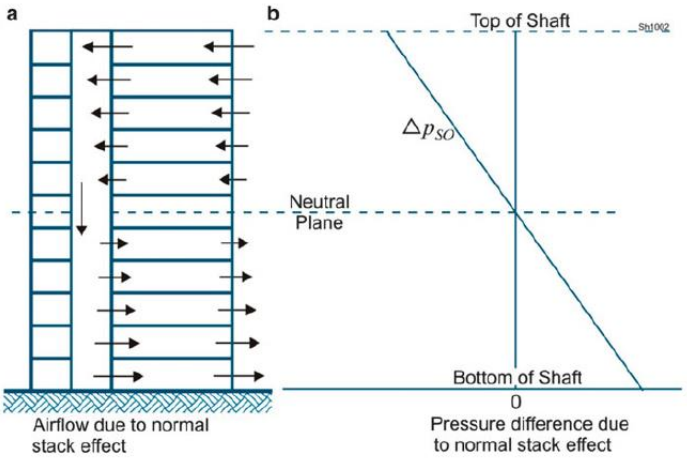

Figure 2.9 – Airflow and pressure difference of reverse stack effect. Image extracted from [1].

Wind

Wind can have a significant impact on the smoke movement within buildings. Wind blowing on a wall exerts the wall with pressure. The pressure increase depends upon wind speed, outdoor air density, and wind direction. As an example, consider a building with a pressurization system that relies on the pressure relief lid on the roof of the stairwell. This pressure relief can be affected by the wind, by limiting the outflow of excess air from the air supply in the pressurization system. The air supply system can also be affected since it collects air from the outside [5].

2.4. Past Validation Experiments

Through time, several full-scale experiments have been conducted to validate pressurization and smoke control systems. Some of these experiments are described briefly in this section.

2.4.1. Henry Grady Hotel Tests

In 1973, a series of smoke control systems were tested in the Henry Grady Hotel in Atlantan, USA. This building was scheduled for demolition. The purpose of the experiment was to evaluate the effectiveness of stairwell pressurization with and without lobby compartments and elevator shaft pressurization. The stairwell pressurization system was intended to safeguard a smoke-free egress route, and the elevator shaft pressurization was intended to prevent smoke-spread within the shaft. The designs of these systems were based on the latest papers and ideas about the topic. The tests were conducted by Atlanta City Building Department, led by N. A. Koplon [6] [7].

Test scenarios were built to measure temperature, smoke obscuration, CO concentration, and pressure difference. In these tests, the fire started in a hotel room on different floors and consisted of materials that are common for such rooms (beds, lamps, and other wooden furniture).

Tests at the Henry Grady Hotel proved that elevator pressurization systems can prevent the spread of smoke through the elevator shafts and that the stairwells can be kept smoke-free with the stairwell pressurization system [8].

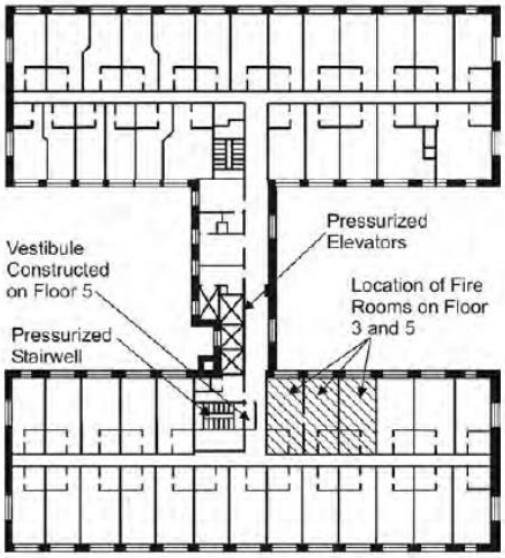

Figure 2.10 – The Henry Grady Hotel. Typical floor plan. Image extracted from [8].

2.4.2. 30 Church Street Tests

In 1973, the effectiveness of stairwell pressurization systems was tested in a 22-story office building, at 30 Church Street in New York, USA. This building was scheduled for demolition. The experiments were conducted by The Brooklyn Polytechnic Institute, led by P. R. DeCicco [9].

Temperatures and pressure difference were measured. The outcome of open doors towards the stairwell and how this affects the pressurization system were also studied. Typical office materials were used for the fires (desks, chairs, boxes with papers). Four fires were set at the office building on the 7th and 10th floor. These tests proved that the pressurization system could keep the stairwell smoke-free.

Based on these tests, a theoretical airflow model was developed, and airflow and pressure measurements from the tests were used to evaluate this model. During the tests, R. J. Cresci documented the visually observed stationary vortices at open doorways [10]. These vortices are the reason that the flow coefficient through an open stairwell door is about half of what it would else be [8].

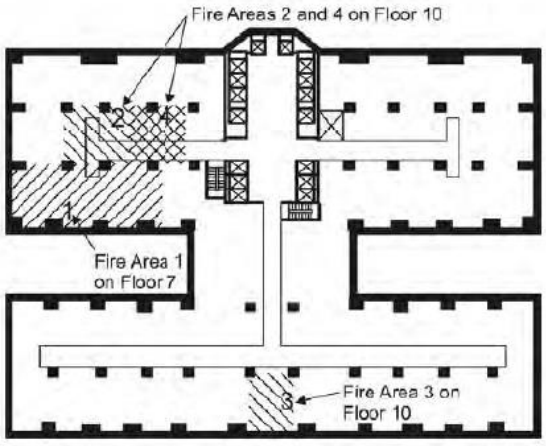

Figure 2.11 – The 30 Church Street office building. Typical floor plan. Image extracted from [8].

2.4.3. Plaza Hotel Tests

In 1989, experiments of stairwell pressurization and zoned smoke control were conducted in the Plaza Hotel Building in Washington D.C., USA. This 7-story building was scheduled for demolition. Exhaust fans were installed on the fire floors, with the intention to keep the floors above and below the fire floor smoke-free. The second floor was defined as the fire floor. A pressurization system was installed in the stairwell with the intention to keep the stairwell smoke-free. The experiments showed that these systems could keep smoke-free conditions as intended. The tests were conducted by the National Institute of Standards and Technology (NIST), led by J. H. Klote [11].

The interaction between the fire and the smoke control system was investigated. For each fire test, solid fuels in terms of two or four wooden cribs (64 kg per crib) were used. Measurements were

made of temperature, wind velocity, pressure difference, smoke obscuration and concentrations of CO, CO_2 and O_2 [8].

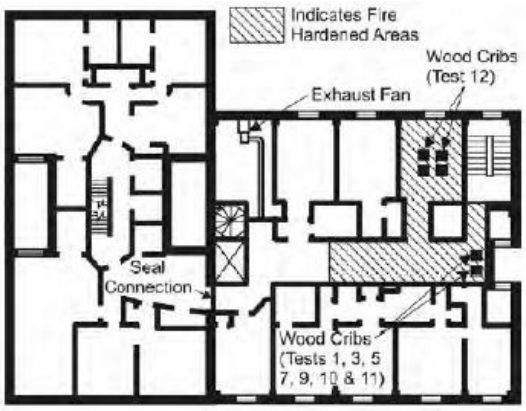

Figure 2.12 – The Plaza Hotel. The second floor plan. Image extracted from [8].

2.4.4. The NRCC Experimental Fire Tower

During the mid-1980s, the National Research Council Canada (NRCC) built an experimental fire tower, which is used for smoke control experiments like stairwell pressurization system [8]. The experimental fire tower is located near Ottawa, Canada. The 10-story experimental fire tower consists of two parts on each floor, the experimental facility and the control room. The core of the experimental facility consists of several compartments which are used as the fire room compartment, a stairwell connecting all the stories, a lobby compartment connecting the stairwell and the compartments, and several shafts (elevator shaft, air supply shafts, exhaust shafts, and others). The fire room compartment has an opening to the outside, which can be blocked or used as a simulated broken window. The building has instruments at many locations on each floor for measuring temperatures, airflows, pressure differences, smoke obstructions and gas concentrations. Gas burners have been used as the fire for most tests. Gas burners are easy to reuse and easy to control [8].

Figure 2.13 – The NRCC Experimental Fire Tower. Typical floor plan. Image extracted from [8].

The tower has been used to develop the foundation of today's known smoke control principles. The National Institute of Standards and Technology (NIST) and the National Research Council Canada (NRCC) used the tower to validate elevator pressurization [8]. Some people can not evacuate through stairwells due to physical disabilities. G. T. Tamura and J. H. Klote conducted in 1987 experiments on elevator pressurization systems for smoke control [12], and mechanical pressurization to control the smoke movement caused by fire pressures [13]. In 1988, they investigated the pressures caused by stack and wind actions [14].

During the 1990s, G. T. Tamura conducted experiments of four stairwell pressurization systems based on pressure relief vents and mechanical extraction systems. This project was split up into three phases. During the first phase, a literature review was made to summarize pressurization principles, review evacuation principles, and to gather requirements from different fire codes. Based on the review, nonfire and fire tests were conducted in the NRCC experimental fire tower, where airflow through different angles of open stairwell doors was measured. During the fire tests, pressure differences and velocity pressures across stairwell doors were measured. This resulted in conclusions of minimum required velocities and pressures differences to prevent smoke backflow from the fire room compartment to the pressurized stairwell [15].

During the second phase, stairwell pressurization principles were evaluated in three existing buildings. The 22-story apartment building had a pressurized stairwell with exit door reliefs. The 39-story office building had a pressurized stairwell with barometric damper reliefs. The 42-story office building had a pressurized stairwell with a variable-supply air system with feedback control. The smoke-flow through various angles of open stairwell shaft doors were analysed, and pressure differences and airflow velocities were measured [16].

During the third phase experiments were conducted in the NRCC experimental fire tower. Four pressurization systems for stairwells were tested: (1) with an exit door relief, (2) with a barometric damper relief, (3) with a fan bypass, and (4) with a variable-speed fan. The fire room compartment was located on the second floor, gas burners were used as the fire source. To avoid having unburnt gasses in the facility, the gas was premixed with air. These scenarios were each performed with natural venting of the fire room compartment, mechanical extraction venting of the fire room compartment, and with no venting of the fire room compartment. The tests were performed during summer and winter conditions. The tests were conducted with and without fires. For the nonfire conditions, pressure differences and average air velocities were measured. For the fire conditions, temperatures on various locations in the fire room compartment, the percentage of smoke backflow of an open door, and the door-opening angle to stop smoke backflow were measured. Different combinations of open-door scenarios were analysed: no stairwell-door open, stairwell-door on floor 1 and 2 open, stairwell-door on floor 1, 2 and 3 open, and stairwell-door on floor 1, 2, 3 and 8 open. The air supply to the stairwell varied between 5,92 m^3/s and 15,6 m^3/s for the case with natural venting of the fire floor, and 0,80 m^3/s to 13,69 m^3/s for the case with mechanical venting of the fire floor [17] [18].

2.5. The fire scenario

The HRR (Heat Release Rate) of a fire is mainly depended upon the fuel load (type and amount of fuel) and the properties of the fire room compartment. The HRR is expressed as a function of the $\dot{m}_f$ (fuel mass loss rate) and the ΔH_c (Heat of Combustion per unit mass of consumed fuel).

$$\dot{Q} = \dot{m}_f \Delta H_c \tag{2.5}$$

The HRR is often viewed as the main controlling factor of the fire scenario, it controls the heat and smoke production. The HRR indicates the fire size, which is determined by the fire source area (A_f) and the HRRPUA ($\dot{Q}''$, Heat Release Rate Per Unit Area).

$$\dot{Q} = A_f \dot{Q}'' = A_f \dot{m}_f'' \Delta H_c \tag{2.6}$$

The HRR varies during the development of the fire scenario. The fire scenario is in various literature described as four stages: (1) ignition, (2) growth, (3) fully developed fire, and (4) decay [19] [20] [21].

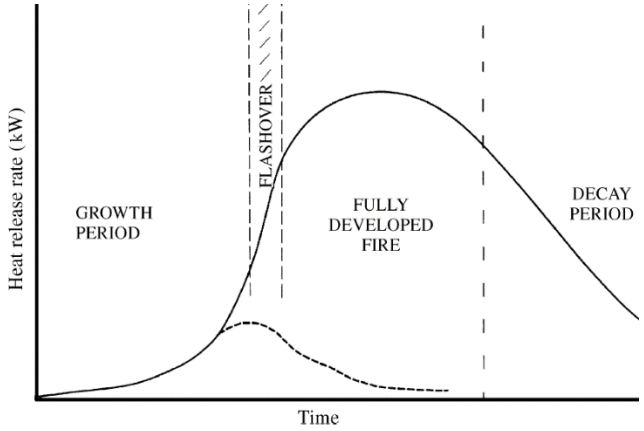

Figure 2.14 – The phases of a fire scenario. The growth phase starts after ignition. Image extracted from [21].

Some literature describes the flashover phase as one of the main stages. This is considered as wrong since the transaction between the growth phase and the fully developed fire phase can occur with and without the flashover. The flashover is by the International Standards Organization defined as "the rapid transition to a state of total surface involvement in a fire of combustible materials within an enclosure". The flashover occurs when the temperatures in the fire room compartment reach 500 - 600 °C, or when the radiation to the floor is 15 - 20 kW/m^2. Everything that can burn will burn. The flashover does not occur when the temperature and radiation are much lower than the flashover criterion during the fully developed fire phase [19].

Ignition

In most cases, fire is initiated by a piloted ignition. The fire is started by an ignition source like a spark or a flaming match. Without an ignition source, a fire can start by a spontaneous ignition, or by self-ignition. Spontaneous ignition is caused by an external radiative source. The external radiative source ignites a material when the radiative source is so great so that the material heats up and reaches its autoignition temperature. An example is a flaming chimney heating a nearby

piece of paper. Self-ignition is caused by the process where an object produces an amount of energy high enough to make itself ignite, for example, a phone charger overheating while charging [20].

Growth

The growth rate is at start depended upon the available fuel. The fuel load controls the growth rate. Liquids and gases burn easier than solid fuels. Solids must vaporize before they can burn because this process demands more energy. It means that the fire must produce more energy to keep up the combustion process.

The fire can develop in three different ways, the fire can be extinguished, burn constantly or continue to grow. The HRR decays when the fire consumes more combustible gases than it produces. When the consumption and production of combustible gases are equal, the fire reaches a steady-state condition and do not grow or decay. The HRR grows when the fire produces more combustible gases than it consumes. The growth can be limited by for example a fire extinguishing system, or by a limited amount of fuel or oxygen. These factors can also extinguish the fire. The growth period can take a long time, this depends upon the fuel load [20].

Fully developed fire

A fully developed fire is defined as the situation where the fire is either fuel-controlled or ventilation-controlled. The fire can not grow further unless more fuel or oxygen is supplied. Unburnt gases are produced in the case where the fire is ventilation-controlled. Unburnt gases flowing out of openings mixes with oxygen, ignite and propagate flames on the outside of the opening since the temperature of the gases are greater than the autoignition temperature.

The average temperature in the compartment can during this phase reach 700 – 1200 °C. All materials that can burn will burn. The temperatures can also be smaller due to limited fuel loads. The fire reaches the decay phase when most of the fuel load is consumed [20].

Decay

The decay starts when the amount of combustible materials that can pyrolyze is reduced, leading to a reduced HRR. The decay phase can take a very long time, the average gas temperature decreases (commonly in compartments) in this phase. A ventilation-controlled fire will become fuel-controlled during this phase [20].

2.6. The design fire in terms of numerical simulations

In terms of numerical calculations, the HRR development is commonly modelled instead of simulated. Simulations of the HRR development are very demanding in terms of computational costs, due to this requiring a very fine grid resolution with short time steps. The phases of the fire are modelled based on assumptions of how the fire scenario will look like. The ignition phase is normally ignored since it is demanding in terms of computational costs. It is just assumed that the fire has started.

The initial growth phase nearly always accelerates in fire scenarios. The accelerating growth of the HRR is commonly described as increasing with the square of time. By implementing a constant factor α various growth velocities can be modelled:

$$\dot{Q} = \alpha t^2 \tag{2.7}$$

where $\dot{Q}$ is the HRR, α is the growth rate, and t is the time [22]. Studies show that this correlation fits well with real fire scenarios after the ignition has occurred and the fire has started to grow. In most literature, α is categorized with the following fire growth rates: slow, medium, fast or ultra-fast [22] [23]. These values have been assessed through real fire tests, and various categories of buildings and fuel loads are often connected to these fire growth rates. For example, a library can contribute to a more rapid fire growth rate compared to an indoor swimming pool. The fuel loads are different in these buildings [22].

Table 2.1 – Fire Growth Rates used in Fire Safety Design. Data collected from [22].

Fire growth rate	α [kW/s^2]	Time to reach 1055 kW [s]
Slow	0,003	600
Medium	0,012	300
Fast	0,047	150
Ultra-fast	0,190	75

The growth rate continues until the fire reaches the defined limit of the design fire. A fully developed fire is either limited by the amount of fuel supplied to the fire, or by the amount of oxygen supplied to the fire, as described in chapter 2.5. The smallest value of the maximum HRR regarding a fuel-controlled fire and the maximum HRR regarding a ventilation-controlled fire determines the largest possible HRR for the scenario.

For ventilation-controlled fires (fully developed), the mass flow rate of air through an opening can be expressed as:

$$\dot{m}_a = 0{,}5 \times A_o\sqrt{H_o} \tag{2.8}$$

where $\dot{m}_a$ is the mass flow rate of air, A_o is the opening area, and H_o is the opening height. The mass flow rate $\dot{m}_a$ can be estimated for several openings, and the total value can be used to define the HRR of the ventilation-controlled fire. Each kilogram of oxygen used for combustion produces

13,1 MJ of energy. The mass fraction of oxygen in the air is 23 % [24]. With this information eq. 2.8 is rewritten to eq. 2.9, which now states the HRR regarding a ventilation-controlled fire:

$$\dot{Q} = 1{,}507 \times A_o\sqrt{H_o} \tag{2.9}$$

Fuel-controlled fires are often in literature specified after the HRRPUA (Heat Release Rate Per Unit Area) and the area of the fire:

$$\dot{Q} = \dot{Q}'' \times A_f \tag{2.10}$$

where $\dot{Q}''$ is the HRRPUA and A_f is the fire source area.

The HRR used to model fires in an FDS simulation can be based upon measured values from a real experiment or upon data from a fire code. Guidelines for design fires with an aspect to time-evolving HRRs are found in, for example, NS-EN 1991-1-2:2002 Eurocode 1 [25]. The growth phase, the fully developed fire phase, and the decay phase is accounted for with this method. The calculations regarding the maximum HRR for the fuel-controlled scenario is based upon the room geometry and the fuel load. The ventilation-controlled scenario is based upon the opening areas to the outside. For fuel-controlled fires, each type of building has a specified HRRPUA. This value multiplied by the total floor area in the fire cell gives the total HRR. For example, apartments have a 250 kW/m^2 HRRPUA. With a total floor area in the fire cell of 100 m^2, the total HRR is 25 MW. The maximum possible HRR when the fire is ventilation-controlled are calculated based on the opening factor, the building properties are not considered in this case. Windows with an average height of 2 meters and a total width of 6,3 meters, or an average height of 1 meter and a total width of 17,8 meter would represent a 25 MW fire, according to the calculations. Mind that the opening height increases the HRR more than the opening width. These window sizes are a lot for apartments of size 100 m^2. The fire becomes ventilation-controlled with smaller windows.

The HRR of a fire starting in a smaller room to an adjacent larger space, should in the early phase be defined after the properties of the available ventilation factors, and the fuel properties of that room [26].

The HRR can, however, be affected by a fire extinguishing system. The fire safety code SN-INSTA/TS 950:2014 [23] describes the calculation procedure for this consideration. A fire of size less than 5 MW, at the time of fire extinguishing system activation, decreases to one-third of the HRR at the time of the fire extinguishing system activation, and remains constant for the rest of the fire scenario. The HRR for larger fires is kept constant at the time of the fire extinguishing system activation. The principles of fire suppression as described in SN-INSTA/TS 950:2014 can with some modifications be implemented into the calculation procedure of NS-EN 1991-1-2:2002 Eurocode 1 [25].

The fire safety code SN-INSTA/TS 950:2014 [23] presents tenable conditions for visibility, temperature, heat flux, CO, CO_2 and the reduction of O_2. With these quantities, the available safety egress time can be assessed.

Parameter	Criteria	
Visibility	Visibility no less than 3 m in the primary fire compartment at area of ≤ 100 m^2). Visibility no less than 10 m at height of 2 m in escape routes and compartments of areas > 100 m^2. As an alternative to determine visibility, a smoke-free height of 1,6 m + 0,1 x H.	
Thermal[a]	Continuous radiation intensity of maximum 2.5 kW/m^2 and,a short-term radiation intensity of maximum 10 kW/m^2 if the maximum radiant dose is less than 60 kJ/m^2.	
Temperature	Gas temperature not higher than 80 °C.	
Toxicity[b]	CO CO_2 O_2	< 2 000 ppm < 5 % > 15 %
[a] In addition to the energy from background radiation. [b] Toxicity does not need to be calculated when the visibility surpasses 5 m.		

Figure 2.15 – Tenable conditions when evaluating the available safety egress time. Image extracted from [23].

Through a vast number of experiments, it has been found that the Froude number correlates to the geometry of a flame. The nondimensional Froude number, Fr, is used in hydraulics when expressing liquid flows [27]. The Froude number is expressed as:

$$Fr = \frac{u^2}{g \times D} \tag{2.11}$$

where u, g and D are the flow velocity, acceleration due to gravity, and the diameter of the flow source respectively. The square root of the Froude number approximately correlates to the ratio of the flame height, L, and the fire source diameter, D:

$$\sqrt{Fr} \propto \frac{L}{D} \propto \sqrt{\frac{\dot{Q}^2}{D^5}} \propto \frac{\dot{Q}}{D^{5/2}} \tag{2.12}$$

A useful way to express the data of a fire is in terms of the nondimensional HRR, $\dot{Q}^*$ [27]. $\dot{Q}^*$ contains information about the HRR, the acceleration due to gravity (g, 9,81 m/s^2), D (fire source diameter) and the properties of air:

$$\dot{Q}^* = \frac{\dot{Q}}{\rho_\infty c_p T_\infty \sqrt{gD} D^2} \tag{2.13}$$

where ρ_∞, c_p and T_∞ are the density, specific heat and temperature of ambient conditions, which in most cases are ambient air. The approximate ambient values of air are [27]:

- ρ_∞ - 1,20 kg/m^3
- c_p - 1,00 J/(g × K)
- T_∞ - 293 K

Figure 2.16 shows several experiments where $\dot{Q}^*$ and L/D has been plotted. Lower values of $\dot{Q}^*$ indicates typical pool fires where the flows are dominated by buoyancy. Higher values indicate jet

flames where momentum dominates the flow. For most natural fires the $\dot{Q}^*$ is less than 10. For most large fires the value is less than 2 [27]. G. Cox and S. Kumar described that a value above anything around 2,5 is not representative for buoyant fire plumes, it is more appropriate for higher momentum jet flames [28].

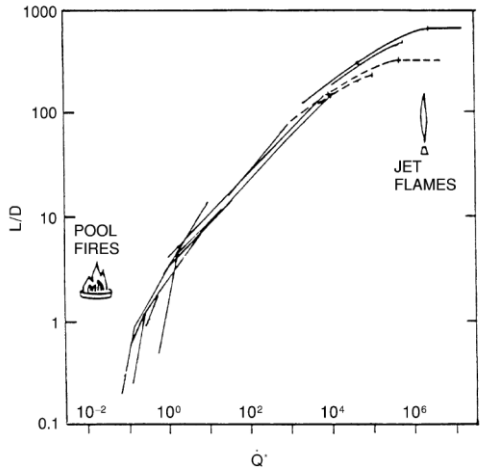

Figure 2.16 – Experiments of fire scenarios, where the nondimensional heat release rate, $\dot{Q}^*$, is plotted against the ratio of the flame height and the fire source diameter, L/D. Image extracted from [27].

Several equations have been developed to predict flame heights based upon the fire source diameter and $\dot{Q}^*$ for the different regimes of the experimental results as presented in Figure 2.16. A well-known equation for the pool fire regime has been developed by G. Heskestad:

$$\frac{L}{D} = 3{,}7 \times \dot{Q}^{*2/5} - 1{,}02 \tag{2.14}$$

A new equation is returned by adding g and the ambient values of ρ_∞, c_p and T_∞ to eq. 2.14:

$$L = 0{,}235 \times \dot{Q}^{2/5} - 1{,}02 \times D \tag{2.15}$$

which is a more convenient way of estimating the flame height as a function of the HRR and the fire source diameter [27].

2.7. Computational Fluid Dynamics

The idea of solving the governing equations for fluid flows by numerical calculations was first addressed in the early 1920s, by Lewis Richardson, for weather prediction. The tools were about 50 years later emerged into the concept of Computational Fluid Dynamics (CFD). CFD is a technique used to analyse, predict and solve problems that involve the behaviour of fluid flows, by solving the governing equations with computational power [29].

CFD is today used in a wide aspect of engineering fields. Some examples are metrology, ventilation design, fire science and vehicle design. CFD was first developed outside of the fire community, but the same techniques have today been adapted to fire technical analyses. The use of CFD codes is an alternative to full-scale experiments, which are often limited to cost. The back draw of CFD codes is the high demand for computational power, which can make the simulation time essentially longer than the length of the current scenario.

CFD has been used to analyze past disasters like the King Cross tragedy in 1987, and the World Trade Center tragedy in 2001. These simulations have been essential to the development of future CFD codes [30].

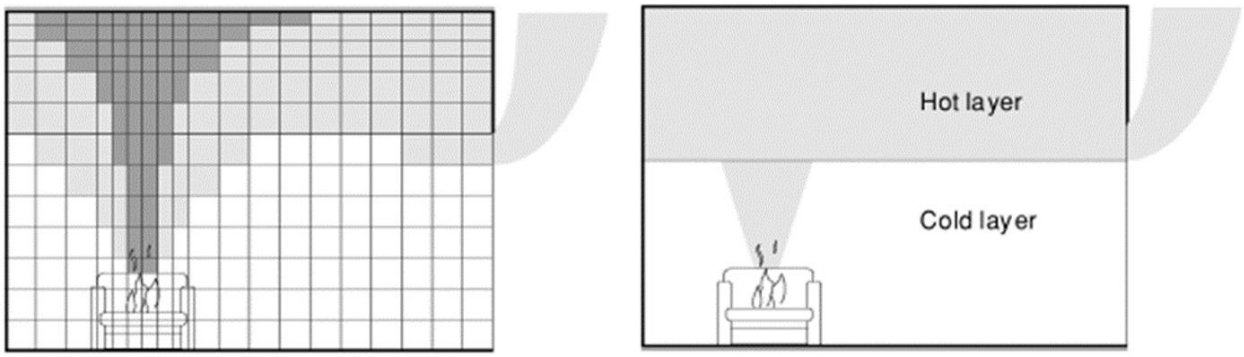

Figure 2.17 – A CFD model (left), in comparison to a two-zone model (right). The two-zone model presents the result data as average values across a cold layer and hot layer. The CFD model is capable to present more detail results in terms of data across a large number of sub-volumes in X, Y and Z direction. Images extracted from [31].

2.7.1. The governing equations

The core of any CFD model is constituted by the conservation equations of mass, momentum and energy.

Conservation of Mass

The conservation equation for mass is:

$$\frac{\partial \rho}{\partial t} + \nabla \cdot \rho u = 0 \tag{2.16}$$

which states that the change of density at a given point is equal to the mass flux across the boundaries of that point (referred to as the control volume in the CFD application). The mass within a sealed domain can neither be created or terminated. For fire simulations, it is necessary to account for the conservation of mass for various gas species, like fire products and air. The mass

conservation equation (eq. 2.16) is often rewritten to set of transport equations for the mass fraction of various gas species, Y_α:

$$\frac{\partial(\rho Y_\alpha)}{\partial t} + \nabla \cdot (\rho Y_\alpha u) = \nabla \cdot (\rho D_\alpha \nabla Y_\alpha) + \dot{m}_\alpha''' \tag{2.17}$$

By summarizing the specific species equations, the mass diffusion and production terms equal zero, as stated by the original mass conservation equation (eq. 2.16) [29].

Conservation of Momentum

The conservation equation for momentum is:

$$\frac{\partial(\rho u)}{\partial t} + \nabla \cdot (\rho u u) = -\nabla p + f + \nabla \cdot \tau \tag{2.18}$$

This equation refers to Newton's second law of motion, which states that the velocity of an object changes when it is subjected to an external force. Momentum is equal to mass times velocity, and force equals mass times acceleration. The forces that control the movement of fluid flows consist of the pressure gradient, ∇p, friction in the form of the viscous stress tensor, τ, and other external forces (like the driving forces of smoke movement, chapter 2.3), f [29].

Conservation of Energy

The conservation equation for energy is:

$$\frac{\partial(\rho h)}{\partial t} + \nabla \cdot (\rho h u) = \frac{Dp}{Dt} + \dot{Q}''' - \nabla \cdot Q + \varepsilon \tag{2.19}$$

which states that the change of enthalpy, h, at any given point is equal to the net energy flux across the boundaries of that point. The net energy flux is, in terms of fire, related to pressure, combustion HRR, radiation and conduction, and kinetic energy dissipation, as shown on the right hand of eq. 2.19 [29].

Further details

The momentum equation consists of three equations, one for each velocity component: u, v and w (the u component is presented in eq. 2.18). The mass and energy equations consist of one set each. This leaves five conservation equations with six unknows, being the three velocity components, the density, the pressure and the sensible enthalpy for the fluid. An equation of state is required to close the system by relating the pressure and the sensible enthalpy. The sensible enthalpy is a function of the specific heat and temperature of the fluid:

$$h = \int_{To}^{T} c_p \, dT \tag{2.20}$$

For fire application it is sufficient to assume a perfect gas (eq. 2.1):

$$PW = \rho RT; W = \frac{1}{\sum \left(\frac{Y_\alpha}{W_\alpha}\right)} \tag{2.21}$$

where $\Sigma (Y_a / W_a)$ is the average molecular weight of the gas mixture. The stated governing equations form the basis for any CFD code, but not without further simplifying assumptions which are unique to each field [29].

2.7.2. Turbulence modelling

Turbulence modelling is one of the most important aspects to account for regarding CFD. Turbulence is one of the most computationally demanding tasks to simulate, therefore it needs further simplifications and assumptions. The transport of mass, momentum and energy occurs through convection and diffusion, two modes that play a significant role in a CFD analysis. The convective mode for transport of heat and combustion products is the dominant part in large-scale fire scenarios. The diffusive mode (viscosity, thermal conductivity, and material diffusivity) is the dominant part around the fire and near boundaries of solid surfaces.

It is computationally demanding to capture the spatial (cell size) and temporal (time) scaling differences between the convective and diffusive modes properly together. For large-scale fire scenarios, techniques have been developed to approximate the diffusive part by modelling the turbulence. Five turbulence modes are briefly described in this section [29].

Direct Numerical Simulation

Direct Numerical Simulation (DNS) is a mode with no modifications and simplifications of the diffusive part. No assumptions are made regarding turbulence. That means that the governing equations are solved directly with consideration to all aspects, like convection and diffusion. The DNS mode requires a very fine spatial and temporal resolution, in ranges of less than 1 mm and 1 ms respectively, to simulate small laminar flames and turbulent jets. Hence the demand for fine spatial and temporal scales, it is not suited for large-scale fire simulations [29].

Reynolds-Averaged Navier-Stokes

The Reynolds-Averaged Navier-Stokes (RANS) equations were introduced by O. Reynolds over a century ago. By using the RANS method in a fire specific CFD model, the turbulence is modelled with a statistically time-averaged form of conservation equations. The idea of RANS is to decompose the velocity components, enthalpy and the species mass fractions from the governing conservation equations, into a time-averaged component and a fluctuating component [29].

$$\phi(x,t) = \bar{\phi}(x,t) + \phi'(x,t) \tag{2.22}$$

The time scale for the time-averaged component is on the order of several seconds, while the fluctuating component is on the order of milliseconds. The time-averaged component changes more slowly in time and space than the original components, the time-averaged component is therefor used to model the turbulence [32].

By substituting eq. 2.22 and applying the time-averaged components into the governing equations (eq. 2.16, 2.18 and 2.19), a new set of equations is yielded. While the mass equation remains unchanged, the momentum and energy equations expand with new terms on the right hand.

$$\frac{\partial(\rho\bar{u})}{\partial t} + \nabla \cdot (\rho\bar{u}\bar{u}) = -\nabla p + f + \nabla \cdot \bar{\tau} - \nabla \cdot \rho\overline{u'u'} \tag{2.23}$$

$$\frac{\partial(\rho\bar{h})}{\partial t} + \nabla \cdot \left(\rho\bar{h}\bar{u}\right) = \frac{Dp}{Dt} + \dot{Q}''' - \nabla \cdot \bar{Q} + \bar{\varepsilon} - \nabla \cdot \rho\overline{u'h'} \tag{2.24}$$

The additional terms are referred to as Reynolds stresses and the turbulent scalar flux. The additional terms leave the equations "unsolvable" (no longer closed), due to the increased number of unknows now being larger than the number of equations. The equations can be closed by introducing an "eddy viscosity turbulence model". The computational cost for large-scale CFD simulations is reduced by using the RANS mode [29].

Large Eddy Simulation

The Large Eddy Simulation (LES) mode is similar to the RANS mode. The RANS mode uses time-averaging to model turbulence, while the LES mode uses spatial-averaging (or filtering). Like for RANS, the LES mode models and solves the same, unresolved convection terms by replacing them with diffusion terms.

The LES technique simulates the large-scale turbulences while the small-scale motions are modelled. This action leads to a neglectable error in turbulence. It is assumed that the smaller eddies (turbulent movements, see Figure 2.18) are self-similar which makes the simulation simpler by modelling them. The conservation equations are not solved for the small-scale motions (as they are with the DNS mode).

With LES, swirling eddies can span just a few grid cells. To achieve this, the eddy viscosity must be small enough to avoid smoothing out these eddies, but large enough to achieve numerical stability and to account for the dissipation of energy at sub-grid scales. The LES mode still requires a large computational cost, but still less than the DNS mode [29] [33].

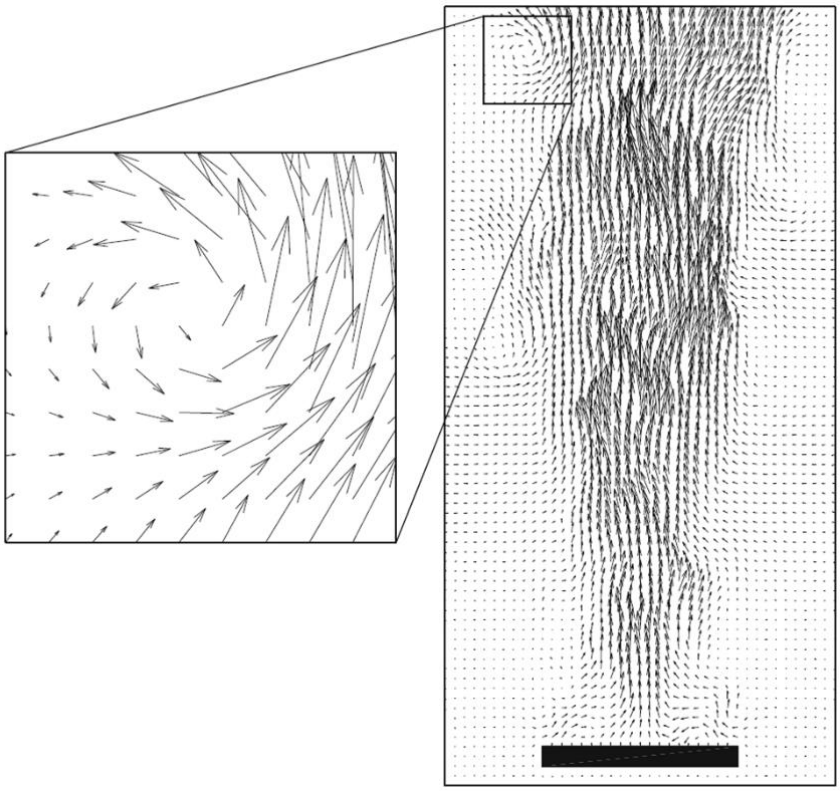

Figure 2.18 – The flow vectors of a Helium plume simulated with the LES mode. The image shows the smallest possible resolvable eddy. Smaller eddies are modelled, instead of simulated like the eddy shown in the image. The grid size is visible by the spacing and distance between the arrows. Image extracted from [29].

Very Large Eddy Simulation

The Very Large Eddy Simulation (VLES) mode is a hybrid model of the RANS and LES methodology. The VLES mode uses the principles of RANS in near boundaries of solid surfaces, in combination with the principles of LES in large-scale turbulent structures [34] [35].

Simple Very Large Eddy Simulation

The Simple Very Large Eddy Simulation (SVLES) mode, is VLES with simplifies physics [34].

2.8. Fire Dynamics Simulator

Fire Dynamics Simulator (FDS) is an open-source CFD code for fire-driven fluid flows designed for fire applications. Fire-driven flows are substantially slower than the speed of sound, therefore FDS solves the conservation equations for low-speed Mach numbers (lower than 0,3) with an emphasis on smoke and heat transport from fires [34].

The development and maintenance of FDS are led by the National Institute of Standards and Technology (NIST) and VTT Technical Research Centre of Finland, with support from other developers, contributors and the international fire community. The first version of FDS was publicly released in February 2000 [34].

The quality of the FDS analysis controls the computational cost, which increases as the number of cells increase and as the time steps decrease. The term computational cost is bound by the capacity of computational hardware and simulation time.

FDS has been validated to many experimental measurements, to ensure the appropriateness of the governing equations. Such documentations in essential to the choice of which CFD code is to be used [36]. Each version of the code is also verified, to control that the equations are solved correctly [37].

The National Institute of Standards and Technology (NIST) and VTT Technical Research Centre of Finland have also developed Smokeview, which is a companion program to FDS. Smokeview visualizes the FDS result data (and other CFD code result data) as a 3D model [34].

2.8.1. Mesh

The specific scenario for analysis must be defined within a domain where all the FDS calculations are performed. The domain consists of rectangular volumes called meshes, and each mesh is divided into rectangular volumes called cells [34].

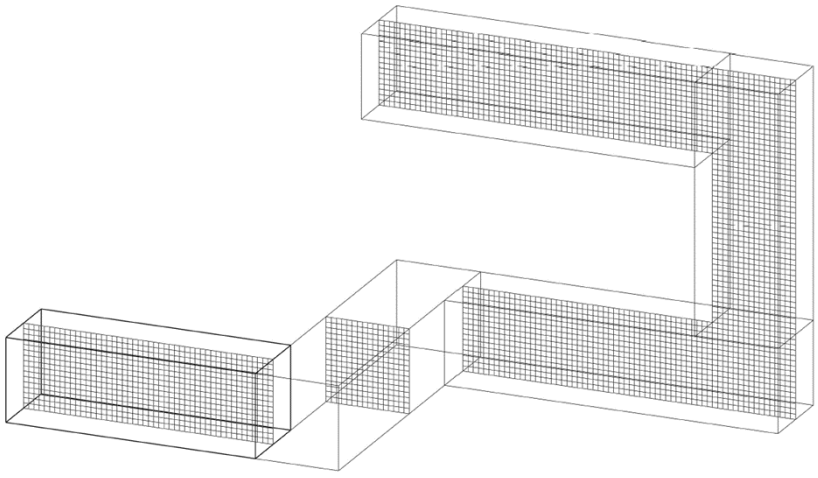

Figure 2.19 – A computational domain consisting of five meshes. The cells are visualized as square shapes. Image extracted from [34].

Any object located outside of the domain does not take part in the calculation. Any object extending to the outside of the domain is cut off at the borders, and the part within the domain participates in the calculation.

An FDS job consists of one or several meshes. Bigger amounts of cells require a bigger computational cost. The computational domain visualized in Figure 2.19 consists of five meshes, which is an advantage comparing to enclosing the same domain within one mesh. The number of cells would increase by at least 10 times if the same domain would be enclosed by one mesh, resulting in a 10 times larger computational cost. That results in 10 times longer computational time with the same computational hardware.

Splitting one mesh into two meshes with the same cell size and the same total number of cells usually returns the same results, but there are some issues to keep in mind. The mesh borders should be avoided to be put where critical actions are expected, like through a fire area. If possible, the mesh borders should be kept free of areas where complicated phenomena are expected. The exchange of information across mesh boundaries are not (yet) as accurate as of the exchange of information between cells in one mesh [34].

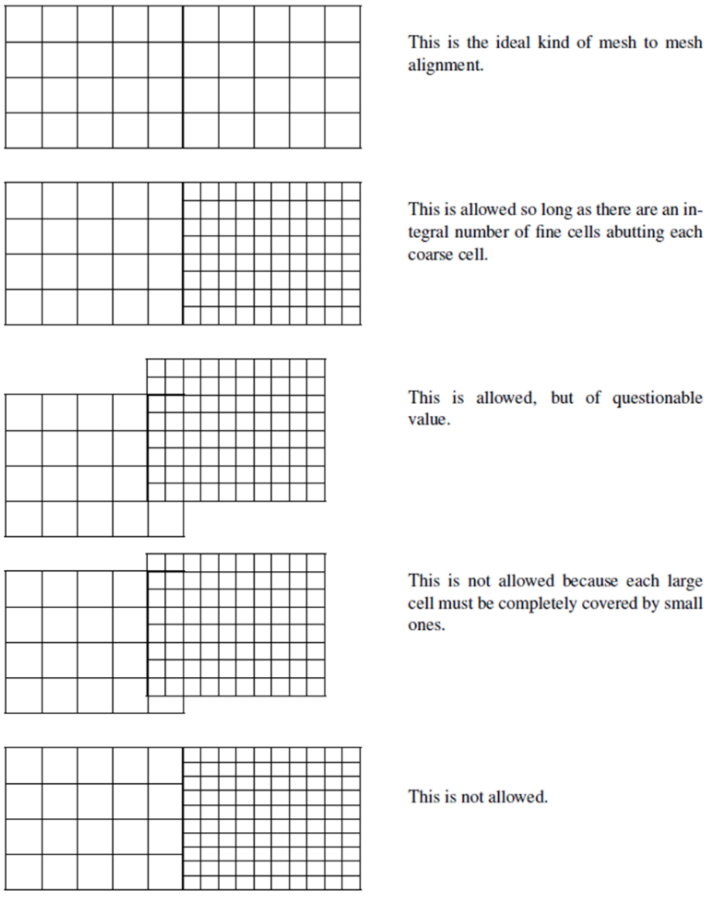

Figure 2.20 – A mesh-alignment guideline. Image extracted from [34].

The right size of a cell must be assessed through a mesh sensitivity analysis. The accurate cell size is depended upon the current scenario. The general process of the mesh sensitivity analysis is to design an FDS input file with a coarse mesh (a mesh with a cell size bigger than for the purpose of the current scenario), and then gradually refine the mesh with smaller cells until the results between the two finest meshes are neglectable [34].

It is more convenient to express the mesh resolution in terms of $D^*/\delta x$ for buoyant plumes, where δx is the nominal cell size [m] and D^* is the characteristic fire source diameter [m] (characteristic, but not physical, diameter of a fire). The expression for D^* is as follows:

$$D^* = \left(\frac{\dot{Q}}{\rho_\infty c_p T_\infty \sqrt{g}}\right)^{\frac{2}{5}} \tag{2.25}$$

where ρ_∞, c_p and T_∞ are the density, specific heat and temperature of ambient air, and g is the acceleration due to gravity (9,81 m/s^2). The approximate ambient values of air are [27]:

- ρ_∞ - 1,20 kg/m^3
- c_p - 1,00 kJ/(kg × K)
- T_∞ - 293 K

The expression $D^*/\delta x$ states the number of computational cells spanning across the characteristic fire source diameter, where larger values return a finer resolution for the calculation. A certain cell size δx which is evaluated to be good for a large fire might not be good for a small fire. A certain value of $D^*/\delta x$ evaluated to be good for a large fire can as well (but not guaranteed) be good for a small fire, since the value of D^* reduces with the reduction of the fire. If the HRR is growing (time-dependent), the value $D^*/\delta x$ grows as well. If $D^*/\delta x$ is evaluated to be fine enough for the maximum expected HRR, the cell size might not be good enough in the early growing phase [34].

There is no clear answer on what the right cell size or right value of $D^*/\delta x$ is for a given situation, except doing a mesh sensitivity analysis. However, recommendations on ranging values are found in various literature [38]. The FDS Validation Guide states the values of $D^*/\delta x$ for several scenarios [36]. These values are good to consider as a starting point when defining the mesh resolution, but it is inappropriate to use them directly without further research. A mesh sensitivity analysis is considered as the prior way to determinate the right mesh resolution.

2.8.2. Simulation mode

FDS supports four simulation modes regarding turbulence modelling, these are DNS, LES, VLES and SVLES. These modes are described in chapter 2.7.2. The default mode of FDS is the VLES mode [34].

2.8.3. Heat release rate

FDS has several approaches for describing the pyrolysis of solids and liquids. The simplest way to describe a fire is by modelling the HRR as an ejection of gaseous fuel from a vent (or any solid

surface). The rectangular geometry of the vent is defined as the fire source area. The HRR is specified by defining the HRRPUA to the same vent (eq. 2.6) [34].

2.8.4. Air Supply

FDS allows the user to create simple vents, fans and heaters, or more advanced HVAC systems (heating, ventilating, and air-cooling systems). The air supply points of a pressurization system can be designed as one or several vents blowing air into a compartment from desired locations. Air is the default gas species to be supplied with this feature, but any other gas species can be specified as the supply gas, for example, soot, CO, CO_2, fire products, etc. An exhaust system can be designed as vents extracting any gas species, which is smoke in a fire situation.

The temperature of the supplied gas species can also be regulated (for example implementation of hot air for HVAC systems). If nothing is specified, gas species is supplied to the computational domain with the same temperature as the ambient conditions.

A blower or an extractor can be designed as a simple fan by assigning a volumetric flow value of a gas species to a vent. A negative flow supplies the specified gas species into the computational domain, and a positive flow extracts out any gas species from the computational domain [34].

2.8.5. Reaction

The reaction, or fuel properties for combustion, must be defined in the FDS input file to run a simulation. The reaction reflects the characteristics of the combustible material involved in the fire. The gas-phase combustion should not be mixed with the solid-phase pyrolysis. The pyrolysis step refers to the generation of fuel vapour at a solid or liquid surface, and the combustion step refers to the reaction of fuel vapour and oxygen [34].

FDS supports two reaction models: the mixing-controlled combustion model and the finite-rate combustion model. A real fire consists of several reactions. Such scenarios have a high computational cost because of the need to solve the transport equations for several gaseous fuels. The default reaction model of FDS is the mixing-controlled combustion model where just one reaction is defined. The finite-rate combustion model allows the user to specify several reactions, using an Arrhenius model. This usually requires a very fine grid resolution which is not practical for large-scale scenarios. It is recommended to use the finite-rate combustion model with the DNS turbulence mode activated. The finite-rate combustion model can also be used with the LES turbulence mode activated, but with caution. In a large-scale calculation performed with the LES turbulence mode and with a coarser grid resolution, the temperatures are averaged across the larger cells, which must be accounted for in the reaction calculations.

The mixing-controlled combustion model has two under-categories: the simple-chemistry combustion model and the complex-stoichiometry combustion model. The simple-chemistry combustion model is used for a single mixing-controlled reaction containing C, O, N and H atoms (carbon, oxygen, nitrogen and hydrogen respectively). The complex-stoichiometry combustion

model is used for other situations, where the reaction stoichiometry is described in greater detail by specifying the gas species or species mixtures along with the stoichiometry of the reaction [34].

The simple-chemistry combustion model is the simplest reaction model. The reaction is considered as a Lumped Species Approach, where various gas species are lumped into reacting groups referred to as lumped species. The following simplified reaction is considered:

$$Fuel + Air \rightarrow Products \tag{2.26}$$

The lumped species approach consists of three reacting groups: air, fuel and products. The byproducts of the lumped species are defined by mass fractions. Air is the default background species consisting of O_2, N_2, CO_2 and H_2O (water vapour). The default values of air in FDS are:

- The ambient mass fraction of O_2: 0.232378.
- The ambient mass fraction of CO_2: 0.000595.
- Relative humidity of the background air species: 40 %.

The fuel is assumed to consist of C, O, N and H atoms (basic fuel chemistry), that reacts with O_2 in one mixing-controlled step to form the products consisting of CO_2, H_2O, CO and soot. The remaining N_2, CO_2 and H_2O from the air transfers to the products. FDS calculates the reaction as:

$$C_x H_y O_z N_v + \upsilon_{O_2} O_2 \rightarrow \upsilon_{CO_2} CO_2 + \upsilon_{H_2O} H_2O + \upsilon_{CO} CO + \upsilon_S Soot + \upsilon_{N_2} N_2 \tag{2.27}$$

Mind that the remaining byproducts from the air are not included in this equation [34]. The basic fuel chemistry (C, H, O and N) and the yields of CO and soot must be defined in the FDS input file. The simple-chemistry approach treats soot as a composition of C and H. The default value for the fraction of H atoms in soot is 0,1. FDS uses this input information to calculate the stoichiometric coefficients as follows:

$$\upsilon_{O_2} = \upsilon_{CO_2} + \frac{\upsilon_{CO}}{2} + \frac{\upsilon_{H_2O}}{2} - \frac{z}{2} \tag{2.28}$$

$$\upsilon_{CO_2} = x - \upsilon_{CO} - (1 - X_H)\,\upsilon_S \tag{2.29}$$

$$\upsilon_{H_2O} = \frac{y}{2} - \frac{X_H}{2}\upsilon_S \tag{2.30}$$

$$\upsilon_{CO} = \frac{W_F}{W_{CO}}\gamma_{CO} \tag{2.31}$$

$$\upsilon_S = \frac{W_F}{W_S}\gamma_S \tag{2.32}$$

$$\upsilon_{N_2} = \frac{v}{2} \tag{2.33}$$

$$W_S = X_H W_H + (1 - X_H) W_C \tag{2.34}$$

Information about the ΔH_c must be specified in the FDS input file, if not then this value is computed automatically by FDS. This calculator step is excluded if this value is known and defined in the FDS input file. The ΔH_c (Heat of Combustion per unit mass of consumed fuel) and the HRR controls the $\dot{m}_f$ (fuel mass loss rate), as stated in eq. 2.5 [34].

2.8.6. Materials and Surfaces

The boundaries of the model have an impact on the fire scenario. The term "boundaries" refers to the obstructions (solid surfaces) within the model (walls, floors, ceilings, openings, etc.) and the mesh borders designed as solid surfaces. These solid surfaces control the airflow and smoke movement within the model. These flows only pass through openings (gaps, cracks, vents, HVAC nodes, etc.). Ventilation openings (openings to the outside) allows these flows to escape the domain [34].

The heat exchange through a solid surface is controlled by defining the material properties. As default, FDS assumes all solids (objects and mesh boundaries) to be inert. A surface defined as inert has the surface fixed at ambient temperature with heat transfer by convection and radiation from the gas to the solid. The opposite of this is to define the surfaces as adiabatic. An adiabatic surface does not allow any heat transfer through the surface, no net heat transfer (radiative and convective) occurs from the gas to the solid. All heat stays in the compartment and contributes to the heat development. Flows exiting the compartment is expected to have a higher temperature if the compartment is adiabatic compared to inert. Mesh boundaries defined as "open" allows ambient conditions outside the computational domain to interfere with the model. Fire plumes should be positioned with some distance from the "open" boundary, to avoid any unrealistic interference on the fire [34].

2.8.7. Output data

The information which is of interest to be extracted from the FDS simulation must be specified in the FDS input file. These are for example devices which records the time history of various parameters, like temperatures, visibility, pressure, heat flux, Fractional Effective Doses, and more. Densities, volume fractions and mass fractions of various gas species can also be recorded. These devices are located by the user at desired locations. The time history of each device is recorded in a comma-delimited ASCII file.

The result data can be visualized with Smokeview. Slice-files or boundary-files of various parameters (like those mentioned above) must also be specified in the FDS input file on desired locations.

3. Methods

The impact of a smoke control system on various HRRs is investigated with the airflow criterion of a pressurization system. Simulations are conducted with FDS (Fire Dynamics Simulator). Six model geometries are used to perform the analysis. Four of the models consist of two compartments connected with an opening. Two models have a lobby compartment between the two same main compartments. Air supply points generate air in the pressurized compartment, and a fire is generated in the fire room compartment. A flow of air is created in the opening between the compartments towards the fire room compartment, which restricts the spread of smoke in the opposite direction. The product density is analysed in each compartment and compared to each scenario due to various generated airflows contra various HRRs.

3.1. Simulations

A description of the conducted simulations and the assessment of the layouts are provided in this section. A total of 74 simulations has been conducted.

3.1.1. Simulation code

There are several CFD codes available with an aspect to fire science. FDS is a CFD code for fire-driven fluid flows designed for fire applications. The simulations are performed with FDS version 6.7.1, released 5th of February 2019, which was the latest version available by the beginning of this study.

The simulations are conducted with default properties of FDS, unless other is specified.

Pyrosim, developed by Thunderhead Engineering [39], is a third-party application which allows the FDS user to develop the FDS input file through a graphical interface. The model geometry is built through a 2D or a 3D view and then generated to an FDS input file. The location of the fire and other elements, like devices, is easily specified. Reactions and material properties are specified through a table interface. An FDS input file can consist of hundreds of lines, due to complicated geometries, many objects and several floors. The location of devices can be hard to specify correctly in a complicated geometry. The design process of the FDS input file is speeded up by using Pyrosim, which generates the FDS input file.

Pyrosim version 2019.2.1002 is only used to generate the FDS input file for the different model geometries, which are described later in this section. The simulations where the fire and the air supply parameters are altered are created by directly modifying the parameter values in the copied FDS input files.

3.1.2. Parameters to consider for the FDS simulation

There are many parameters which can affect a fire scenario and a pressurization system. Some of them have a greater impact than others, depending on the situation. Parameters relevant to consider for an FDS simulation with an aspect to the fire scenario and the pressurization system are summarized in Table 3.1 and Table 3.2 respectively.

The scenario outcome of the fire room compartment is bound by the fire and the boundaries of the compartment. The pressurized compartment is affected by the air supply system and the boundaries of the compartment.

Only the HRR and the air supply is altered in the simulations for each model geometry. The remaining parameters are kept constant to limit the number of simulation scenarios. Details on the further parameters are given in the remaining parts of chapter 3.1.

Table 3.1 – Parameters which can affect the scenario relevant to the fire room compartment.

The fire	Presence of fuel and oxygen	Fuel-controlled fire
		Ventilation-controlled fire
	Heat Release Rate, HRR	Fuel load
		Heat Release Rate Per Unit Area, HRRPUA
		Fire source area, A_f
		Growth rate, α
	The fire location	Distance to adjacent compartments
		Distance to openings
		Distance to fuel
The boundaries	Volume of the compartment	Floor area
		Room height
	Objects	Objects within the compartment
		Other rooms and its openings
	Ventilation factor	Number of ventilation openings (example: windows and vents)
		Size of each ventilation opening
		Location of the ventilation opening
		State of ventilation opening (open, closed or variating)
	Openings to adjacent compartments	State of the adjacent compartment – Non-pressurized – Pressurized – Depressurized
		Size of openings
		Location of openings
		State of opening (open, closed or variating)
	Construction materials	– Density – Specific Heat – Conductivity

Table 3.2 – Parameters which can affect the scenario relevant to the pressurized compartment.

The pressurization system	Air supply rate into the compartment	Number of air supply points
		Location of air supply points
		Total air supply rate into the compartment
	Relief vents	Size
		Location
	Lobby / no lobby	Lobby compartment between the fire room compartment and the pressurized compartment
		Other adjoining unpressurized compartments
	Leaks	Openings, gaps and cracks
The boundaries	Volume of the compartment	Height
		Floor area
	Objects within the compartment	Other rooms and its openings
		Objects
		Stairs
	Ventilation factor	Number of ventilation openings (example: windows and vents)
		Size of each ventilation opening
		Location of the ventilation opening
		State of ventilation opening (open, closed or variating)
	Openings to adjacent compartments	State of the adjacent compartment – Non-pressurized – Pressurized – Depressurized
		Size of openings
		Location of openings
		State of opening (open, closed or variating)
	Construction materials	– Density – Specific Heat – Conductivity

3.1.3. Heat release rate

HRRs up to 10000 kW are analysed in this study, contra various levels of generated airflows. Two models are constructed in FDS regarding the fire room compartment geometry. The difference is the size of the fire room compartment, larger fires require a larger fire source area and a larger opening area to the outside. The smaller compartment hosts fire scenarios up to 2000 kW. The bigger compartment hosts fire scenarios up to 10000 kW. The fire room compartments are well ventilated (large openings) to sustain stable and fuel-controlled conditions for the largest HRR. The HRRs are constant (not time-evolving).

The HRR is a function of the fire source area (A_f) and the HRRPUA (eq. 2.6). The $\dot{Q}^*$ parameter is adjusted to be maximum 2 (a value suited for most large fires [27]). In FDS, the fire source area is defined with a rectangular shape. The fire source diameter (D) is found by adopting a value of $\dot{Q}^*$ to eq. 2.13 along with the HRR. The circular fire source area (calculated upon the fire source

diameter) is converted to a square shape and adapted to the conducted FDS simulations. The side of the square can be adjusted with intervals of 0,1 meters (based on the mesh sensitivity analysis described in chapter 3.2). The HRRPUA ranges around the value 1000 kW/m^2. The HRRs and the related parameters used to conduct the simulations are presented in Table 3.3. The input values for $\dot{Q}^*$ are presented in chapter 2.6.

Table 3.3 – HRRs and details for the conducted simulations.

HRR [kW]	HRRPUA [kW/m^2]	Fire source area, A_f [m^2]	Side length [m]	Fire source diameter, D [m]	The nondimensional HRR, $\dot{Q}^*$ [-]
500,00	1020,49	0,49	0,70	0,79	0,82
1000,00	1000,00	1,00	1,00	1,13	0,67
1500,00	1041,67	1,44	1,20	1,35	0,64
2000,00	1020,49	1,96	1,40	1,58	0,58
2500,00	976,57	2,56	1,60	1,81	0,52
5000,00	1033,06	4,84	2,20	2,48	0,47
7500,00	1028,81	7,29	2,70	3,05	0,42
10000,00	976,57	10,24	3,20	3,61	0,37

3.1.4. Airflow

Simulations, where the air supply is altered, are conducted for each of the defined HRRs. The air supplied to the pressurized compartment generates a flow of air through openings. An airflow in the range of 0,5 to 3,0 m/s is necessary to steer the smoke in the desired direction. An airflow of minimum 0,7 m/s through an opening is necessary to prevent the spread of smoke in the opposite direction [40].

The volume flux (volume per second) of air supplied to a compartment by a pressurization system is assumed to equal the volume flux of air escaping the compartment at steady-state conditions. The considered models have one opening from the pressurized compartment, 0,80 m × 2,00 m (width × height). The airflow in terms of m/s is calculated by dividing the volume flux of air with the opening area.

Simulations, where the air supply is activated and deactivated, are conducted. For the cases where the air supply is activated, simulations of airflows in the range of 0,7 and 3,0 m/s are conducted. The air supply rates and the related parameters used in the conducted simulations are presented in Table 3.4.

The location and number of air supply points are important to consider. Generally, more uniform pressure distribution in the pressurized compartment can be achieved by increasing the number of supply points. It should be avoided to position them too close to one another since they can affect each other. It is reasonable to assume that a supply point should not be positioned in direct contact with a door. The pressure that a supply point exerts on a door can be high enough to prevent the doors opening and closing function (human force or a self-closing mechanism). The total pressure distribution in the compartment must be designed so that the pressure range is safeguarded, a single supply point can surpass these limits locally.

For each of the models, two air supply points are positioned in the pressurized compartment. The total volumetric supply is distributed equally on these two points, as presented in Table 3.4.

Table 3.4 – Airflows HRRs and details for the conducted simulations.

Air supply rate [m^3/s]	Air supply rate per vent [m^3/s]	Opening area [m^2]	Generated Airflow [m/s]
0,00	0,00	1,60	0,00
1,12	0,56	1,60	0,70
1,60	0,80	1,60	1,00
2,40	1,20	1,60	1,50
4,80	2,40	1,60	3,00

3.1.5. Model geometries

Six model geometries are used to perform the analysis. Three parameters are altered in each geometry: the fire source area, the HRRPUA and the volume flow from the air supply point. The centre-point of the fire source area is kept on the same coordinate in all instances.

The models are prefixed as A1, A2, B1, B2, C and D. Model A1 and Model A2 refers to a fire room compartment and an adjacent pressurized compartment. The difference between Model A1 and Model A2 is the size of the fire room compartment. Model B1 and Model B2 are the same as Model A1 and Model A2, the difference is that there is a lobby compartment between the fire room compartment and the adjacent pressurized compartment. Model C and Model D is the same as Model A1, besides that the fire room compartment is expanded for Model C, and the pressurized compartment is expanded for Model D.

Model A1

Model A1 consists of a fire room compartment and an adjacent pressurized compartment. Both compartments have a dimension of 4,80 m × 4,80 m × 2,40 m (width × length × height). The two compartments are connected with an opening of dimension 0,80 m × 2,00 m (width × height). The model has one ventilation opening (opening to the outside), to supply the fire with oxygen. The opening is located in the fire room compartment, the dimensions of the opening are 1,20 m × 2,00 m (width × height),

The dimensions of the compartment are based on the ISO 9705 room dimensions (2,40 m × 3,60 m × 2,40 m (width × length × height)) [41], where the width is expanded times 2,0 and the length is expanded times 1,5. The opening connecting the compartments equals to the opening of the ISO 9705 room (0,80 × 2,00 m (width × height)) [41]. The width of the ventilation opening is expanded times 1,5 (the height is unchanged).

The fire is represented by a red-coloured vent located in the centre of the fire room compartment. The borders of the largest fire source (2000 kW) are positioned with some distance from the walls and openings to avoid any affections. The vent is located 0,4 meters above the floor, positioned on an obstruction (which is as large as the vent), to avoid any affection from the floor.

The two air supply points are represented by green-coloured vents located in the pressurized compartment. Two vents are chosen, to achieve symmetrical conditions and uniform pressure distribution. The vents are positioned behind walls to avoid interference with one another and to avoid a direct air supply exertion on the opening to the fire room compartment. The vents are located mid-height to achieve less interference on the airflow, from the ceiling or the floor.

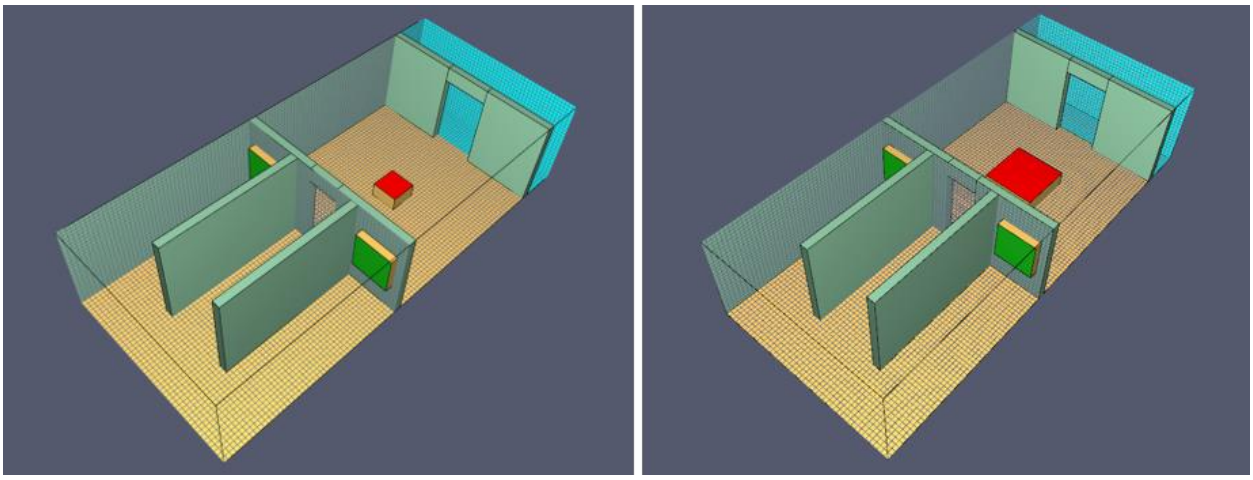

Figure 3.1 – Model A1 geometry. 500 kW HRR to the left, 2000 kW HRR to the right. Images extracted from the Pyrosim model.

Model A2

Model A2 is similar to Model A1, where the difference is the size of the fire room compartment and the number of ventilation openings from the fire room compartment. The width and length are expanded times 1,5 compared to Model A1, the dimensions are 7,20 m × 7,20 m × 2,40 m (width × length × height). The number of openings is increased from one to four with the same dimensions per opening, 1,20 m × 2,00 m (width × height).

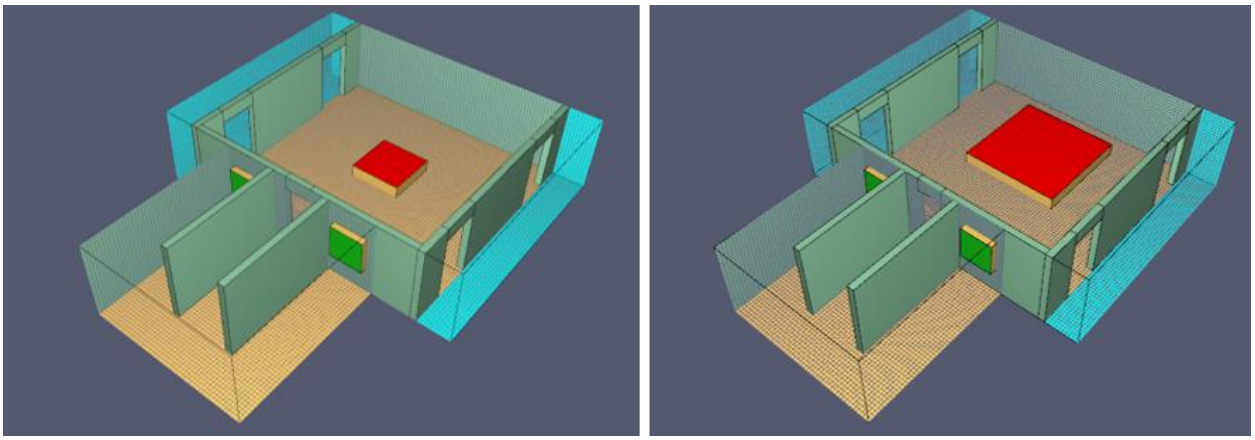

Figure 3.2 – Model A2 geometry. 2500 kW HRR to the left, 10000 kW HRR to the right. Images extracted from the Pyrosim model.

Model B1

Model B1 is similar to Model A1, where the difference is that there is a lobby compartment between the fire room compartment and the pressurized compartment. There is one opening between the lobby compartment and the fire room compartment, and one opening of equal size between the lobby compartment and the pressurized compartment.

The dimensions of the lobby compartment are 2,00 m × 3,00 m × 2,40 m (width × length × height), and the dimensions of the other compartments are unchanged. The dimensions of the openings connecting the compartments are 0,80 m × 2,00 m (width × height).

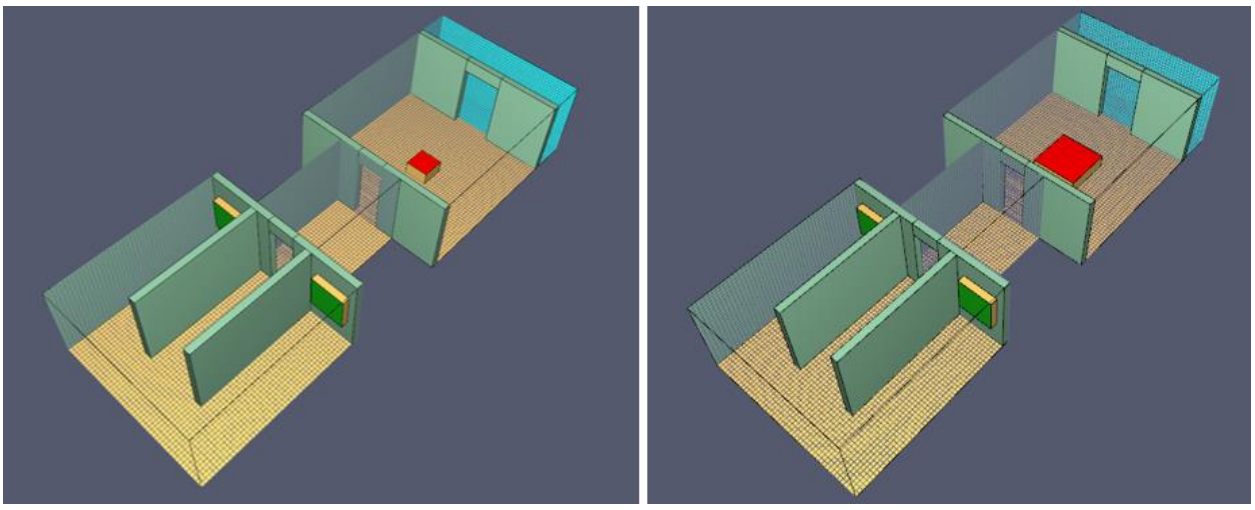

Figure 3.3 – Model B1 geometry. 500 kW HRR to the left, 2000 kW HRR to the right. Images extracted from the Pyrosim model.

Model B2

Model B2 is similar to Model A2, where the difference is that there is a lobby compartment between the fire room compartment and the pressurized compartment. There is one opening between the lobby compartment and the fire room compartment, and one opening of equal size between the lobby compartment and the pressurized compartment.

The dimensions of the lobby compartment are the same as for Model B1, and the dimensions of the other compartments are unchanged. The dimensions of the openings connecting the compartments are the same as for Model B1.

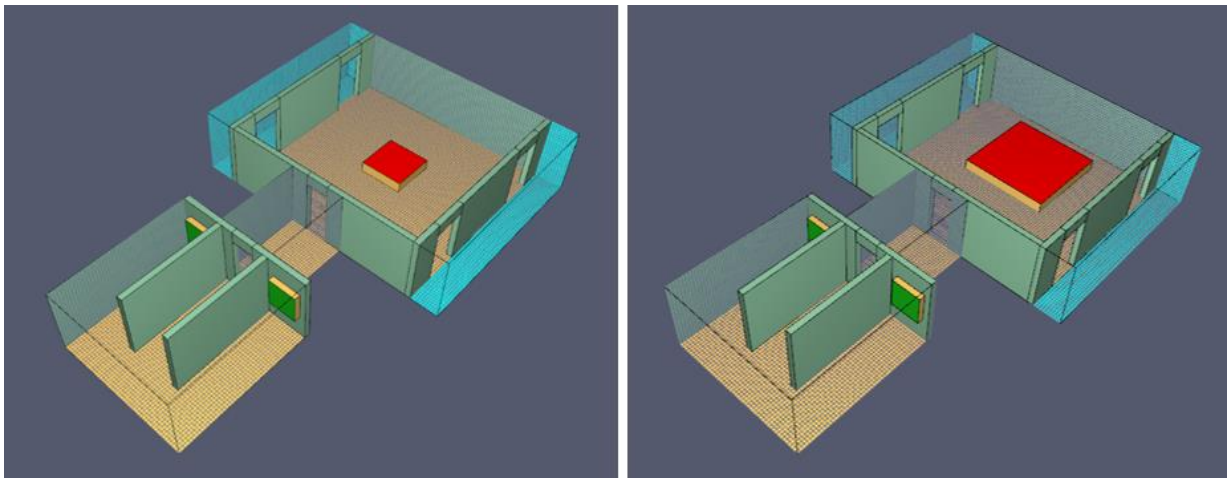

Figure 3.4 – Model B2 geometry. 2500 kW HRR to the left, 10000 kW HRR to the right. Images extracted from the Pyrosim model.

Model C

Model C is similar to Model A1. The difference is that the fire room compartment is expanded 2,25 times, the width and length are expanded 1,5 times each. No other vents or openings are added.

Model C is also similar to Model A2. The difference is the number of ventilation openings, which is decreased from four to one.

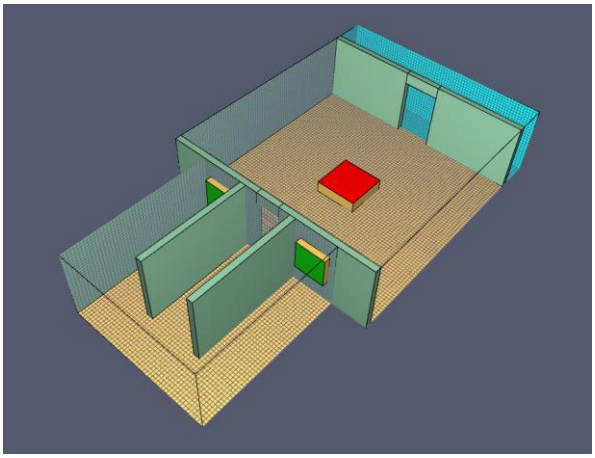

Figure 3.5 – Model C geometry. 2000 kW HRR. Image extracted from the Pyrosim model.

Model D

Model D is similar to Model A1. The difference is that the pressurized compartment is expanded 2,25 times, the width and length are expanded 1,5 times each. No other vents or openings are added.

Model D is also similar to Model C. The difference is that the size of the two compartments is reversed. The fire room compartment of Model D has the same dimensions as the pressurized compartment of Model C. The pressurized compartment of Model D has the same dimensions as the fire room compartment of Model C.

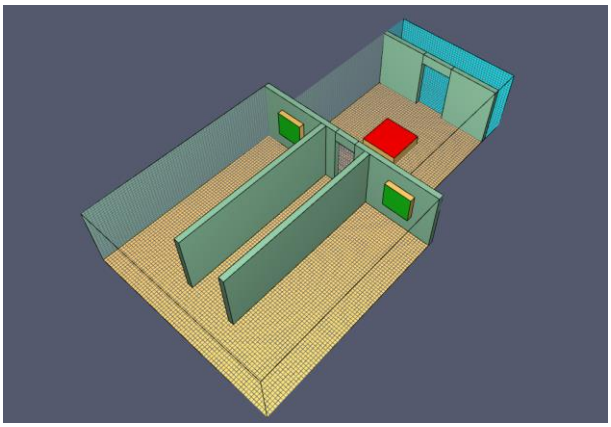

Figure 3.6 – Model D geometry. 2000 kW HRR. Image extracted from the Pyrosim model.

3.1.6. Measurements

FDS calculates the development of flows in each cell over time. The average value across these cells plotted over time can be extracted by specifying a volume bound by several cells.

The product density development is analysed in each compartment due to various air supply rates contra various HRRs. The specified volume where the quantity is recorded is defined as the whole volume of a compartment. The product density development is recorded in each compartment of each model.

3.1.7. Boundaries

The walls, roofs and ceilings of the model are designed as 60-minute fire-resistant constructions (EI 60 classification according to European standards) to ensure realistic fire scenarios.

The walls are designed as a 172 mm five-layered structure as illustrated in Figure 3.7. The floors and ceilings are designed as a 200 mm four-layered structure, as illustrated in Figure 3.8. The stands are neglected in both cases.

The layer structure must be defined in a certain order in FDS. The surface towards the compartment must be ranged as number one. Two surface properties are defined for the floor and ceiling structure, and one for the wall structure. The FDS input values regarding layering order and layer

thickness are presented in Table 3.5, Table 3.6 and Table 3.7. The density, specific heat and conductivity are specified for each material, presented in Table 3.8.

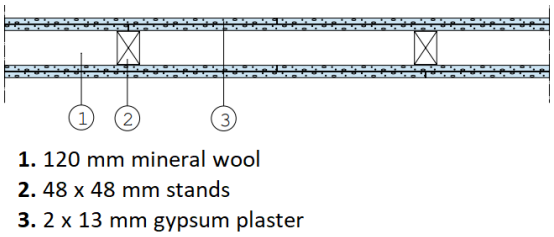

Figure 3.7 – An EI 60 wall structure. Image extracted and modified from [42].

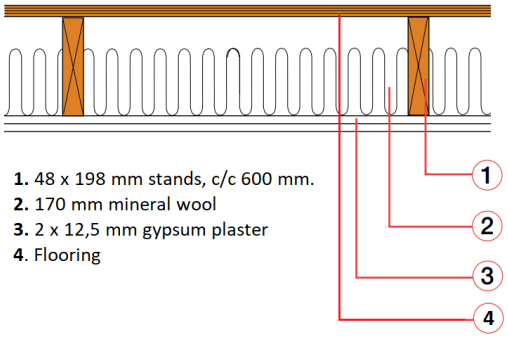

Figure 3.8 – An EI 60 structure between two floors. Image extracted and modified from [43].

Table 3.5 – Wall layers used as input for the FDS calculations, based on [42].

Layer No.	Material	Thickness, d [m]
1	Gypsum plaster	0,013
2	Gypsum plaster	0,013
3	Mineral wool, plates	0,12
4	Gypsum plaster	0,013
5	Gypsum plaster	0,013

Table 3.6 – Floor layers used as input for the FDS calculations, based on [43].

Layer No.	Material	Thickness, d [m]
1	Yellow Pine	0,005
2	Mineral wool, plates	0,17
3	Gypsum plaster	0,0125
4	Gypsum plaster	0,0125

Table 3.7 – Ceiling layers used as input for the FDS calculations, based on [43].

Layer No.	Material	Thickness, d [m]
1	Gypsum plaster	0,0125
2	Gypsum plaster	0,0125
3	Mineral wool, plates	0,17
4	Yellow Pine	0,005

Table 3.8 – Material properties for the layers within the wall, floor and ceiling constructions used as input for the FDS calculations. Data collected from [24] and [44].

Material	Density, ρ [kg/m^3]	Specific Heat, c_p [J/(g × K)]	Conductivity, k [W/(m × K)]
Gypsum plaster	1440,00	0,84	0,48
Mineral wool, plates	100,00	0,80	0,041
Yellow Pine	640,00	2,85	0,14

3.1.8. Fuel properties

The reaction is defined with the simple-chemistry combustion model. The fuel properties are designed as a constant parameter, by the recommendations specified in the Swedish Fire Safety Code BFS 2013:12 BBRAD 3 [45]. The code specifies fuel properties for a severe apartment fire scenario, the data are presented in Table 3.9.

Table 3.9 – Fuel properties for a severe apartment fire scenario. Data collected from [45].

Unit	Value
ΔH_c [MJ/kg]	20,00
Soot yield [g/g]	0,10
CO yield [g/g]	0,10

A fire source regularly consists of woods and plastics in a typical apartment fire. The ΔH_c (Heat of Combustion per unit mass of consumed fuel) for wood and plastics are (typically) respectively 17,5 MJ/kg and 30 MJ/kg [25]. The fuel with a ΔH_c of 20,0 MJ/kg is (based on these values) assessed to consist of about 80 % wood and 20 % plastics. An example of the stochiometric properties for C, H, O and N is presented in Table 3.10. These values reflect a ΔH_c of 19,8 MJ/kg, which is assessed to be an acceptable value regarding the ΔH_c of 20,0 MJ/kg [46]. The values presented in Table 3.9 and Table 3.10 are used as input values in the FDS calculations.

Table 3.10 – Stochiometric values for a ΔH_c of 19,8 MJ/kg. Data collected from [46].

Atom	Value [mol]
C	4,56
H	6,56
O	2,34
N	0,40

3.1.9. Simulation series

The conducted simulations for each model are summarized in the following tables. A total of 74 simulations has been conducted. The FDS input files are presented in Appendix B.1. FDS input files.

Model A1 and Model A2 consist of two compartments each. Four HRRs are simulated for each model geometry. For each of the HRRs, five air supplies are simulated. A total of 20 simulations are conducted for each of the model geometries.

Model A1, Model A2, Model C and Model D are simulated locally with two MPI processes and one OpenMP thread. Model B1 and Model B2 are simulated locally with three MPI processes and one OpenMP thread.

Table 3.11 – Conducted simulation for Model A1.

Simulation No.	HRR [kW]	Air Supply [m^3/s]	Simulation No.	HRR [kW]	Air Supply [m^3/s]
1	500,00	0,00	11	1500,00	0,00
2	500,00	1,12	12	1500,00	1,12
3	500,00	1,60	13	1500,00	1,60
4	500,00	2,40	14	1500,00	2,40
5	500,00	4,80	15	1500,00	4,80
6	1000,00	0,00	16	2000,00	0,00
7	1000,00	1,12	17	2000,00	1,12
8	1000,00	1,60	18	2000,00	1,60
9	1000,00	2,40	19	2000,00	2,40
10	1000,00	4,80	20	2000,00	4,80

Table 3.12 – Conducted simulation for Model A2.

Simulation No.	HRR [kW]	Air Supply [m^3/s]	Simulation No.	HRR [kW]	Air Supply [m^3/s]
21	2500,00	0,00	31	7500,00	0,00
22	2500,00	1,12	32	7500,00	1,12
23	2500,00	1,60	33	7500,00	1,60
24	2500,00	2,40	34	7500,00	2,40
25	2500,00	4,80	35	7500,00	4,80
26	5000,00	0,00	36	10000,00	0,00
27	5000,00	1,12	37	10000,00	1,12
28	5000,00	1,60	38	10000,00	1,60
29	5000,00	2,40	39	10000,00	2,40
30	5000,00	4,80	40	10000,00	4,80

Model B1 and Model B2 consist of three compartments each. Four HRRs are simulated for each model geometry. For each of the HRRs, three air supplies are simulated. A total of 12 simulations are conducted for each of the model geometries.

Table 3.13 – Conducted simulation for Model B1.

Simulation No.	HRR [kW]	Air Supply [m^3/s]	Simulation No.	HRR [kW]	Air Supply [m^3/s]
41	500,00	0,00	47	1500,00	0,00
42	500,00	1,12	48	1500,00	1,12
43	500,00	2,40	49	1500,00	2,40
44	1000,00	0,00	50	2000,00	0,00
45	1000,00	1,12	51	2000,00	1,12
46	1000,00	2,40	52	2000,00	2,40

Table 3.14 – Conducted simulation for Model B2.

Simulation No.	HRR [kW]	Air Supply [m^3/s]	Simulation No.	HRR [kW]	Air Supply [m^3/s]
53	2500,00	0,00	59	7500,00	0,00
54	2500,00	1,12	60	7500,00	1,12
55	2500,00	2,40	61	7500,00	2,40
56	5000,00	0,00	62	10000,00	0,00
57	5000,00	1,12	63	10000,00	1,12
58	5000,00	2,40	64	10000,00	2,40

Model C and Model D consist of two compartments each. One HRR is simulated. Five air supplies are simulated. A total of five simulations are conducted for each of the model geometries.

Table 3.15 – Conducted simulation for Model C.

Simulation No.	HRR [kW]	Air Supply [m^3/s]	Simulation No.	HRR [kW]	Air Supply [m^3/s]
65	2000,00	0,00	68	2000,00	2,40
66	2000,00	1,12	69	2000,00	4,80
67	2000,00	1,60			

Table 3.16 – Conducted simulation for Model D.

Simulation No.	HRR [kW]	Air Supply [m^3/s]	Simulation No.	HRR [kW]	Air Supply [m^3/s]
70	2000,00	0,00	73	2000,00	2,40
71	2000,00	1,12	74	2000,00	4,80
72	2000,00	1,60			

3.2. Mesh Sensitivity Analysis

A mesh sensitivity analysis is performed for each model geometry to verify a correct mesh resolution. A coarse mesh resolution is chosen at the start. The same simulation is performed repeatedly with a finer mesh resolution, until the simulation of the finest mesh resolution returns the same results as for the second-finest mesh resolution, with low deviations.

In a mesh sensitivity analysis, the smallest value of planed HRRs must be used. The HRR is directly connected to the characteristic fire source diameter, D^*, and smaller HHRs results in smaller D^*. As described in chapter 2.8.1, smaller values of D^* demand a finer mesh resolution. A mesh resolution adapted to a certain HRR is generally sufficient for larger HRRs, given that there are no other changes.

The HRR and the air supply must be considered in the mesh sensitivity analysis since this study involves direct flows generated by a fire and air supply points. Smaller values for flows require more detailed calculations, therefore the smallest air supply value must also be considered (besides having the air supply deactivated).

The air supply is deactivated in some simulations. These simulations are less complex, regarding calculations, than those with the air supply activated, since they only generate flows from a fire. Scenarios with the HRR and the air supply activated is therefore considered in this mesh sensitivity analysis. It is assumed that a proper mesh resolution for a scenario with the HRR and the air supply activated is sufficient for the same scenario but with the air supply deactivated.

As a conclusion, the smallest value of HRR and air supply is used for each model in the mesh sensitivity analyses. The lowest values for each model are listed in Table 3.17. The input values for D^* are presented in chapter 2.8.1.

Table 3.17 – Summarized input values for the mesh sensitivity analyses.

Model	HRR [kW]	D^* [m]	Air Supply [m^3/s]
A1	500,00	0,73	1,12
A2	2500,00	1,39	1,12
B1	500,00	0,73	1,12
B2	2500,00	1,39	1,12
C	2000,00	1,27	1,12
D	2000,00	1,27	1,12

3.2.1. Model A1

Model A1 consists of two meshes where Mesh 1 is the pressurized compartment and Mesh 2 is the fire room compartment and the outside volume. Three grid resolutions are analysed in this mesh sensitivity analysis. The smallest HRR and air supply are used as input values, 500 kW (D^* = 0,73 m) and 1,12 m^3/s respectively. No smaller HRRs or air supply rates are used for this model, besides for those with the air supply deactivated.

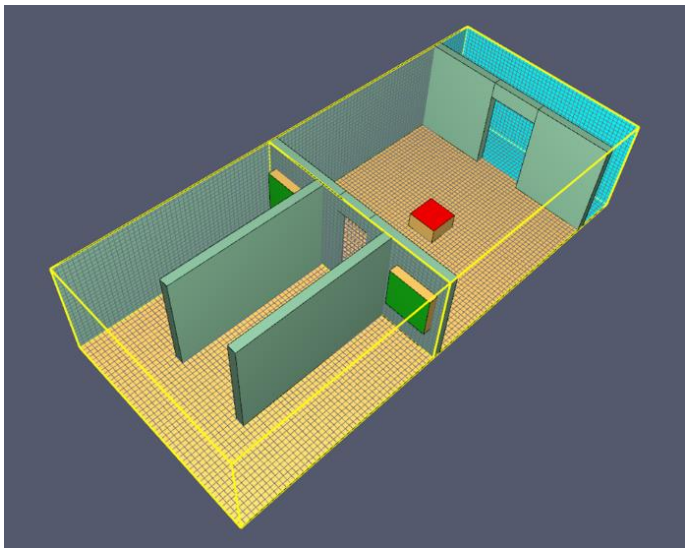

Figure 3.9. Model A1. The two meshes are separated with yellow outlines. Image extracted from the Pyrosim model.

Table 3.18 – Mesh resolutions for the mesh sensitivity analysis of Model A1.

Mesh resolution, cell size, δx [m]	$D^*/\delta x$ [-]	Number of cells		Total number of cells
		Mesh 1	Mesh 2	
0,20	3,65	6 912	8 928	15 840
0,10	7,29	55 296	71 424	126 720
0,075	9,72	131 072	167 936	299 008

The development of the product density in the fire room compartment and the pressurized compartment are analysed and compared for the mesh resolutions. The results are presented in Figure 3.10. Steady-state conditions (stabilized values) are achieved in the timeframe of 360 to 600 seconds. The average values during this timeframe are listed in Table 3.19. The average difference in percentage between the grid resolutions is listed in Table 3.20. For the two finest mesh resolutions the difference for the fire room compartment is 1,85 %, and the difference for the pressurized compartment is 7,66 %. The difference for the pressurized compartment is considered as high, but the graphed results of the product density development match very well for the two finest resolutions during the whole timeframe (0 to 600 seconds). The conclusion of this is that a mesh resolution δx=0,1 is sufficient for Model A1. $D^*/\delta x$ values for the Model A1 simulations are listed in Table 3.21.

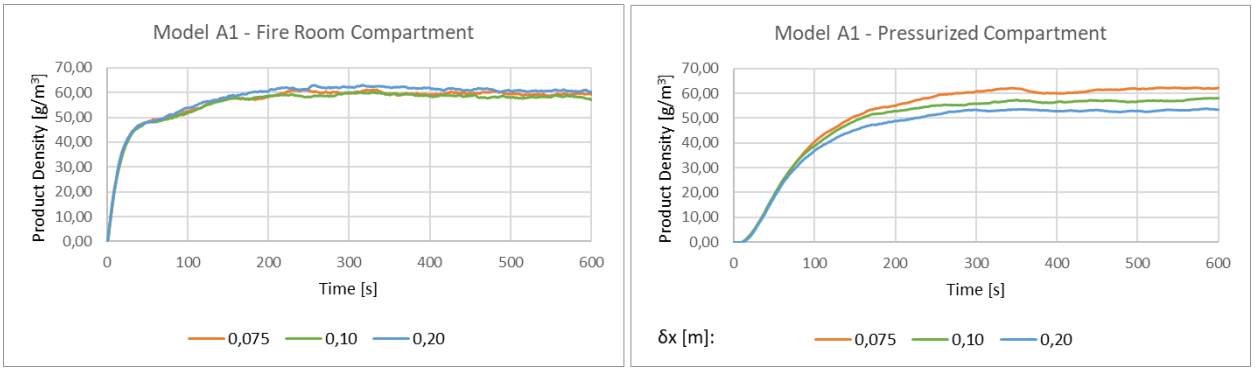

Figure 3.10 – Mesh sensitivity analysis results, Model A1.

Table 3.19 – Mesh sensitivity analysis, Model A1. Average product density during steady-state conditions.

Compartment	Average product density during steady-state conditions [g/m^3]		
	δx = 0,20 m	δx = 0,10 m	δx = 0,075 m
Fire Room Compartment	61,24	58,50	59,58
Pressurized Compartment	53,07	56,93	61,29

Table 3.20 – Mesh sensitivity analysis, Model A1. Mesh resolution comparison.

Compartment	Average product density difference between mesh resolutions [%]	
	δx = 0,20 m VS. δx = 0,10 m	δx = 0,10 m VS. δx = 0,075 m
Fire Room Compartment	4,68	1,85
Pressurized Compartment	7,27	7,66

Table 3.21 – Mesh sensitivity analysis, Model A1. $D^*/\delta x$ values.

HRR [kW]	D^* [m]	δx [m]	$D^*/\delta x$ [-]
500,00	0,73	0,10	7,29
1000,00	0,96	0,10	9,62
1500,00	1,13	0,10	11,32
2000,00	1,27	0,10	12,70

3.2.2. Model A2

Model A2 consists of two meshes where Mesh 1 is the pressurized compartment and Mesh 2 is the fire room compartment and the outside volume. Three grid resolutions are analysed in this mesh sensitivity analysis. The smallest HRR and air supply are used as input values, 2500 kW (D^* = 1,38 m) and 1,12 m^3/s respectively. No smaller HRRs or air supply rates are used for this model, besides for those with the air supply deactivated.

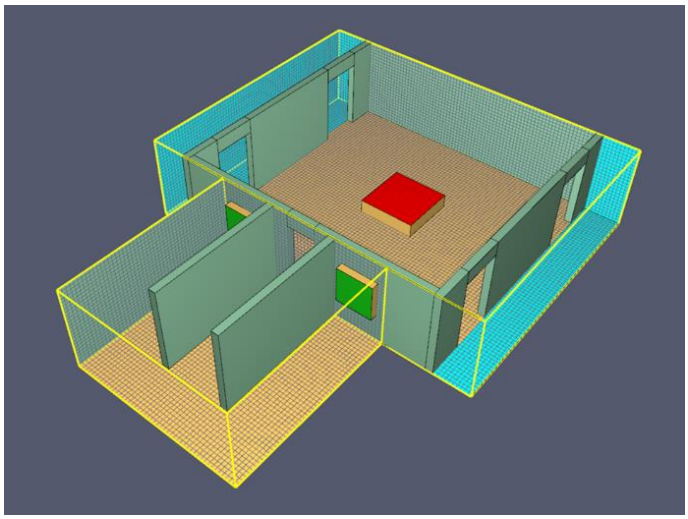

Figure 3.11. Model A2. The two meshes are separated with yellow outlines. Image extracted from the Pyrosim model.

Table 3.22 – Mesh resolutions for the mesh sensitivity analysis of Model A2.

Mesh resolution, cell size, δx [m]	$D^*/\delta x$ [-]	Number of cells		Total number of cells
		Mesh 1	Mesh 2	
0,20	6,94	6 912	21 312	28 224
0,10	13,88	55 296	170 496	225 792
0,075	18,51	131 072	395 136	526 208

The development of the product density in the fire room compartment and the pressurized compartment are analysed and compared for the mesh resolutions. The results are presented in Figure 3.12. Steady-state conditions (stabilized values) are achieved in the timeframe of 360 to 600 seconds. The average values during this timeframe are listed in Table 3.23. The average difference in percentage between the grid resolutions is listed in Table 3.24. For the two finest mesh resolutions the difference for the fire room compartment is 0,83 %, and the difference for the pressurized compartment is 6,06 %. The difference for the pressurized compartment is considered as high, but the graphed results of the product density development match very well for the two finest resolutions during the whole timeframe (0 to 600 seconds). The conclusion of this is that a mesh resolution δx=0,1 is sufficient for Model A2. $D^*/\delta x$ values for the Model A2 simulations are listed in Table 3.25.

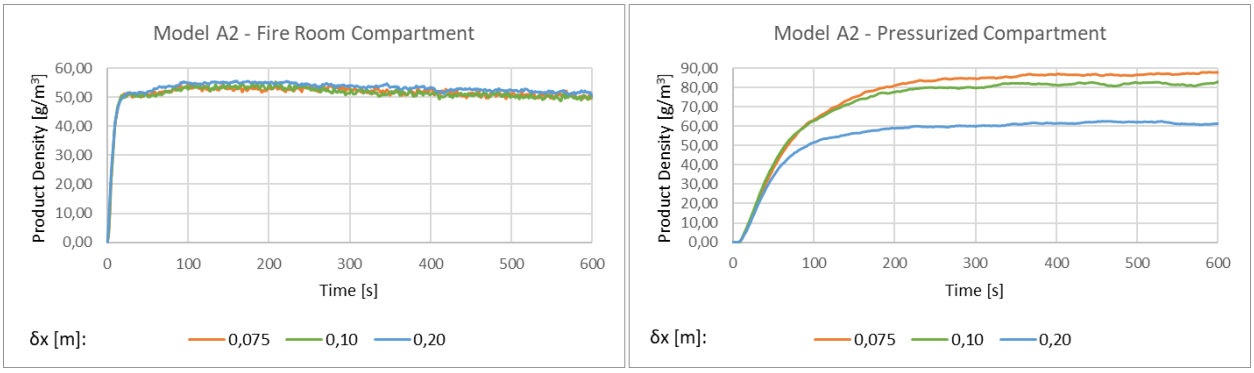

Figure 3.12 – Mesh sensitivity analysis results, Model A2.

Table 3.23 – Mesh sensitivity analysis, Model A2. Average product density during steady-state conditions.

Compartment	Average product density during steady-state conditions [g/m^3]		
	δx = 0,20 m	δx = 0,10 m	δx = 0,075 m
Fire Room Compartment	52,38	50,51	50,93
Pressurized Compartment	61,91	81,65	86,60

Table 3.24 – Mesh sensitivity analysis, Model A2. Mesh resolution comparison.

Compartment	Average product density difference between mesh resolutions [%]	
	δx = 0,20 m VS. δx = 0,10 m	δx = 0,10 m VS. δx = 0,075 m
Fire Room Compartment	3,70	0,83
Pressurized Compartment	31,88	6,06

Table 3.25 – Mesh sensitivity analysis, Model A2. $D^*/\delta x$ values.

HRR [kW]	D^* [m]	δx [m]	$D^*/\delta x$ [-]
2500,00	1,39	0,10	13,88
5000,00	1,83	0,10	18,32
7500,00	2,15	0,10	21,54
10000,00	2,42	0,10	24,17

3.2.3. Model B1

Model B1 consists of three meshes where Mesh 1 is the pressurized compartment, Mesh 2 is the fire room compartment and the outside volume, and Mesh 3 is the lobby compartment. Three grid resolutions are analysed in this mesh sensitivity analysis. The smallest HRR and air supply are used as input values, 500 kW (D^* = 0,73 m) and 1,12 m^3/s respectively. No smaller HRRs or air supply rates are used for this model, besides for those with the air supply deactivated.

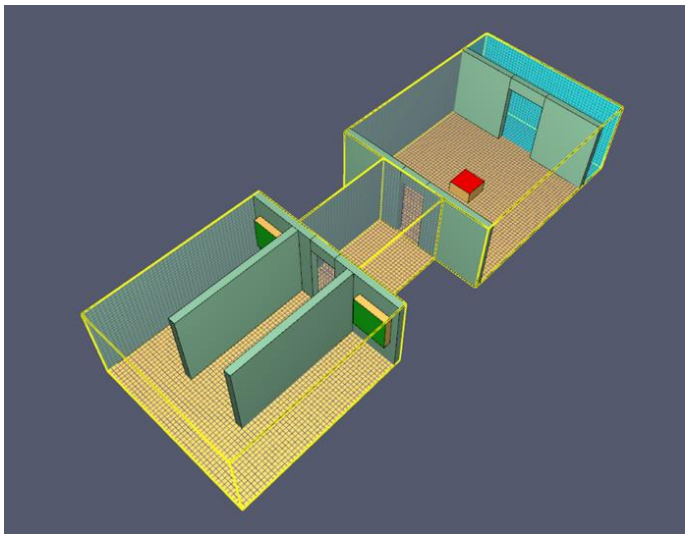

Figure 3.13. Model B1. The three meshes are separated with yellow outlines. Image extracted from the Pyrosim model.

Table 3.26 – Mesh resolutions for the mesh sensitivity analysis of Model B1.

Mesh resolution, cell size, δx [m]	$D^*/\delta x$ [-]	Number of cells			Total number of cells
		Mesh 1	Mesh 2	Mesh 3	
0,20	3,65	7 200	8 928	1 800	17 928
0,10	7,29	57 600	71 424	14 400	143 424
0,075	9,72	137 216	167 936	34 560	339 712

The development of the product density in the fire room compartment, the pressurized compartment and the lobby compartment are analysed and compared for the mesh resolutions. The results are presented in Figure 3.14. Steady-state conditions (stabilized values) are achieved in the timeframe of 360 to 600 seconds. The average values during this timeframe are listed in Table 3.27. The average difference in percentage between the grid resolutions is listed in Table 3.28. For the two finest mesh resolutions the difference for the fire room compartment is 0,09 %, the difference for the pressurized compartment is 10,28 %, and the difference for the lobby compartment is 5,03 %. The difference for the pressurized compartment and lobby compartment is considered as high, but the graphed results of the product density development match very well for the two finest resolutions during the whole timeframe (0 to 600 seconds). The conclusion of this is that a mesh resolution δx=0,1 is sufficient for Model B1. $D^*/\delta x$ values for the Model B1 simulations are listed in Table 3.29.

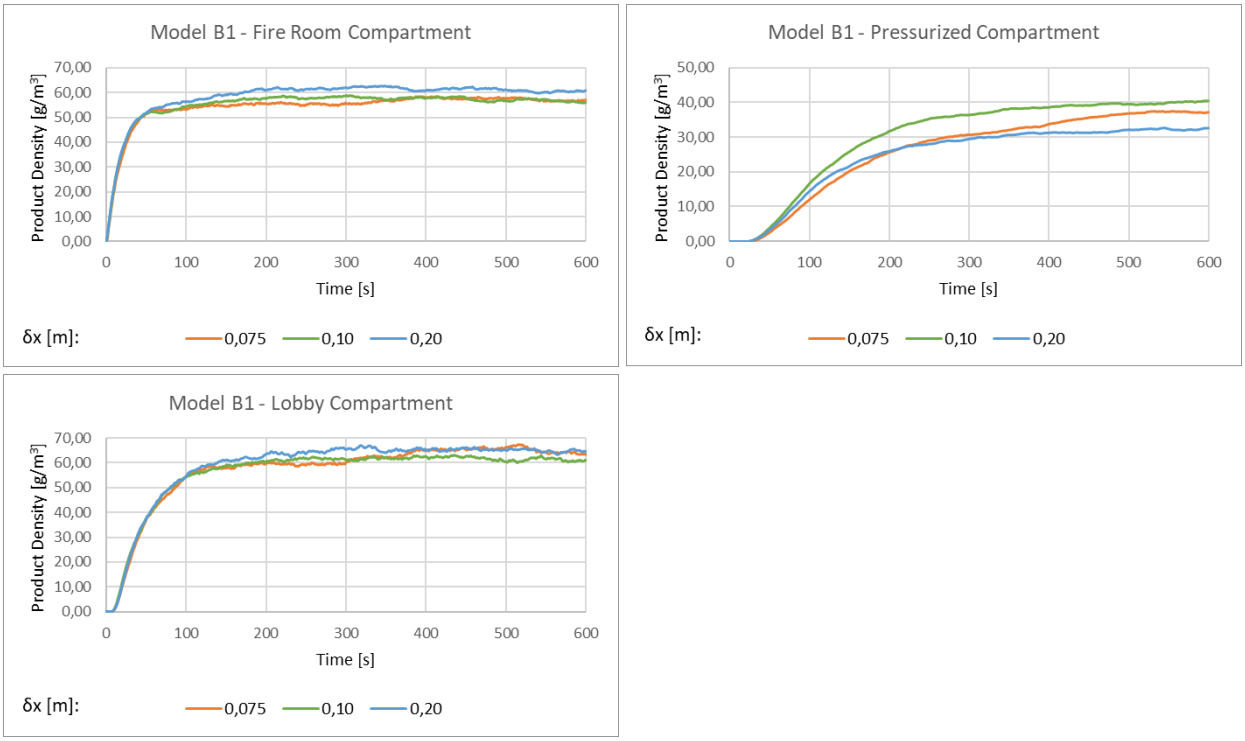

Figure 3.14 – Mesh sensitivity analysis results, Model B1.

Table 3.27 – Mesh sensitivity analysis, Model B1. Average product density during steady-state conditions.

Compartment	Average product density during steady-state conditions [g/m^3]		
	δx = 0,20 m	δx = 0,10 m	δx = 0,075 m
Fire Room Compartment	61,04	57,35	57,30
Pressurized Compartment	31,78	39,38	35,71
Lobby Compartment	65,13	61,86	64,97

Table 3.28 – Mesh sensitivity analysis, Model B1. Mesh resolution comparison.

Compartment	Average product density difference between mesh resolutions [%]	
	δx = 0,20 m VS. δx = 0,10 m	δx = 0,10 m VS. δx = 0,075 m
Fire Room Compartment	6,43	0,09
Pressurized Compartment	23,91	10,28
Lobby Compartment	5,29	5,03

Table 3.29 – Mesh sensitivity analysis, Model B1. $D^*/\delta x$ values.

HRR [kW]	D^* [m]	δx [m]	$D^*/\delta x$ [-]
500,00	0,73	0,10	7,29
1000,00	0,96	0,10	9,62
1500,00	1,13	0,10	11,32
2000,00	1,27	0,10	12,70

3.2.4. Model B2

Model B2 consists of three meshes where Mesh 1 is the pressurized compartment, Mesh 2 is the fire room compartment and the outside volume, and Mesh 3 is the lobby compartment. Three grid resolutions are analysed in this mesh sensitivity analysis. The smallest HRR and air supply are used as input values, 2500 kW (D^* = 1,38 m) and 1,12 m^3/s respectively. No smaller HRRs or air supply rates are used for this model, besides for those with the air supply deactivated.

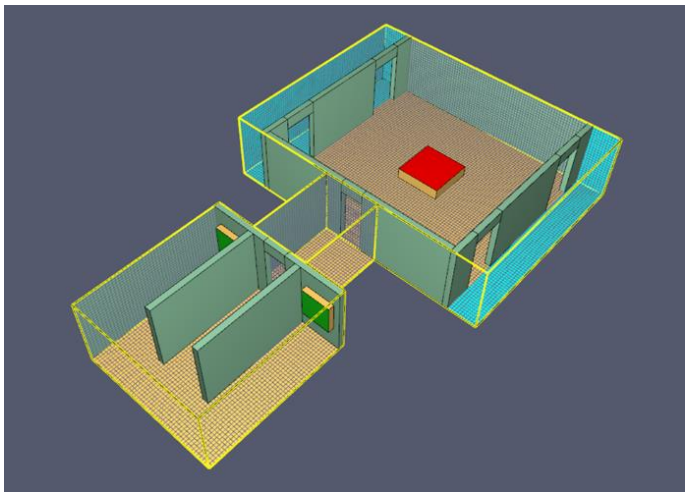

Figure 3.15. Model B2. The three meshes are separated with yellow outlines. Image extracted from the Pyrosim model.

Table 3.30 – Mesh resolutions for the mesh sensitivity analysis of Model B2.

Mesh resolution, cell size, δx [m]	$D^*/δx$ [-]	Number of cells			Total number of cells
		Mesh 1	Mesh 2	Mesh 3	
0,20	6,94	7 200	21 312	1 800	30 312
0,10	13,88	57 600	170 496	14 400	242 496
0,075	18,51	135 168	395 136	34 560	564 864

The development of the product density in the fire room compartment, the pressurized compartment and the lobby compartment are analysed and compared for the mesh resolutions. The results are presented in Figure 3.16. Steady-state conditions (stabilized values) are achieved in the timeframe of 360 to 600 seconds. The average values during this timeframe are listed in Table 3.31. The average difference in percentage between the grid resolutions is listed in Table 3.32. For the two finest mesh resolutions the difference for the fire room compartment is 1,18 %, the difference for the pressurized compartment is 0,98 %, and the difference for the lobby compartment is 0,02 %. The differences are considered as neglectable, the graphed results of the product density development match very well for the two finest resolutions during the whole timeframe (0 to 600 seconds). The conclusion of this is that a mesh resolution δx=0,1 is sufficient for Model B2. $D^*/δx$ values for the Model B2 simulations are listed in Table 3.33.

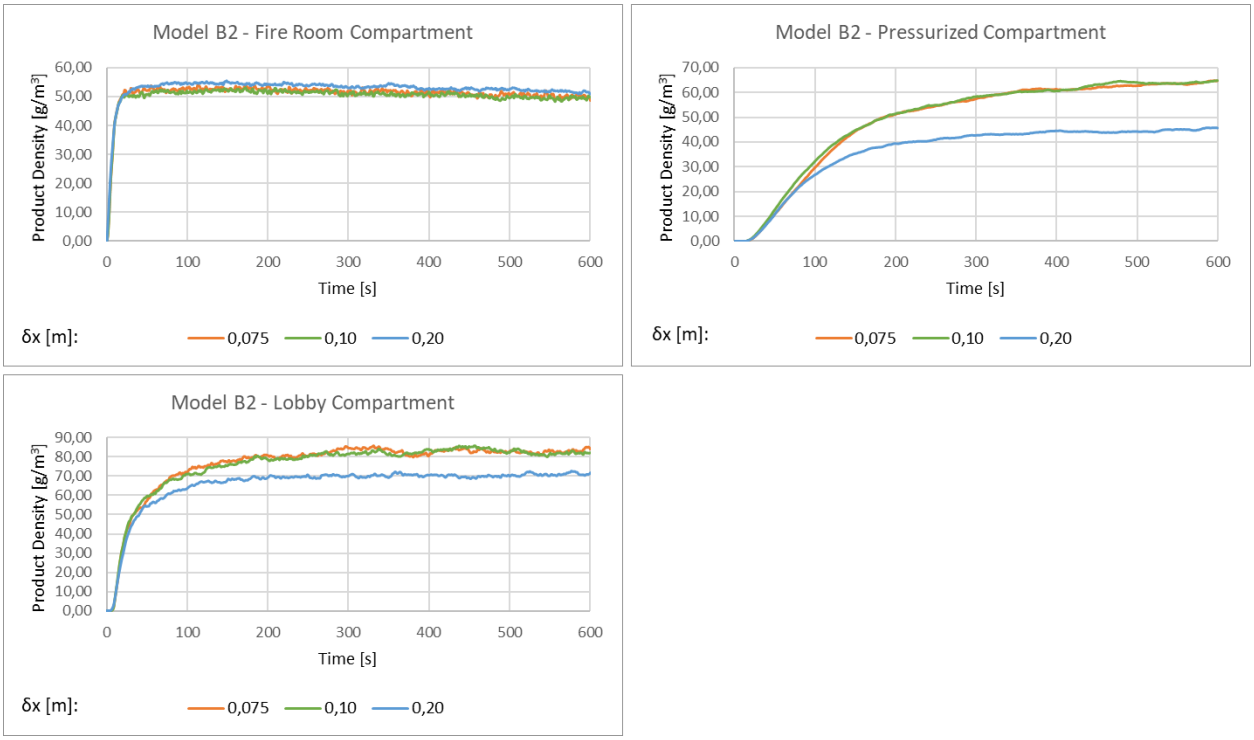

Figure 3.16 – Mesh sensitivity analysis results, Model B2.

Table 3.31 – Mesh sensitivity analysis, Model B2. Average product density during steady-state conditions.

Compartment	Average product density during steady-state conditions [g/m^3]		
	δx = 0,20 m	δx = 0,10 m	δx = 0,075 m
Fire Room Compartment	52,42	50,15	50,74
Pressurized Compartment	44,30	62,98	62,37
Lobby Compartment	70,38	82,73	82,75

Table 3.32 – Mesh sensitivity analysis, Model B2. Mesh resolution comparison.

Compartment	Average product density difference between mesh resolutions [%]	
	δx = 0,20 m VS. δx = 0,10 m	δx = 0,10 m VS. δx = 0,075 m
Fire Room Compartment	4,53	1,18
Pressurized Compartment	42,17	0,98
Lobby Compartment	17,55	0,02

Table 3.33 – Mesh sensitivity analysis, Model B2. $D^*/\delta x$ values.

HRR [kW]	D^* [m]	δx [m]	$D^*/\delta x$ [-]
2500,00	1,39	0,10	13,88
5000,00	1,83	0,10	18,32
7500,00	2,15	0,10	21,54
10000,00	2,42	0,10	24,17

3.2.5. Model C

Model C consists of two meshes where Mesh 1 is the pressurized compartment and Mesh 2 is the fire room compartment and the outside volume.

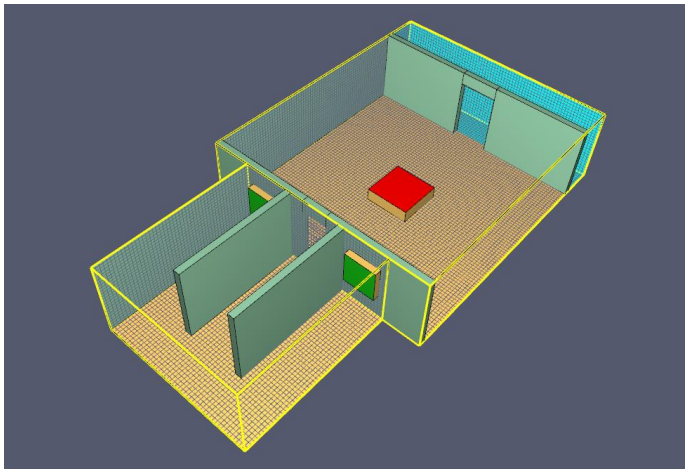

Figure 3.17. Model C. The two meshes are separated with yellow outlines. Image extracted from the Pyrosim model.

Model C is similar to Model A1. The difference is that the fire room compartment is expanded, no other vents or openings are added. Simulations with HRRs of 2000 kW is conducted for Model C. Since Model A1 is approved for HRRs of 500 kW, it is concluded that no mesh sensitivity analysis is required for Model C. Model C can therefore only be used for simulations where the HRR is minimum 2000 kW (D^* = 1,27 m), the air supply rate is minimum 1,12 m^3/s, and that the grid size δx is maximum 0,1 m. The information is summarized in Table 3.34.

Table 3.34 – Mesh resolution for Model C.

Mesh resolution, cell size, δx [m]	$D^*/\delta x$ [-]	Number of cells		Total number of cells
		Mesh 1	Mesh 2	
0,10	12,70	55 296	148 608	203 904

3.2.6. Model D

Model D consists of two meshes where Mesh 1 is the pressurized compartment and Mesh 2 is the fire room compartment and the outside volume.

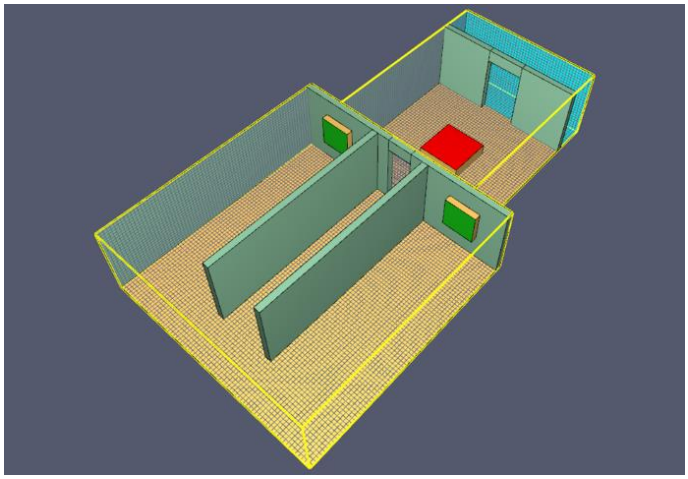

Figure 3.18. Model D. The two meshes are separated with yellow outlines. Image extracted from the Pyrosim model.

Model D is similar to Model A1. The difference is that the pressurized compartment is expanded, no other vents or openings are added. Simulations with HRRs of 2000 kW is conducted for Model D. Since Model A1 is approved for HRRs of 500 kW, it is concluded that no mesh sensitivity analysis is required for Model D. Model D can therefore only be used for simulations where the HRR is minimum 2000 kW ($D^* = 1,27$ m), the air supply rate is minimum 1,12 m^3/s, and that the grid size δx is maximum 0,1 m. The information is summarized in Table 3.35.

Table 3.35 – Mesh resolution for Model D.

Mesh resolution, cell size, δx [m]	$D^*/\delta x$ [-]	Number of cells		Total number of cells
		Mesh 1	Mesh 2	
0,10	12,70	127 872	69 120	196 992

3.3. Evaluation

Each scenario as listed in chapter 3.1.9 is simulated until steady-state conditions of the average product density in each compartment is reached. The average value of the average product density during steady-state conditions is calculated and compared for each model series. Results between the geometries are compared and discussed. The airflow criterion of the pressurization system is analysed, to assess the impact on the product density development due to various HRRs contra various air supply rates. The principle is analyzed in each compartment of each model geometry.

4. Results

Results from the conducted simulations are presented in this section. The product density development is recorded in each compartment and the values at steady-state conditions are plotted and compared for each model geometry.

4.1. The product density development

The simulations are conducted until steady-state conditions of the product density are established in each compartment. Most of the simulations are conducted in the time aspect of 600 seconds. Some simulations with large HRRs or large compartment volumes are conducted in the time aspect of 1200 seconds, due to late establishment of steady-state conditions. Results for each model, each HRR and each compartment are presented in Appendix A.1. Additional result data. The results show that as the air supply increases, the product density decreases.

4.2. The average product density at steady-state conditions

The scenarios due to different HRRs are compared by extracting the average product density results from the steady-state time aspect, and plotting the results into new graphs. The steady-state values of the product density are plotted and summarized in this section. One graph is presented for each model geometry and compartment. Each plot is bound by the HRR and the air supply rate, which is generated by two air supply points and creates an airflow in the opening between the compartments. In general, the product density in a compartment increases as the HRR increases. The product density decreases as the air supply increases.

Comments to Model A1

Deactivated air supply rates contribute to a higher level of product density in the pressurized compartment, compared to the fire room compartment. The pressurized compartment has no ventilation opening. Smoke continues to enter the pressurized compartment until the product density reaches a saturated level (steady-state conditions).

As the air supply increases, the product density decreases in each compartment. The decrease rate is higher in the pressurized compartment compared to the fire room compartment, due to the location of the fire. At some point, the product density in the pressurized compartment becomes lower than the product density in the fire room compartment.

Larger HRRs produce more fire products which lead to a larger product density in the pressurized compartment. Larger HRRs require a larger air supply to reduce the product density to desired levels. Results for the pressurized compartment of Model A1 show that the product density is 155 g/m^3 for the 500 kW HRR with the air supply deactivated. To reach the same level for larger HRRs, the air supply must increase. An air supply rate of 1,12 m^3/s reduces the product density to 142 g/m^3 for the 1500 kW HRR. An air supply rate of 1,60 m^3/s reduces the product density to 110 g/m^3 for the 2000 kW HRR.

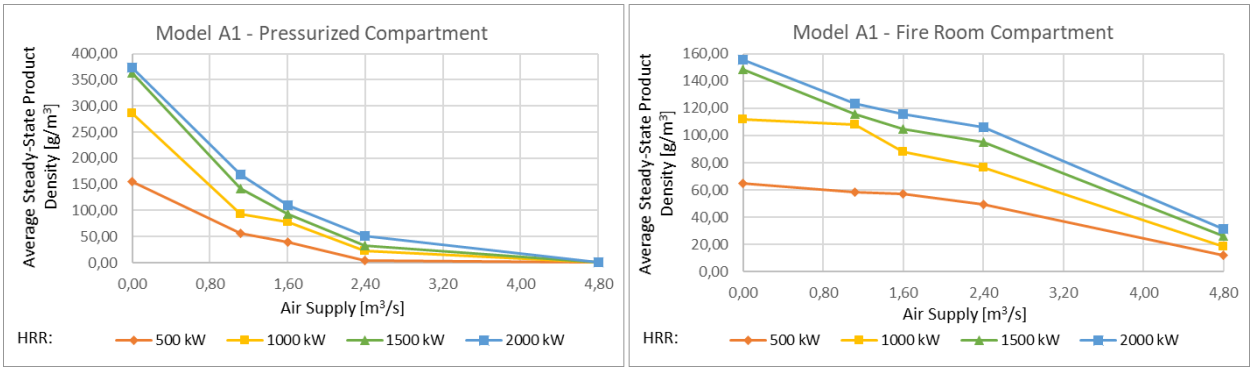

Figure 4.1 – Model A1. Results of the average product density at steady-state conditions in the different compartments, as a result of various HRRs contra various air supply rates.

Comments to Model A2

Similar decrease rates as for Model A1 are registered for Model A2 in the pressurized compartment. By comparing the results for Model A1 with Model A2 it is found that larger HRRs of Model A2 return smaller product densities compared to Model A1. The HRR of 2000 kW for Model A1 develops the product density to 373 g/m^3 in the pressurized compartment with the air supply deactivated. The HRRs of 2500 kW and 5000 kW of Model A2 return lower values, 188 g/m^3 and 309 g/m^3 respectively, with the air supply deactivated. This is directly affected by the larger area of ventilation openings (openings to the outside) for Model A2 compared to Model A1. The larger opening contributes to a larger smoke loss fraction. The same situation occurs for Model B1 compared to Model B2.

The product density in the fire room compartment develops differently for Model A1 and Model A2. As seen for Model A2, the product density is nearly unchanged by increased air supply rates. In Model A1 the product density decreases as the air supply increases. The differences most likely occur due to the larger size of the fire room compartment, the increased number of openings, and the position of the openings for Model A2.

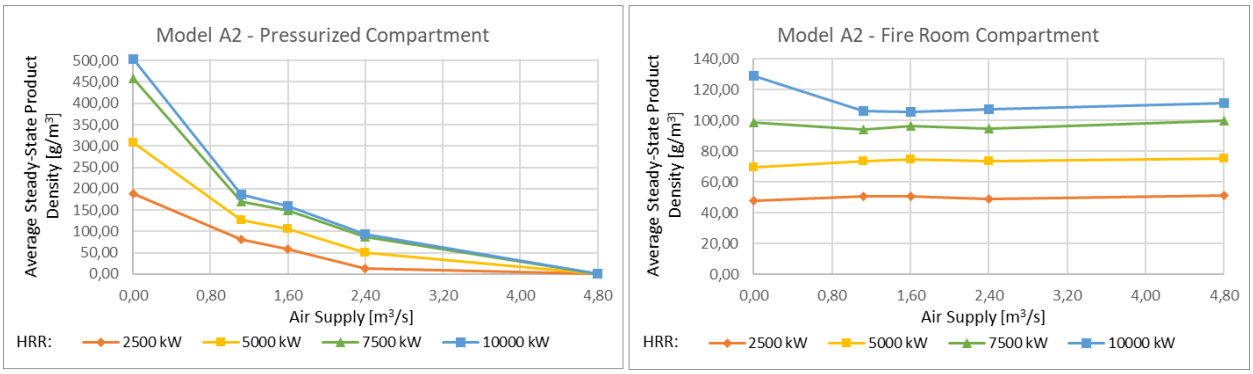

Figure 4.2 – Model A2. Results of the average product density at steady-state conditions in the different compartments, as a result of various HRRs contra various air supply rates.

Comments to Model B1 and Model B2

The same simulations as for Model A1 and Model A2 are conducted in Model B1 and Model B2 but with a lobby compartment implemented between the fire room compartment and the pressurized compartment. The results show that the lobby compartment has an impact on the product density development in the pressurized compartment. With the air supply deactivated a slightly higher product density is established in the pressurized compartment of Model B1 and Model B2, compared to Model A1 and Model A2. As the air supply is activated, the product density decrease rate becomes higher in the pressurized compartment of Model B1 and Model B2, compared to Model A1 and Model A2. At some point, the product density becomes equal in the pressurized compartment of the models (Model A1 compared to Model B1, Model A2 compared to Model B2), and eventually the product density is lower for Model B1 and Model B2, compared to Model A1 and Model A2.

The results show that the demand for air supply is much smaller for the lobby compartment cases. With an air supply rate of 2,40 m^3/s, the product density is decreased to 0 g/m^3 in the pressurized compartment with the lobby compartment. For the same case but without a lobby compartment, the product density is greater than 0 g/m^3.

The fire room compartment is affected differently due to the different geometries. In Model B2, the product density is nearly unchanged, while the product density decreases as the air supply increases for Model B1. The same outcome occurs for Model A1 and Model A2.

The lobby compartment is exerted to a product density level lower than the product density in the pressurized compartment, with the air supply deactivated. With the air supply activated, the product density is higher in the lobby compartment compared to the pressurized compartment. With an air supply rate of 2,40 m^3/s, the product density decreases to 0 g/m^3 in the pressurized compartment of Model B1 and Model B2. The product density is also at this point higher in the lobby compartment compared to the pressurized compartment of Model A1 and Model A2.

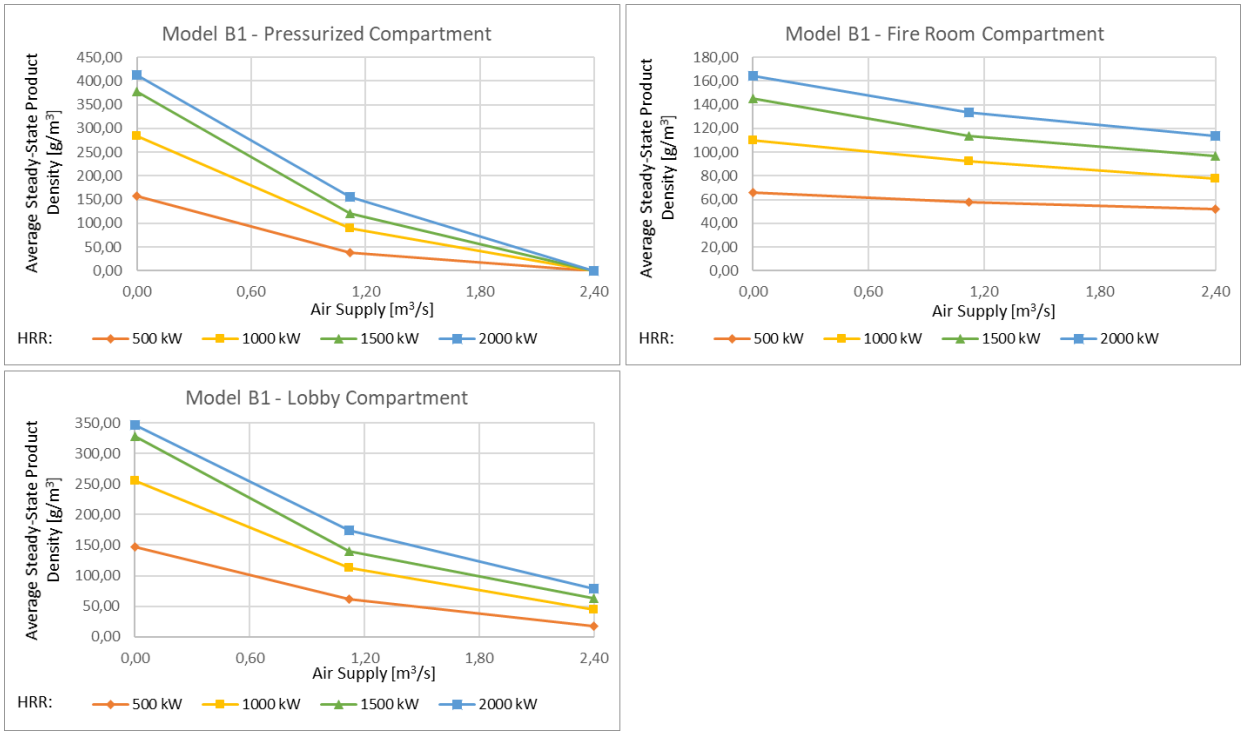

Figure 4.3 – Model B1. Results of the average product density at steady-state conditions in the different compartments, as a result of various HRRs contra various air supply rates.

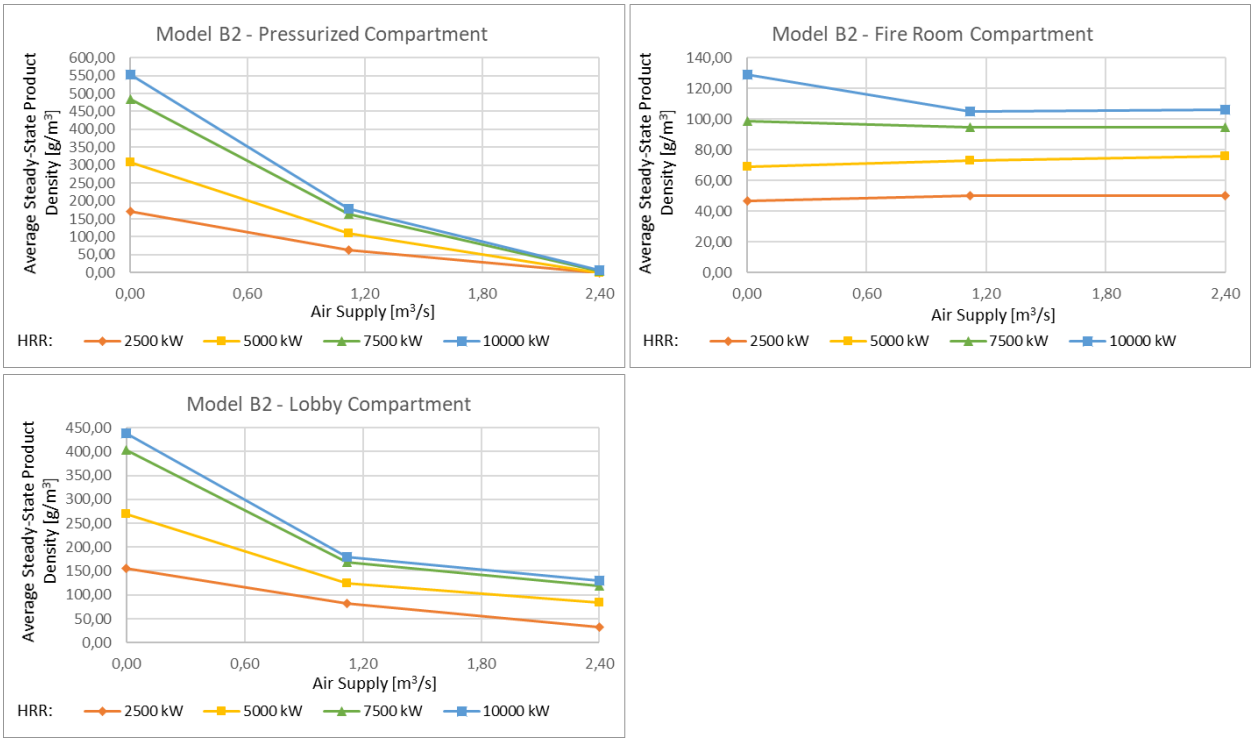

Figure 4.4 – Model B2. Results of the average product density at steady-state conditions in the different compartments, as a result of various HRRs contra various air supply rates.

Comments to Model C and Model D

Simulations, where the geometry of Model A1 is altered, are conducted to study the outcome of the changes. For Model C the fire room compartment is expanded compared to Model A1. For Model D the pressurized compartment is expanded compared to Model A1. Only the HRR of 2000 kW is investigated.

By comparing Model D with Model A1, it is noticed that the product density for Model D in both compartments is slightly higher than for Model A1. The product density is besides this quite equal for the models.

Model C has a greater product density in the pressurized compartment compared to Model A1 and Model D as the air supply is deactivated. With the air supply activated, the product density decreases to the levels of the other models. The product density in the fire room compartment is highest for Model C in each air supply scenario.

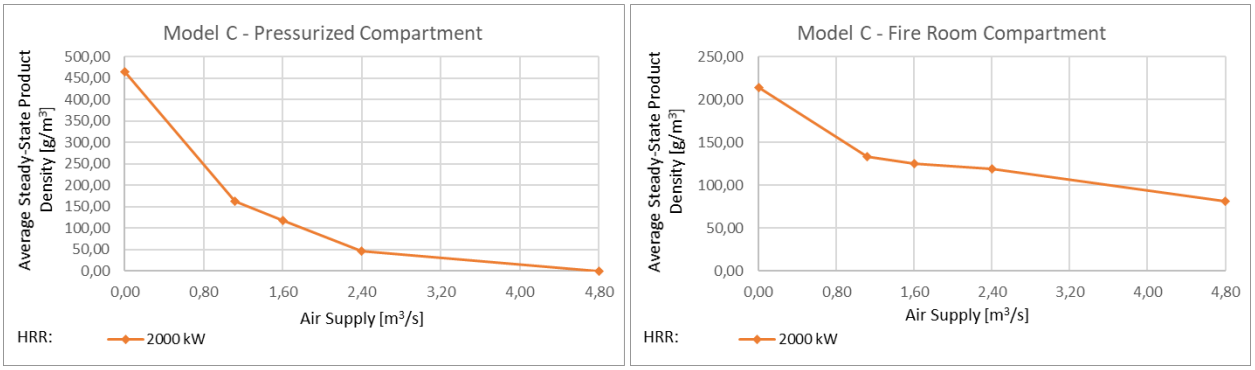

Figure 4.5 – Model C. Results of the average product density at steady-state conditions in the different compartments, as a result of a 2000 kW HRRs contra various air supply rates.

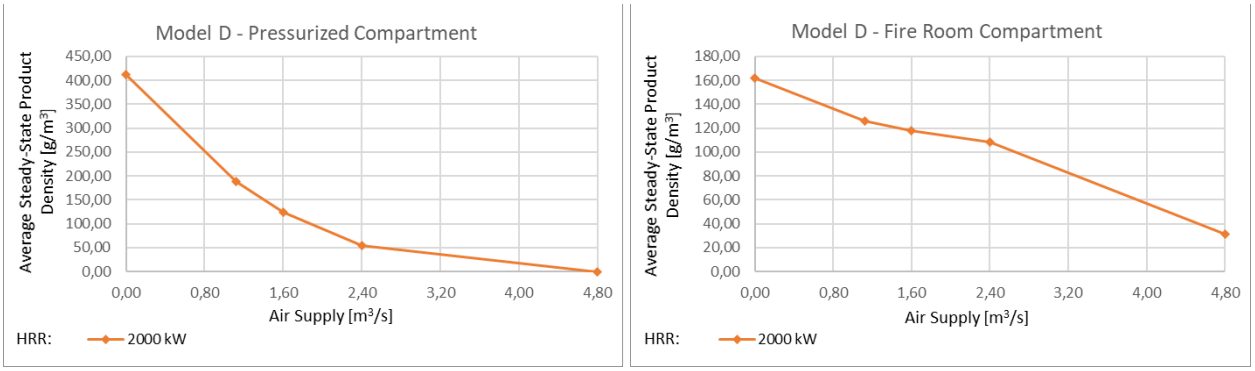

Figure 4.6 – Model D. Results of the average product density at steady-state conditions in the different compartments, as a result of a 2000 kW HRRs contra various air supply rates.

5. Discussion

Simulations are performed to study the reduction of fire products in different compartments of several model geometries, due to the airflow criterion of a pressurization system. The product density is analysed due to the impact of various HRRs contra various air supply rates. The pressurization system, tenable conditions, results and airflows are discussed in this section.

5.1. Pressurization system

A pressurization system consists of many components which must be carefully designed with proper functionality to co-work with other components. The Norwegian site "Brannforum" describes a pressurization system as a system depended upon 16 factors [47]. Further, the site claims that if one of these factors fail, then the whole system fails. The 16 factors are:

1. Lobby compartment between the pressurized compartment and the fire room compartment.
2. Shaft with vents in the lobby compartment.
3. Pressurization fan / air supply unit.
4. Power supply to the pressurization fan.
5. Backup-power to the pressurization fan.
6. Pressure relief vent in the pressurized compartment.
7. Pressure relief vent in the lobby compartment.
8. Smoke detectors in the pressurized compartment and the lobby compartment.
9. Fire alarm central with backup-power.
10. A programmed fire alarm central which activates the pressurization system and the pressure relief vents at the right detector-signal.
11. Fire-protected electrical cables to the pressurization fan.
12. Fire-protected electrical cables to the pressure relief vents.
13. Pressurization fan with the right air supply rate.
14. Pressure relief vents with the right air relief capacity.
15. An airflow of 0,75-2,00 m/s with one door to the pressurized compartment open.
16. An airflow of 0,75-2,00 m/s with one or two doors to the pressurized compartment open.

In addition to this, it is important to consider that doors and other openings towards the pressurized compartment must have a self-closing mechanism. If the pressurized compartment is not airtight or if leaks appear, the system can fail unless it is accounted for some leaks.

Through fire protection engineering many of these factors are eliminated by following a suited standard (for example, NS-EN 12101-6:2005 [4]) for the design of a pressurization system. For example, with a standard it is determined if the pressurization system should rely on a lobby compartment (with shafts) or not. Fire-protected cables are usually not a demand, since the pressurization system is kept in a compartment which is not intended to be the fire room compartment. The right airflow through one or several door openings is safeguarded by designing the proper air supply and air relief capacity. The backup generators, and the fire alarm central with

proper system communication between the smoke detectors and the pressurization system, are safeguarded by the electrical engineers.

The most crucial factors to safeguard for a pressurization system are (1) the pressure criterion and (2) the airflow criterion (as described in NS-EN 12101-6:2005 [4]).

- The pressure criterion defines the minimum and maximum pressure interval difference between the pressurized compartment and the fire room compartment when all the doors between the compartments are closed.
- The airflow criterion defines the minimum airflow through one or several openings (open doors) between the pressurized compartment and the fire room compartment to keep the pressurized compartment smoke-free.

A too low pressure difference between the pressurized compartment and the fire room compartment (or the lobby compartment) results into smoke flowing into the pressurized compartment through small gaps and cracks (unless other factors prevent this). A too high pressure difference results into doors being difficult to open. This can affect the ability to enter the egress route.

Air supply points and relief vents must be designed with proper communication. The air supply points increase the pressure in the pressurized compartment, and the relief vents regulate the pressure level by releasing excess air in controlled amounts. The overpressure can also be regulated by time-changing air supply rates, which adapts to the situation by increasing or decreasing the supply rate. If the relief vent reacts too slow or fails, the pressure can increase to above the maximum level. If the pressure is within the allowed interval and a door suddenly opens, air will flow from the pressurized compartment to the adjacent compartment and create a flow of air across the opening and prevent a smoke-flow in the opposite direction. In this case, the relief vent must close. If the relief vent does not close or reacts to slow, the airflow across the opening can decrease to a level smaller than intended.

It can become difficult to close a door if the airflow through the same opening is too large. This situation can occur when the pressurized compartments have several doors open with the right airflow through each opening. If some doors suddenly close, the airflow will theoretically increase through the remaining doors, unless the relief vent reacts instantly to release the excess air.

The pressurization system is sensitive to this operation and is depended upon the reliability of the components.

5.2. Tenable conditions in the pressurized compartment

It is difficult and demanding to keep the pressurized compartment 100 % smoke-free, considering the need to keep the doors openable and closable. Creating a flow of air through an opening, with a flow rate high enough to reduce the smoke-flow to 0 % in the opposite direction, is theoretically possible. In practice, it requires a level of extreme optimization considering the operation of doors and due to the demand for accuracy in the system.

To achieve a 100 % smoke-free situation in the pressurized compartment, along with controlling the doors, the components must operate with a high level of reliability. Components must communicate with each other without errors, and regulative functions like the air supply rate, the relief vent opening factor and door closing mechanisms much react without delay. Any deviation from this can lead to failure in the system.

A fire can expose humans to life-threatening components, like soot, toxic gases and heat. However, the human tolerates these components up to a certain dose. Some exposure to smoke can be accepted if the tenable conditions are safeguarded. Considering this, the pressurization system does not have to be as demanding as for a system where the pressurized compartment is kept 100 % smoke-free.

The fire safety code SN-INSTA/TS 950:2014 [23] presents tenable conditions for visibility, temperature, heat flux, CO, CO_2 and the reduction of O_2. FDS supports calculations of these quantities. Regarding the gas species, information about, among other things, the mass densities, mass fractions and volumetric fractions can be extracted. Further, it is focused on the toxicity of gases due to increased levels of CO and CO_2, and the reduction of O_2.

The reaction is defined with the simple-chemistry combustion model for the conducted simulations. With the simple-chemistry approach, various gas species are lumped into reacting groups referred to as lumped species. The lumped species consist of three reacting groups: air, fuel and products. More details on this are found in chapter 2.8.5. A compartment, which is originally filled with air and which becomes exerted to fire products, do in terms of volumetric fractions and mass fractions consist of the lumped species air and products, unless the fire products take up the whole volume. That means that the sum of air and product is 1.

With the air supply deactivated, the pressurized compartment is exerted to fire products which after a certain time reaches steady-state conditions regarding the density, mass fraction and volumetric fraction. These quantities decrease (the O_2 increase) as air supply activates and reduces the amount of fire products entering the pressurized compartment. The air supplied to the pressurized compartment contributes to achieving tenable conditions by reducing the fire products.

SN-INSTA/TS 950:2014 recommends the following values for tenable conditions in terms of volumetric fractions:

- CO: maximum 0,2 %
- CO_2: maximum 5%
- O_2: minimum 15 %

The major components of dry air in terms of volumetric fraction are N_2 (78,08 %), O_2 (20,95 %) and argon (0,93 %). The remaining volumetric fraction (0,04 %) consists of other gas species [48]. To accept the volumetric fraction of minimum 15 % O_2, the volumetric fraction of air can decrease to minimum 71,6 %. The remaining 28,4 % consists of fire products.

By analysing the result data, we find that the volumetric fraction of CO in the fire products is approximately 1,6 %. The volumetric fraction of CO_2 in the fire products is approximately 14,3 %. These values originate from the specified fuel properties, as specified in chapter 3.1.8, and is different for different reactions. In FDS, the default volumetric fraction of O_2 in air is 0,20782285, and the default volumetric fraction of CO_2 in air is 0,00038690337. Based on this information, the following correlations between the lumped species and its background species for the current reaction is generated:

$$(m^3/m^3\ CO) = (m^3/m^3\ products) \times 0{,}0160856533057541 \tag{5.1}$$

$$(m^3/m^3\ CO2) = (m^3/m^3\ products) \times 0{,}143433586759932 + 0{,}00038690337 \tag{5.2}$$

$$(m^3/m^3\ O2) = \left(1 - (m^3/m^3\ products)\right) \times 0{,}20782285 \tag{5.3}$$

The maximum product density volumetric fraction is calculated based on the recommended values for tenable conditions:

- Maximum 0,2 % CO = Maximum 12,4 % products
- Maximum 5 % CO_2 = Maximum 34,6 % products
- Minimum 15 % O_2 = Maximum 27,8 % products

For the current reaction input, CO is the most critical gas species since it requires the lowest volumetric fraction of products. As a conclusion, tenable conditions are safeguarded by allowing maximum 12,4 % of Products in the pressurized compartment (the remaining 87,6 % consists of air).

The air supplied to the pressurized compartment reduces the volumetric fraction of products, by creating an airflow through openings and preventing the flow of fire products in the opposite direction. The air supply rate can be increased until the desired volumetric fraction of products is reached.

However, a safety margin should be considered to safeguard Fire Safety Engineering principles, by defining a lower value than 12,4 % for the fire products. In this study, the development of visibility, temperature, and thermal energy have not been analysed. The recommended tenable conditions for these parameters can contribute to a stricter volumetric fraction of fire products.

Figure 5.1 shows the average volumetric fractions of the fire products at steady-state conditions, for the pressurized compartment of Model A1. In addition, the same fractions of CO, CO_2 and O_2 are extracted, and the tenable condition criteria are implemented for the same gas species. The minimum air supply, necessary to safeguard the tenable conditions for various HRRs, is illustrated in Figure 5.1. The tenable condition of CO requires the strictest volumetric fraction of products. A 500 kW HRR require an air supply rate of 1,12 m^3/s to achieve tenable conditions. The 1000

kW, 1500 kW and 2000 kW HRRs require an air supply rate of 1,12 m^3/s, 1,60 m^3/s and 2,40 m^3/s respectively. A 100 % smoke-free pressurized compartment is not demanded.

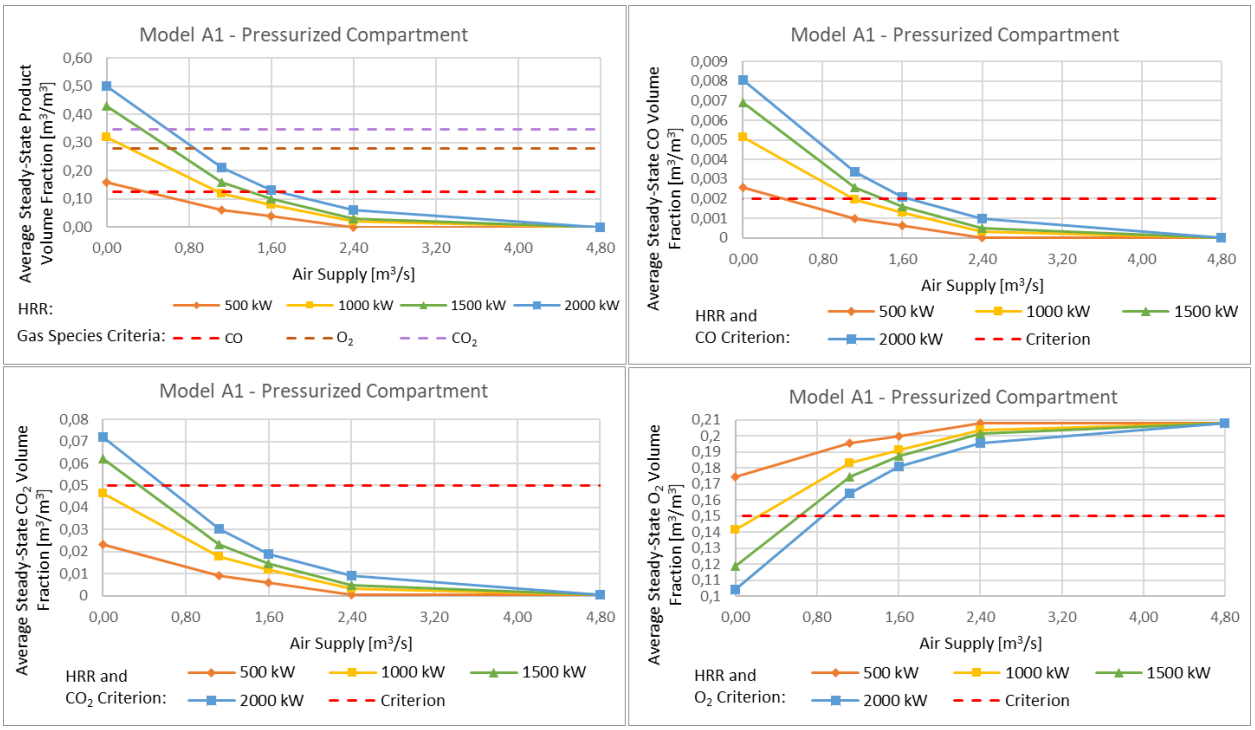

Figure 5.1 – Tenable conditions calculations for the pressurized compartment of Model A1. The average volumetric fractions of the fire products, CO, CO_2 and O_2, at steady-state conditions.

5.3. Simulation results

The simulation results as presented in chapter 4.2 is discussed in this section. Factors such as increased HRRs, ventilation opening positions, the impact of the lobby compartment, and the expansion of compartments are discussed.

5.3.1. The effect of increased heat release rate

The main difference between Model A1 and Model A2, besides the HRR, is the size of the fire room compartment and the opening area. The fire room compartment is 2,25 times larger for Model A2, and the opening area is four times larger, distributed on four equal-sized openings. The purpose of this is to support larger fires, which demands more space and oxygen.

During the pre-studies of the model setup, it was found that Model A1 is not able to support much larger HRRs than 2000 kW. Eventually, the fire becomes ventilation-controlled due to the limited opening area to the outside. The fire room compartment, and the area of ventilation openings, is expanded in Model A2. The openings of Model A2 are located on the sidewalls of the fire room compartment, two on each side. The opening of Model A1 is located on the wall right in front of

the opening connecting the pressurized compartment and the fire room compartment. Model A2 is simulated with fires which is up to five times larger than the largest HRRs in Model A1 (10000 kW for Model A2, 2000 kW for Model A1). As for Model A1, fires larger than 10000 kW eventually become ventilation-controlled in Model A2.

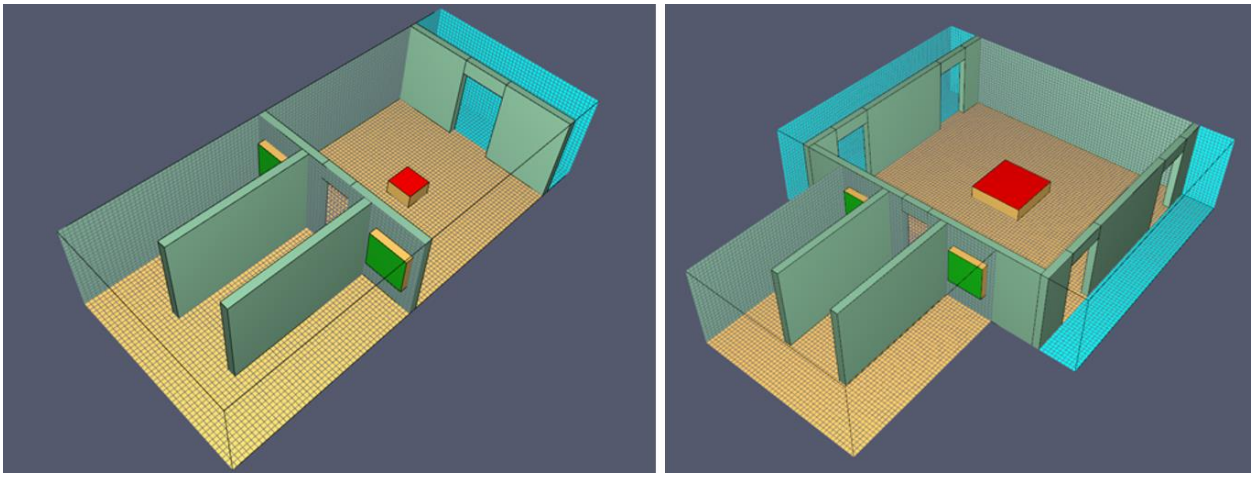

Figure 5.2 – Ventilation openings. The sample to the left shows the ventilation opening location of Model A1, and the sample to the right shows the ventilation opening locations of Model A2. Images extracted from the Pyrosim model.

The distance between the fire source area and the openings is important to consider too. The purpose of the openings is to supply the fire with oxygen and to release smoke from the model. During pre-studies of the model setup, it was found that flames would stretch out of the openings if the fire was located too close to the ventilation openings. This situation is avoided with a distance between the fire and the openings. For larger fires where more openings are demanded, the flames would move away from the fire source area unless the fire was surrounded by these openings. The impact of the opening positions on the smoke-flow has not been investigated, but to avoid any uncertainties the opening locations were designed to avoid any interference on the flame, with consideration to the largest HRR of the current model.

It was found that the fire had to be positioned in the middle of the fire room compartment, with a distance of at least half the fire source side length between the fire source area and any opening to avoid interference on the flame. For the case with one opening, the flame would be stable enough with the ventilation opening positioned in front of the opening connecting the two compartments. For the case with four openings, several combinations were tried before ending up with the current model. At first, one large opening was positioned on the wall in front of the opening connecting the two compartments. This would pull the flames away from the fire source area. Having two openings on the sidewalls between the fire and the pressurized compartment (one on each side) would also pull the flames away from the fire source area. By surrounding the fire with four openings, the flames would remain stable around the fire vent.

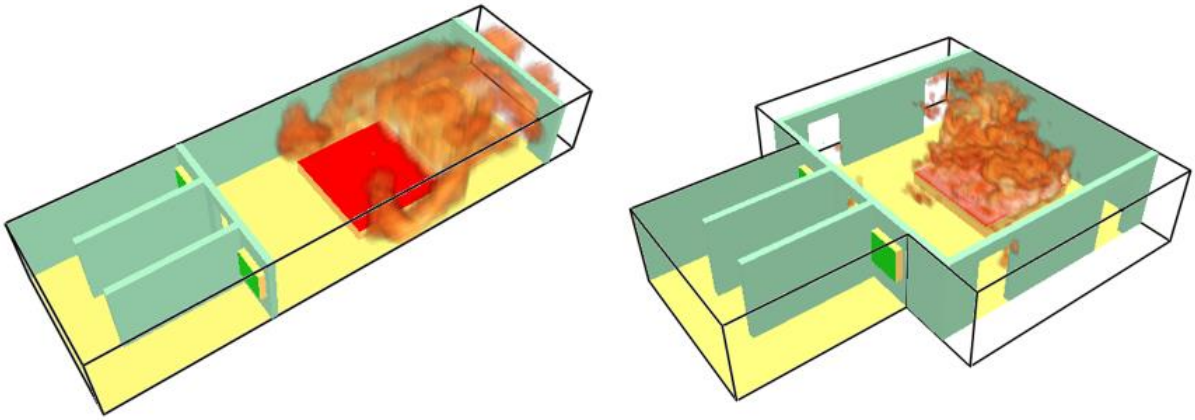

Figure 5.3 – Pre-studies of the opening positions for the model geometries. The sample to the left shows one opening which pulls the flames away from the fire source area. The sample to the right shows the same opening area distributed on four openings, which surrounds the fire source area and keeps the flames stable. Image extracted from Smokeview, which presents the FDS result data.

The opening area to the outside affects the smoke development in the pressurized compartment. Because of the larger area of ventilation openings in Model A2, a larger fraction of smoke spreads to the outside and less to the pressurized compartment, compared to Model A1. This is a positive effect regarding the smoke development in the pressurized compartment for a fuel-controlled fire. A fire of size 2000 kW simulated in Model A2 would contribute to a much lower product density in the pressurized compartment. Mind that a ventilation-controlled fire is depended upon the opening area and grows as the number of opening grows. Results for Model A1 show that for a fire of size 2000 kW with the air supply deactivated, the product density develops to 370 g/m^3. Results for Model A2 show that for a fire of size 5000 kW with the air supply deactivated, the product density develops to 305 g/m^3.

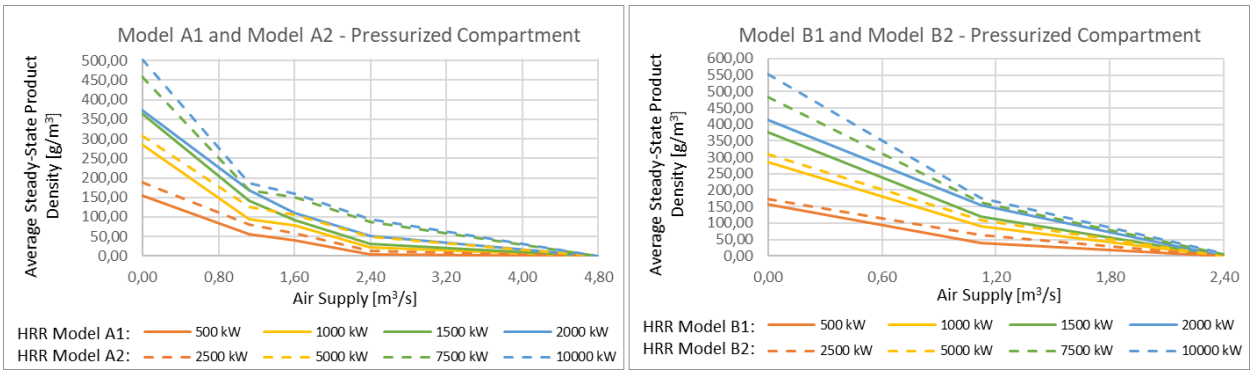

Figure 5.4 – Pressurized compartment. Model A1 compared to Model A2, Model B1 compared to Model B2.

Since the product density reaches steady-state conditions, while the fire still produces more fire products, smoke which spreads to the pressurized compartment also circles back to the fire room compartment.

5.3.2. The positions of the ventilation openings

The position of the ventilation openings impacts the product density development in the fire room compartment. For Model A1 and Model B1, the one opening is located on the wall right in front of the opening connecting the fire room compartment and the pressurized compartment. For Model A2 and Model B2, the four openings are located on the sidewalls.

The average product density during steady-state conditions is unchanged as the air supply is altered, for the fire room compartment of Model A2 and Model B2. The average product density during steady-state conditions decreases in the fire room compartment of Model A1 and Model B1, as the air supply is altered.

This effect most likely occurs due to the ventilation opening for Model A1 and Model B1 being located right in front of the opening connecting the two compartments. The velocity of air entering the fire room compartment creates a momentum of air ejected towards the in front laying opening. A higher level of fire product is pressed out through the opening. For Model A2 and Model B2, the momentum of air is exerted on the in front laying wall and is further distributed across the fire room compartment before it exits through the four openings at a lower but stabilized rate.

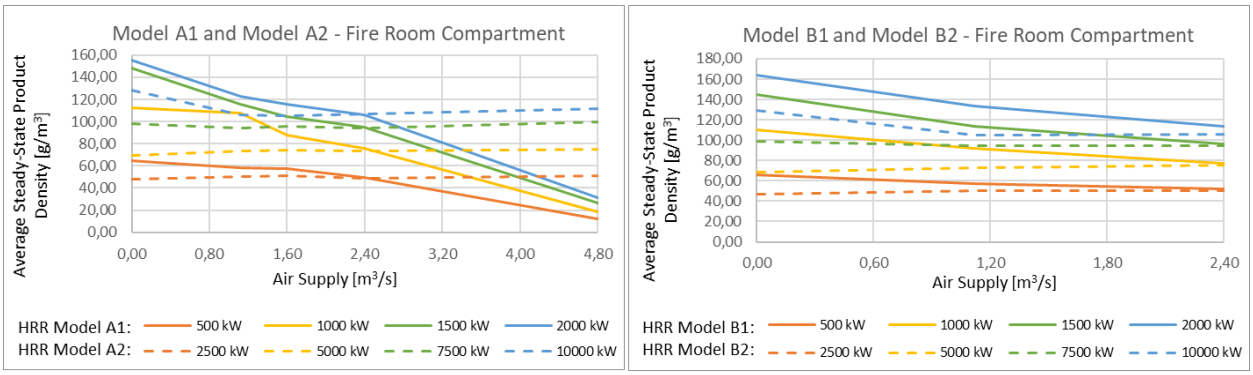

Figure 5.5 – Fire room compartment. Model A1 compared to Model A2, Model B1 compared to Model B2.

5.3.3. Impact of the lobby compartment

It is found that a lobby compartment, located between the fire room compartment and the pressurized compartment, has an impact on the product density development. With the air supply deactivated, the product density at steady-state conditions in the pressurized compartment with a lobby compartment (Model B1 and Model B2) is slightly higher, than for the same case but without a lobby compartment (Model A1 and Model A2). This most likely occurs due to the one extra opening between the fire room compartment and the pressurized compartment.

The product density in the pressurized compartment decreases as the air supply is activated. The product density decreases at a higher rate for the case with a lobby compartment, compared to the same case without a lobby compartment. The product density is equal at one point. With an air supply rate of 1,12 m^3/s, the product density difference in the pressurized compartment is surpassed. The product density is lower for the case with a lobby compartment than without a lobby compartment.

As the air supply increases to 2,40 m^3/s, the product density decreases to 0 g/m^3 for the case with a lobby compartment, while the product density is greater than 0 g/m^3 without a lobby compartment. For Model B2, the fire of 7500 kW results into a product density of 4,11 g/m^3, and for 10000 kW the value is 7,19 g/m^3, but these values are far below those without a lobby compartment. As a conclusion to this, the minimum volumetric air supply rate to establish a maximum product density in the pressurized compartment can be reduced by having a lobby compartment between the pressurized compartment and the fire room compartment.

While the lobby compartment brings an advantage to the pressurized compartment, the lobby compartment itself is subjected to an increased product density. The product density is lowest in the lobby compartment with the air supply deactivated. The product density is highest in the lobby compartment with the air supply activated, compared to the pressurized compartment with and without a lobby compartment.

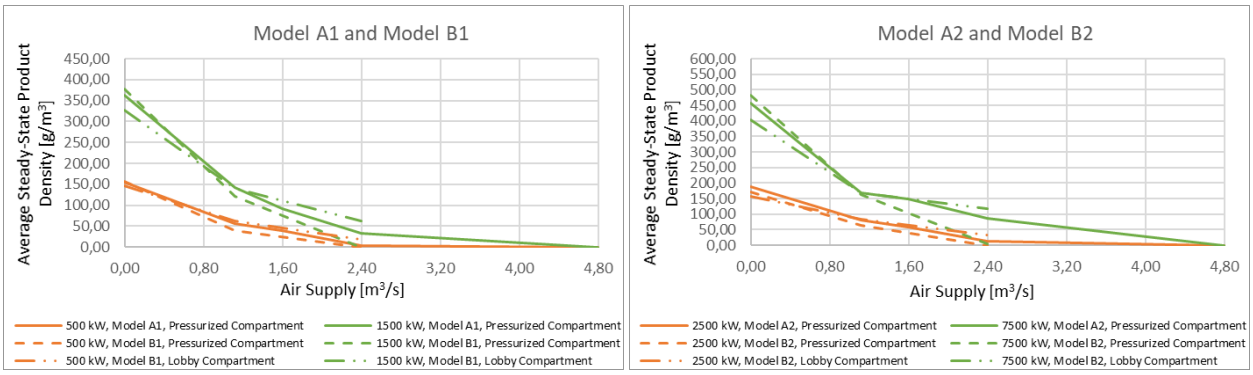

Figure 5.6 – Pressurized compartment and lobby compartment. 500 kW and 1500 kW HRR. Model A1 compared to Model B1, Model A2 compared to Model B2.

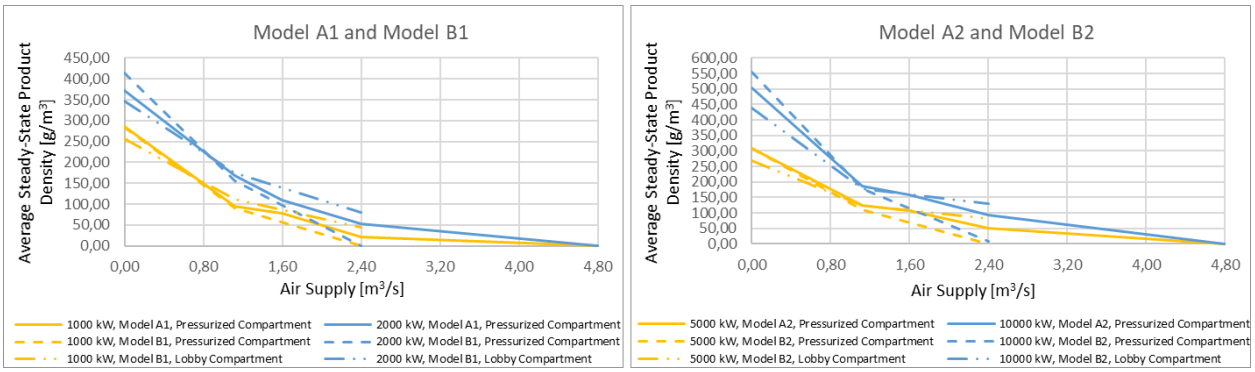

Figure 5.7 – Pressurized compartment and lobby compartment. 1000 kW and 2000 kW HRR. Model A1 compared to Model B1, Model A2 compared to Model B2.

During the pre-studies, a solution where the lobby compartment is pressurized were investigated. The results indicated that it is more difficult to achieve a successful solution by pressurizing the lobby compartment, due to the supplied air being concentrated to one opening instead of both. No flow of air was established towards the fire room compartment, leading to fire products spreading to the lobby compartment and the other adjacent compartment.

5.3.4. Expansion of the compartments

Model A1 consists of two equal-sized compartments, the fire room compartment and the pressurized compartment. Simulations, where the size of these rooms are expanded, are conducted to study the impact on the product density development. Fires of size 2000 kW are simulated with altered air supply rates.

Model C is similar to Model A1, the difference is that the fire room compartment is expanded 2,25 times. Model D is similar to Model A1, the difference is that the pressurized compartment is expanded 2,25 times.

The results show that the product density development, and the decrease rate due to increased air supply rate, are similar for Model A1 and Model D. The product density is slightly higher for Model D in both compartments, due to the size of the pressurized compartment being bigger.

The product density development results for Model C differ from the results for Model A1 and Model D. The product density is highest in the pressurized compartment of Model C with the air supply deactivated. As the air supply is activated, the product density decrease rate is most effective for Model C.

In the fire room compartment, the product density is highest for Model C for each air supply scenario, compared to Model A1 and Model D. As the air supply is activated, the product density reduction is at first most effective for Model C, but apart from that, the reduction is least effective when higher air supply rates are activated.

Expanding the pressurized compartment has for this case little impact on the product density development. Expanding the fire room compartment results in more changes in the product density development.

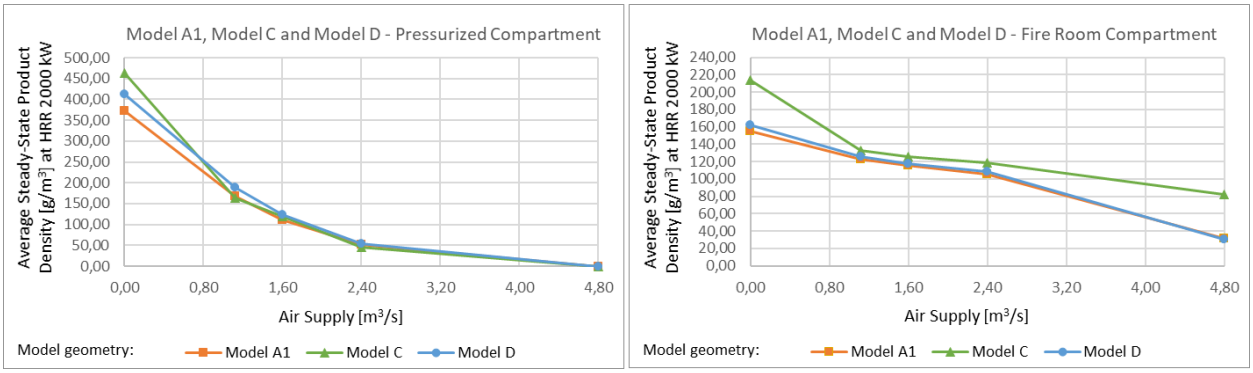

Figure 5.8 – Pressurized compartment and fire room compartment. Model A1, Model C and Model D.

5.4. Airflow

The airflow through the opening connecting the two compartments is an important factor to consider when designing the pressurization system. As previously discussed, the product density development depends primarily upon the HRR and the air supply rate. The ventilation opening area controls the amount of smoke being released from the model, and the amount of smoke spreading to the pressurized compartment. The geometrical shape has an impact on the development too.

For a given geometrical scenario, the air supplied to the pressurized compartment affects the amount of smoke spreading into the same compartment. Since smoke is less dense than air (due to the temperature difference), smoke spreads from the fire room compartment to the pressurized compartment through the top of the opening connecting the compartments. Air flows in the opposite direction, through the bottom of the same opening.

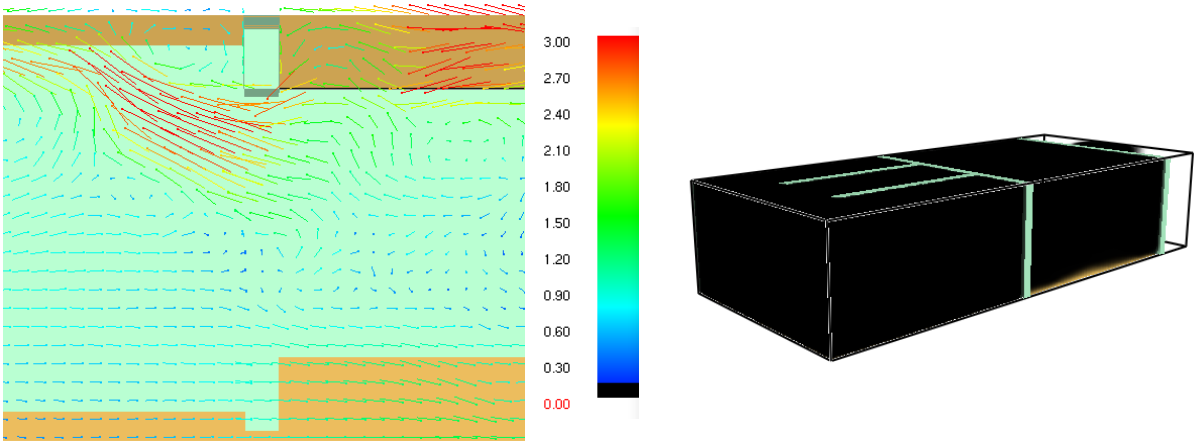

Figure 5.9: Airflow and smoke-flow at steady-state conditions, through the opening connecting the compartments of Model A1. 2000 kW HRR. 0,00 m³/s air supply rate. 0,00 m/s airflow through the opening. Image extracted from Smokeview, which presents the FDS result data.

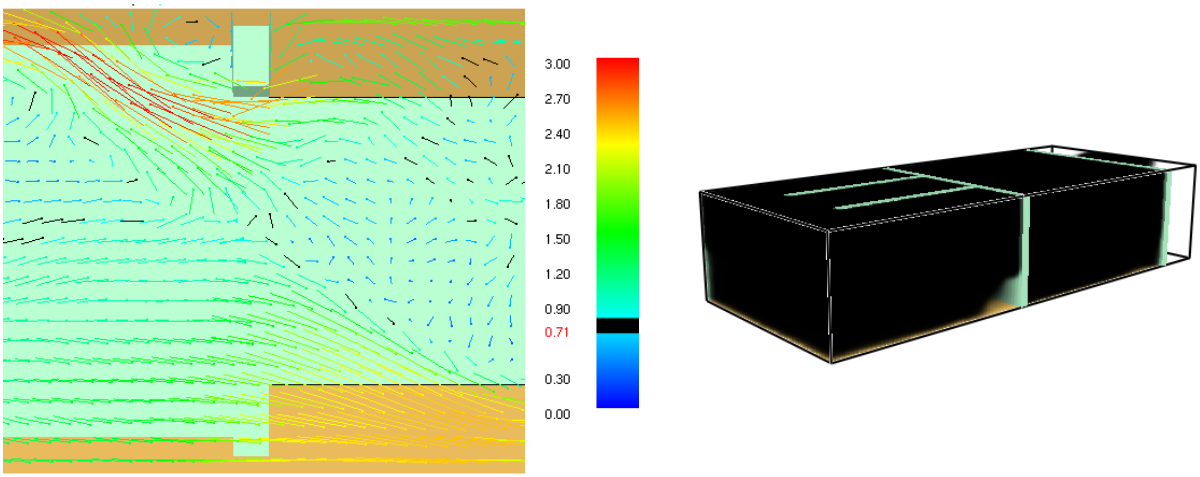

Figure 5.10: Airflow and smoke-flow at steady-state conditions, through the opening connecting the compartments of Model A1. 2000 kW HRR. 1,12 m³/s air supply rate. 0,70 m/s airflow through the opening. Image extracted from Smokeview, which presents the FDS result data.

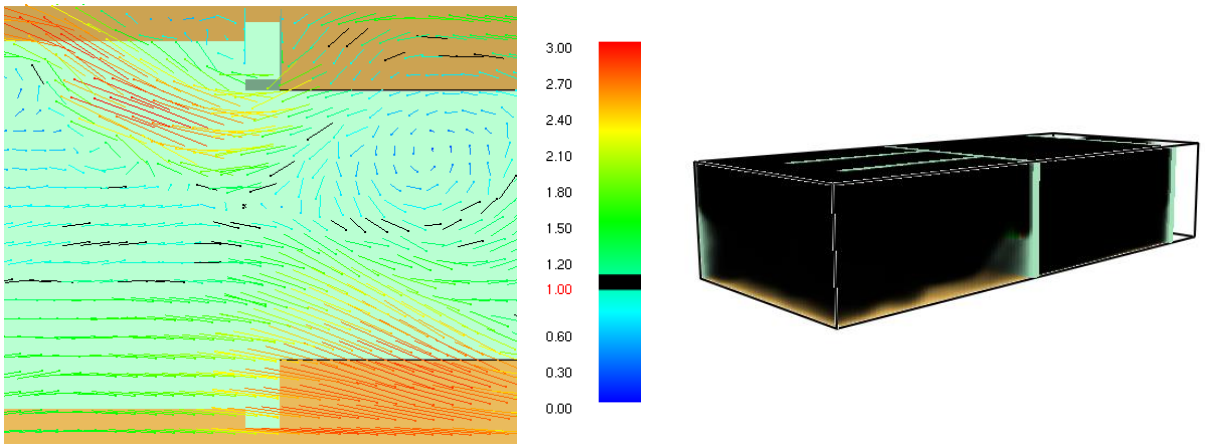

Figure 5.11: Airflow and smoke-flow at steady-state conditions, through the opening connecting the compartments of Model A1. 2000 kW HRR. 1,60 m^3/s air supply rate. 1,00 m/s airflow through the opening. Image extracted from Smokeview, which presents the FDS result data

.

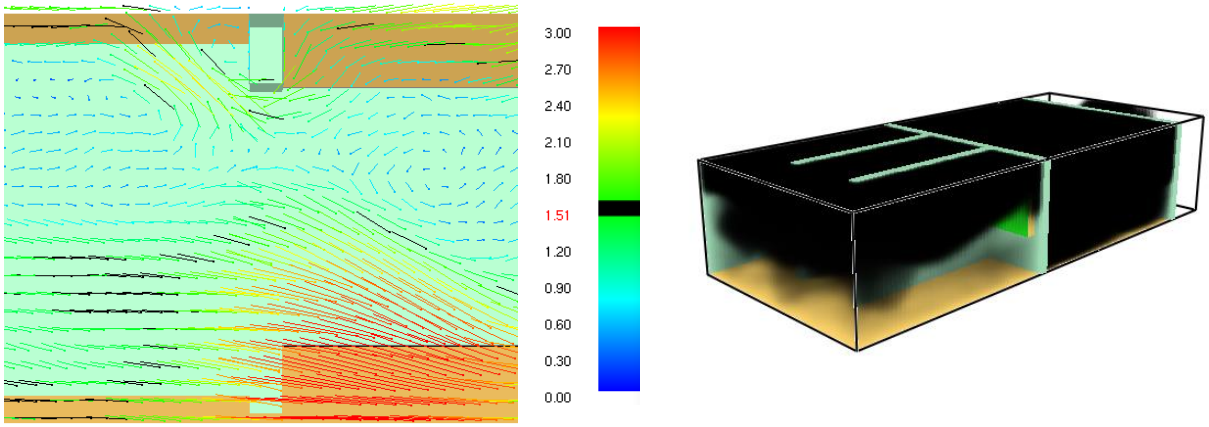

Figure 5.12: Airflow and smoke-flow at steady-state conditions, through the opening connecting the compartments of Model A1. 2000 kW HRR. 2,40 m^3/s air supply rate. 1,50 m/s airflow through the opening. Image extracted from Smokeview, which presents the FDS result data.

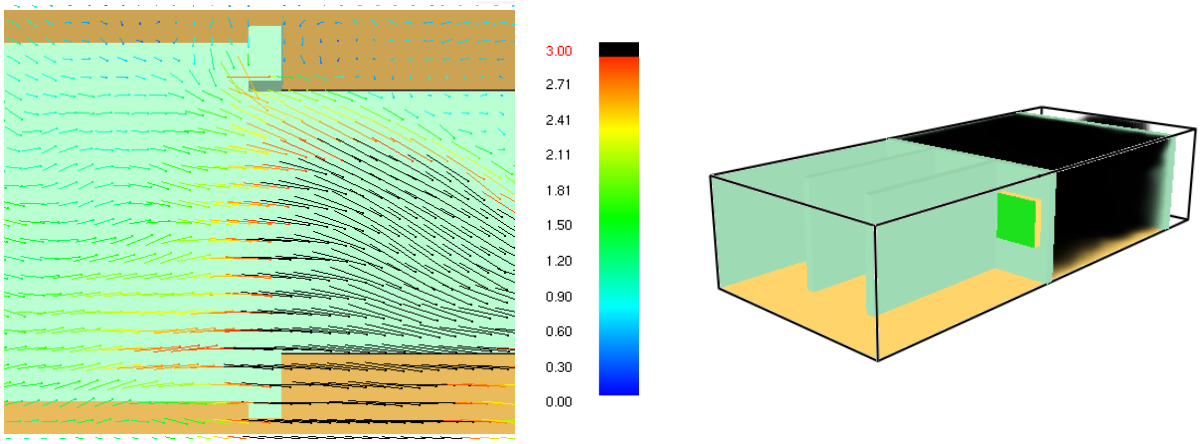

Figure 5.13: Airflow and smoke-flow at steady-state conditions, through the opening connecting the compartments of Model A1. 2000 kW HRR. 4,80 m^3/s air supply rate. 3,00 m/s airflow through the opening. Image extracted from Smokeview, which presents the FDS result data.

The flow of air and smoke is illustrated in Figure 5.9, Figure 5.10, Figure 5.11, Figure 5.12 and Figure 5.13. The model geometry A1, 2000 kW HRR, is used as a reference. The position of the neutral plane is mid-height of the opening, with the air supply deactivated. Hot smoke flows into the pressurized compartment in the top of the opening, other gas species flow out in the opposite direction. Since the air supply is deactivated in this situation, the outflowing gas species consist of smoke which has been cooled down in the pressurized compartment. It also consists of byproducts of air, like N_2 and unconsumed O_2. The byproducts of air enter the fire room compartment through the ventilation openings and spread to the pressurized compartment along with the smoke, and then circle back to the fire room compartment.

As the air supply is activated, the neutral plane rises to a higher level above the floor. The air being supplied is concentrated to exit through the bottom of the opening and demands a larger part of the opening area. This means that a smaller part of the opening area is left for the smoke to enter the compartment. The velocity is higher further away from the neutral plane, that is in the top and bottom of the opening.

As the air supply increases, the neutral plane rises further above the floor, closer to the top of the opening. At a point, the air supply rate is high enough to stop the flow of smoke to the pressurized compartment. In the opposite direction, the flow of air takes up the whole opening. The neutral plane reaches the top of the opening.

The figures illustrate increased airflow velocity towards the fire room compartment, and decreased smoke-flow velocity in the opposite direction, as the air supply increases. By studying the images, we notice that the velocity of air is the highest right outside of the opening on the fire room compartment side. The velocity of smoke is the highest right outside of the opening on the pressurized compartment side.

6. Conclusion

Smoke control systems are used to control and restrict the spread of fire and smoke to adjacent spaces. The airflow criterion of a pressurization system controls the spread of smoke by generating a flow of air through any opening, which prevents the spread of smoke in the opposite direction.

This principle has been investigated with FDS (Fire Dynamics Simulator). A total of 74 simulations has been conducted to assess the impact of the generated airflow on various HRRs.

Six model geometries have been used to perform the analysis, where four of them consist of a fire room compartment and a pressurized compartment, which are connected with an opening. Two model geometries have a lobby compartment between the fire room compartment and the pressurized compartment. The fire source area is located in the fire room compartment, which generates various HRRs. Air supply points are located in the pressurized compartment. The HRR generates fire products which spread to the pressurized compartment. The air supplied to the model generates a flow of air in the opening connecting the compartment, which restricts the amount of fire products spreading in the opposite direction. The product density development is recorded in each compartment due to various HRRs contra various air supply rates.

It is found that the product density in each compartment grows as the HRR grows. The product density in the pressurized compartment decreases as the air supply rate increases, and at a high enough air supply rate, the pressurized compartment becomes 100 % smoke-free. By increasing the ventilation openings in the fire room compartment, more smoke will escape the model. An increased ventilation opening area results in a lower product density in the pressurized compartment. The product density development in the fire room compartment is affected by the air supply rate from the pressurized compartment. With the ventilation opening being in front of the opening connecting the two compartments, more smoke escapes the model at higher air supply rates due to a direct momentum from the air supply to the ventilation opening. The product density decreases as the air supply rate increases. With the ventilation openings located on the sidewalls and not in front of the opening connecting the two compartments, the product density remains unchanged as the air supply rate is altered.

By implementing a lobby compartment between the pressurized compartment and the fire room compartment, the air supply rate can be decreased to achieve the same product density in the pressurized compartment as without a lobby compartment. To achieve a 100 % smoke-free pressurized compartment with a lobby compartment, the air supply rate can be decreased by 50 % compared to the same case without a lobby compartment. The lobby compartment works as a barrier, due to it having two openings between the fire room compartment and the pressurized compartment, which restricts the flow of smoke. It should be noticed that the product density in the lobby compartment is higher than the product density in the pressurized compartment without a lobby compartment, with the air supply activated.

It is found that an expansion of the pressurized compartment does not affect the product density development in either the fire room compartment or the pressurized compartment. By expanding the fire room compartment the product density with the air supply deactivated is increased in the pressurized compartment, compared to the other models. By expanding the fire room compartment

the product density with the air supply activated is decreased in the pressurized compartment, compared to the other models. The product density in the fire room compartment is increased as the fire room compartment is expanded, for each air supply rate scenario.

The airflow created through the opening connecting the compartments, and the smoke flowing in the opposite direction, creates a neutral plane. The neutral plane is visually been observed in the result data. As the airflow increases, the height of the neutral plane increases. It is noticed that the flow velocities are the highest right outside of each side of the opening. The neutral plane rises to the top of the opening when the air supply rate is high enough to prevent the flow of smoke in the opposite direction.

7. Further studies

The following suggestions are made regarding further studies of the airflow smoke control criterion.

- **Increased height of the pressurized compartment:** By increasing the height of the pressurized compartment, a smoke-free layer is expected to form below a smoke layer. It is suggested to investigate if higher ceilings require an increased air supply rate to keep the pressurized compartment smoke-free. Perhaps more supply points are required in the heights to achieve tenable conditions on the top of the compartment.
- **Ventilation controlled fires:** Simulations of fuel-controlled fires were conducted in this study. The HRR of a ventilation-controlled fire increases as the ventilation opening area increase. Further work on the assessment of the product density development for ventilation-controlled fires is suggested to be investigated. Perhaps the product density development in the pressurized compartment remains unchanged as the HRR increase. The air supplied to a ventilation controlled fire can also increase the HRR.
- **Time-depended openings:** FDS supports the function to remove and add obstructions at a certain time. By keeping the opening between the fire room compartment and the pressurized compartment open for a shorter time, the mass of smoke entering the pressurized compartment can be recorded for various HRRs. It is suggested to study how this amount of smoke can be removed in an effective way.
- **Pressurized lobby compartment:** By locating the air supply points in the lobby compartment, a flow of air is generated in the openings towards the fire room compartment and the "protected" compartment. Pre-studies to this thesis indicated that it is more difficult to achieve a successful solution by pressurizing the lobby compartment, due to the supplied air being concentrated to one opening instead of both. It is suggested to investigate the possibility to prevent the spread of smoke to the protected compartment, using a pressurized lobby compartment.
- **Leaks:** FDS supports the possibility to model leaks through very small openings in for example a door, with the HVAC function. These leaks are typically smaller than the cell sizes. This function can be used to investigate the overpressure criterion, by analysing the pressure difference between the pressurized compartment and the fire room compartment for various HRRs and various air supply rates.

8. Bibliography

[1] J. H. Klote, "Smoke Control," in *SFPE Handbook of Fire Protection Engineering, Fifth Edition*, New York, Springer, 2016.

[2] B. Karlsson and J. G. Quintiere, "Pressure Profiles and Vent Flows for Well-Ventilated Enclosures," in *Enclosure Fire Dynamics*, Boca Raton, CRC Press, 2000.

[3] J. H. Klote, "Pressurized Stairwells," in *Handbook of Smoke Control Engineering*, Atlanta, ASHRAE, 2012.

[4] Standard Norge, "NS-EN 12101-6:2005, Smoke and heat control systems - Part 6: Specification for pressure differential systems - Kits - (Corrigendum AC:2006 incorporated)," Standard Norge, 2005.

[5] J. H. Klote, "Flow of Air and Smoke," in *Handbook of Smoke Control Engineering*, Atlanta, ASHRAE, 2012.

[6] N. A. Koplon, "Report of the Henry Grady fire tests," City of Atlanta Building Department, Atlanta, 1973.

[7] N. A. Koplon, "A partial report of the Henry Grady fire tests," Symposium on Experience and Applications on Smoke and Fire Control, ASHRAE Annual Meeting, Louisville, 1973.

[8] J. H. Klote, "Basics of Passive and Pressurization Systems," in *Handbook of Smoke Control Engineering*, Atlanta, ASHRAE, 2012.

[9] P. R. DeCicco, "Smoke and fire control in high-rise office buildings—Part I: full-scale tests for establishing standards," Symposium on Experience and Applications on Smoke and Fire Control, ASHRAE Annual Meeting, Louisville, 1973.

[10] R. J. Cresci, "Smoke and fire control in high-rise office buildings—Part II: analysis of stair pressurization systems," Symposium on Experience and Applications on Smoke and Fire Control, ASHRAE Annual Meeting, Louisville, 1973.

[11] J. H. Klote, "Fire experiments of zoned smoke control at the Plaza Hotel in Washington, DC," ASHRAE Transactions 96 (2), 1990.

[12] G. T. Tamura and J. H. Klote, "Experimental fire tower studies on elevator pressurization systems for smoke control," ASHRAE Transactions 93(2)., p. 1987.

[13] G. T. Tamura and J. H. Klote, "Experimental fire tower studies on mechanical pressurization to control smoke movement caused by fire pressures," Proceedings of the 2nd International Symposium on Fire Safety Science, Tokyo, 1987.

[14] G. T. Tamura and J. H. Klote, "Experimental fire tower studies on adverse pressures caused by stack and wind action: studies on smoke movement and control," ASTM International Symposium on Characterization and Toxicity of Smoke, Phoenix, 1988.

[15] G. T. Tamura, "Stair pressurization systems for smoke control - design considerations," in *ASHRAE Transactions, Vol. 95*, ASHRAE, 1989.

[16] G. T. Tamura, "Field tests of stair pressurization systems with overpressure relief," in *ASHRAE Transactions, Vol. 96*, ASHRAE, 1990.

[17] G. T. Tamura, "Fire tower tests of stair pressurization systems with overpressure relief," in *ASHRAE Transactions Vol 96*, ASHRAE, 1990.

[18] G. T. Tamura, "Fire tower tests of stair pressurization systems with mechanical venting of the fire floor," in *ASHRAE Transactions, Vol. 96*, ASHRAE, 1990.

[19] B. Karlsson and J. G. Quintiere, "A Qualitative Description of Enclosure Fires," in *Enclosure Fire Dynamics*, Boca Raton, CRC Press, 2000.

[20] B. C. Hagen, Grunnleggende brannteknikk, Haugesund: B.C. Hagen, 2004.

[21] D. Drysdale, "The Pre-flashover Compartment Fire," in *An Introduction to Fire Dynamics. Third Edition*, Chichester, John Wiley & Sons, Ltd , 2011.

[22] B. Karlsson and J. G. Quintiere, "Energy Release Rates," in *Enclosure Fire Dynamics*, Boca Raton, CRC Press, 2000.

[23] Standard Norge, "SN-INSTA/TS 950:2014 Fire Safety Engineering - Comparative method to verify fire safety design in buildings," Standard Norge, 2014.

[24] B. Karlsson and J. G. Quintiere, "Gas Temperatures in Ventilated Enclosure Fires," in *Enclosure Fire Dynamics*, Boca Raton, CRC Press, 2000.

[25] Standard Norge, "NS-EN 1991-1-2:2002 Eurocode 1: Actions on structures - Part 1-2: General actions - Actions on structures exposed to fire.," Standard Norge, 2002.

[26] L. Staffansnon, "Selecting design fires," Lunds Universitet, Lund, 2010.

[27] B. Karlsson and J. G. Quintiere, "Fire Plumes and Flame Heights," in *Enclosure Fire Dynamics*, Boca Raton, CRC Press, 2000.

[28] G. Cox and S. Kumar, "Modeling enclosure Fires Using CFD," in *SFPE Handbook of Fire Protection Engineering, Third edition*, Quincy, Massachusetts, The National Fire Protection Association, 2002.

[29] K. McGrattan and S. Miles, "Modeling Fires Using Computational Fluid Dynamics (CFD)," in *SFPE Handbook of Fire Protection Engineering, Fifth Edition*, New York, Springer, 2016.

[30] G. H. Yeoh and K. K. Yuen, "Introduction," in *Computational Fluid Dynamics in Fire Engineering*, Burlington, Elsevier Inc, 2009.

[31] B. Karlsson and J. G. Quintiere, "Introduction," in *Enclosure Fire Dynamics*, Boca Raton, CRC Press, 2000.

[32] "caefn.com," [Online]. Available: https://caefn.com/openfoam/rans. [Accessed 20 01 2020].

[33] "southampton.ac.uk," [Online]. Available: http://www.southampton.ac.uk/~zxie/SESS6021/CCMP/online1/143-usingLargeEddySimulation-02.html. [Accessed 20 01 2020].

[34] NIST, NIST Special Publication 1019, Sixth Edition, Fire Dynamics Simulator, User's Guide, NIST, 2019.

[35] H. Cheng, L. J. Zhou and Y. Z. Zhao, "Very large eddy simulation of swirling flow in the Dellenback," IOP Publishing, https://iopscience.iop.org/article/10.1088/1755-1315/163/1/012084/pdf, 2018.

[36] NIST, NIST Special Publication 1018-3, Sixth Edition, Fire Dynamics Simulator, Technical Reference Guide, Volume 3: Validation, NIST, 2019.

[37] NIST, NIST Special Publication 1018-2, Sixth Edition, Fire Dynamics Simulator Technical Reference Guide Volume 2: Verification, NIST, 2019.

[38] CFD Best Practice, Best Practice gruppen, 2009.

[39] "Thunderhead Engineering," [Online]. Available: https://www.thunderheadeng.com/pyrosim/. [Accessed 08 05 2020].

[40] Sintef, "520.380 Røykkontroll i bygninger," Sintef, 2006.

[41] "ISO 9705-1:2016, Reaction to fire tests — Room corner test for wall and ceiling lining products — Part 1: Test method for a small room configuration," 2006.

[42] "Gyproc (page 8)," [Online]. Available: https://www.gyproc.no/sites/gypsum.nordic.master/files/gyproc-site/document-files/MONTBranncellebegrensedeVegger.pdf. [Accessed 12 12 2019].

[43] "Norgips (page 2)," [Online]. Available: https://norgips.no/assets/planningpdfs/Prosjekteringsh%C3%A5ndbok/Himling-og-etasjeskillere.pdf. [Accessed 12 12 2019].

[44] D. Drysdale, "Heat Transfer," in *An Introduction to Fire Dynamics, Third Edition*, Chichester, John Wiley & Sons, Ltd, 2011.

[45] "BFS 2013:12 BBRAD 3 Boverkets ändring av verkets allmänna råd (2011:27) om analytisk dimensionering av byggnaders brandskydd.," Boverket, 2011.

[46] "BIV:s tillämpningsdokument 2/2013 – Utgåva 1, CFD-beräkningar med FDS," Föreningen för brandteknisk ingenjörsvetenskap, 2013.

[47] "Brannforum.no - Pressurization system factors," [Online]. Available: http://www.brannforum.com/Presentasjoner/Trykksetting%20trapperom%20GJEN%20April%202007.pdf. [Accessed 15 01 2020].

[48] "Engineering Toolbox," [Online]. Available: https://www.engineeringtoolbox.com/air-composition-d_212.html. [Accessed 15 02 2020].

Appendix

A.1. Additional result data

The time history of the product density development for each scenario and each compartment is presented in this section. In addition, the time history of the product volume fraction development is presented for Model A1.

A.1.1. Model A1

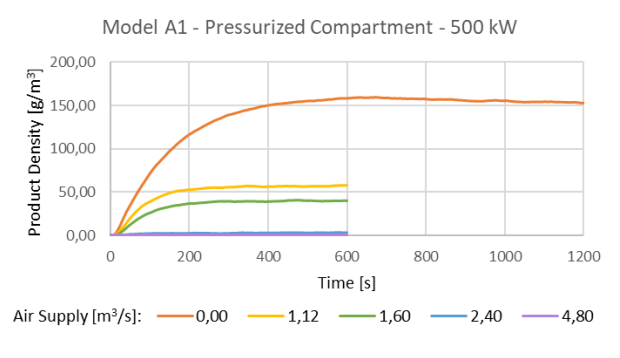
Model A1 - Pressurized Compartment - 500 kW
Product Density [g/m³]
200,00
150,00
100,00
50,00
0,00
0
200
400
600
800
1000
1200
Time [s]
Air Supply [m³/s]: 0,00 1,12 1,60 2,40 4,80

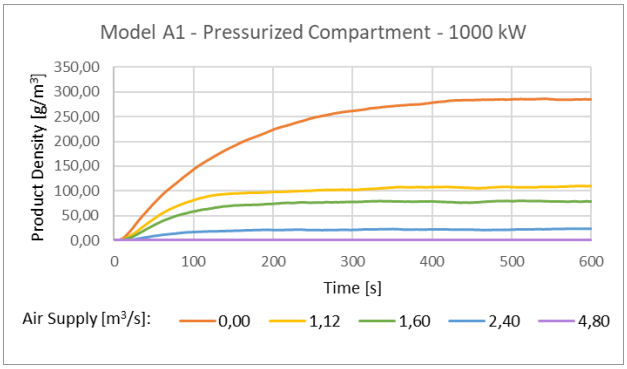
Model A1 - Pressurized Compartment - 1000 kW
Product Density [g/m³]
350,00
300,00
250,00
200,00
150,00
100,00
50,00
0,00
0
100
200
300
400
500
600
Time [s]
Air Supply [m³/s]: 0,00 1,12 1,60 2,40 4,80

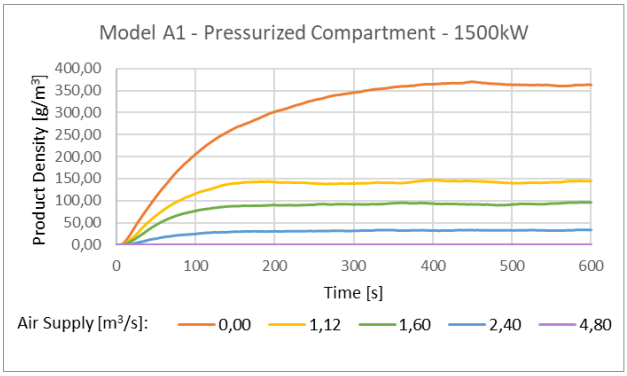
Model A1 - Pressurized Compartment - 1500kW
Product Density [g/m³]
400,00
350,00
300,00
250,00
200,00
150,00
100,00
50,00
0,00
0
100
200
300
400
500
600
Time [s]
Air Supply [m³/s]: 0,00 1,12 1,60 2,40 4,80

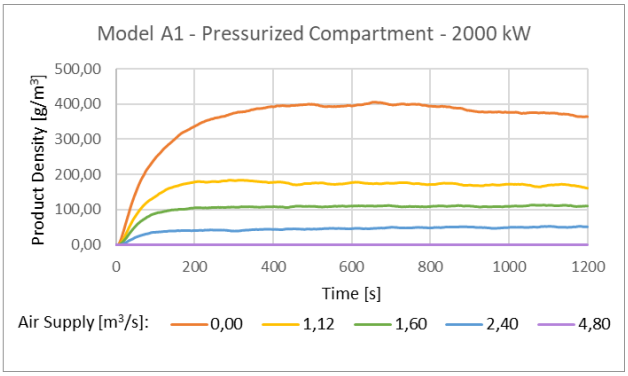
Model A1 - Pressurized Compartment - 2000 kW
Product Density [g/m³]
500,00
400,00
300,00
200,00
100,00
0,00
0
200
400
600
800
1000
1200
Time [s]
Air Supply [m³/s]: 0,00 1,12 1,60 2,40 4,80

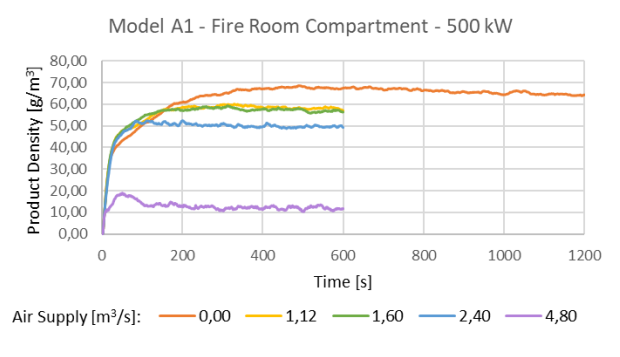
Model A1 - Fire Room Compartment - 500 kW
Product Density [g/m³]
80,00
70,00
60,00
50,00
40,00
30,00
20,00
10,00
0,00
0
200
400
600
800
1000
1200
Time [s]
Air Supply [m³/s]: 0,00 1,12 1,60 2,40 4,80


Model A1 - Fire Room Compartment - 1000 kW
Product Density [g/m³]
140,00
120,00
100,00
80,00
60,00
40,00
20,00
0,00
0
100
200
300
400
500
600
Time [s]
Air Supply [m³/s]: 0,00 1,12 1,60 2,40 4,80

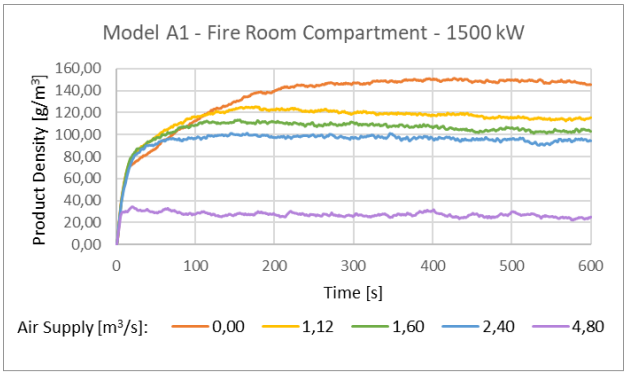
Model A1 - Fire Room Compartment - 1500 kW
Product Density [g/m³]
160,00
140,00
120,00
100,00
80,00
60,00
40,00
20,00
0,00
0
100
200
300
400
500
600
Time [s]
Air Supply [m³/s]: 0,00 1,12 1,60 2,40 4,80

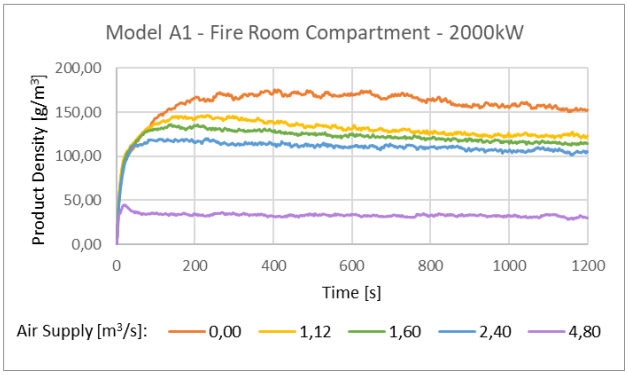
Model A1 - Fire Room Compartment - 2000kW
Product Density [g/m³]
200,00
150,00
100,00
50,00
0,00
0
200
400
600
800
1000
1200
Time [s]
Air Supply [m³/s]: 0,00 1,12 1,60 2,40 4,80

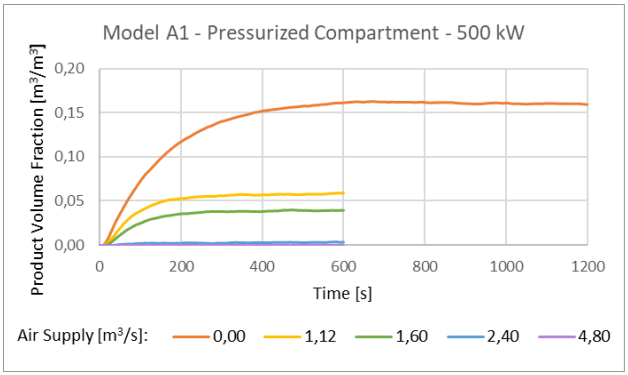
Model A1 - Pressurized Compartment - 500 kW
Product Volume Fraction [m³/m³]
0,20
0,15
0,10
0,05
0,00
0
200
400
600
800
1000
1200
Time [s]
Air Supply [m³/s]:
0,00
1,12
1,60
2,40
4,80

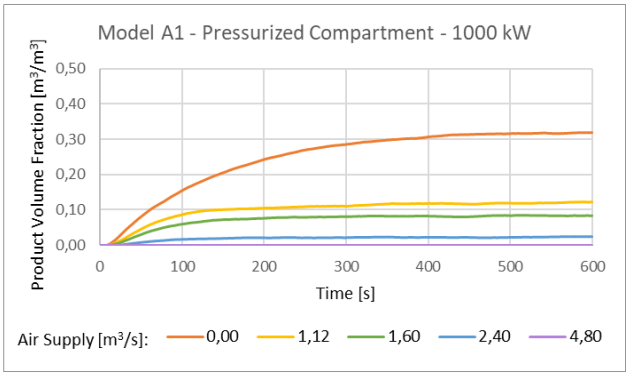
Model A1 - Pressurized Compartment - 1000 kW
Product Volume Fraction [m³/m³]
0,50
0,40
0,30
0,20
0,10
0,00
0
100
200
300
400
500
600
Time [s]
Air Supply [m³/s]:
0,00
1,12
1,60
2,40
4,80

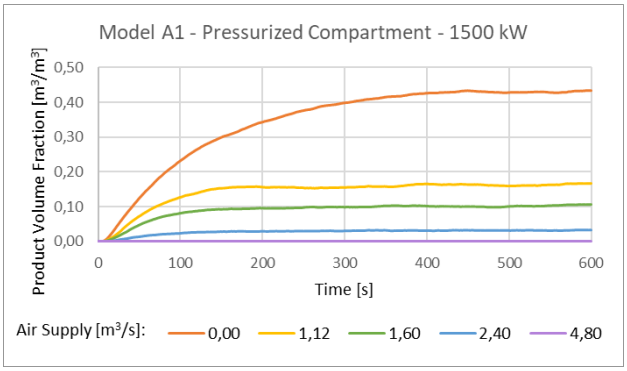
Model A1 - Pressurized Compartment - 1500 kW
Product Volume Fraction [m³/m³]
0,50
0,40
0,30
0,20
0,10
0,00
0
100
200
300
400
500
600
Time [s]
Air Supply [m³/s]:
0,00
1,12
1,60
2,40
4,80

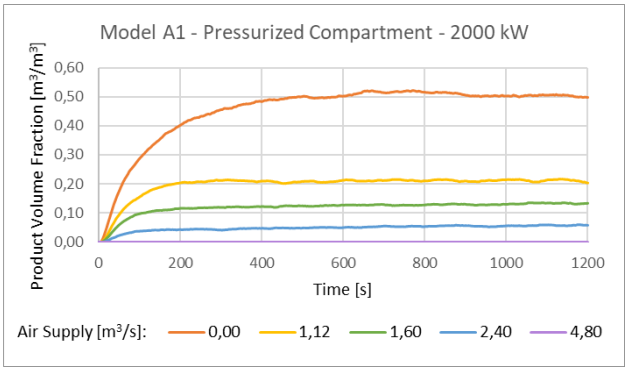
Model A1 - Pressurized Compartment - 2000 kW
Product Volume Fraction [m³/m³]
0,60
0,50
0,40
0,30
0,20
0,10
0,00
0
200
400
600
800
1000
1200
Time [s]
Air Supply [m³/s]:
0,00
1,12
1,60
2,40
4,80

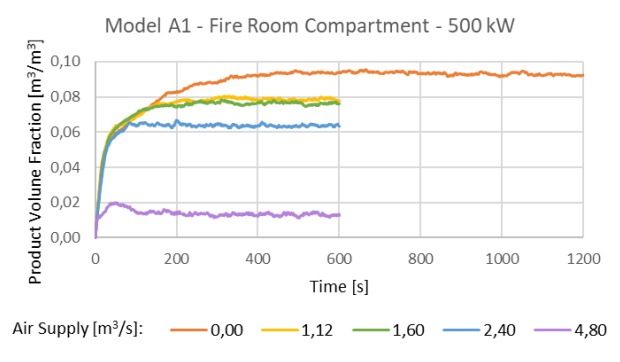
Model A1 - Fire Room Compartment - 500 kW
Product Volume Fraction [m³/m³]
0,10
0,08
0,06
0,04
0,02
0,00
0
200
400
600
800
1000
1200
Time [s]
Air Supply [m³/s]:
0,00
1,12
1,60
2,40
4,80

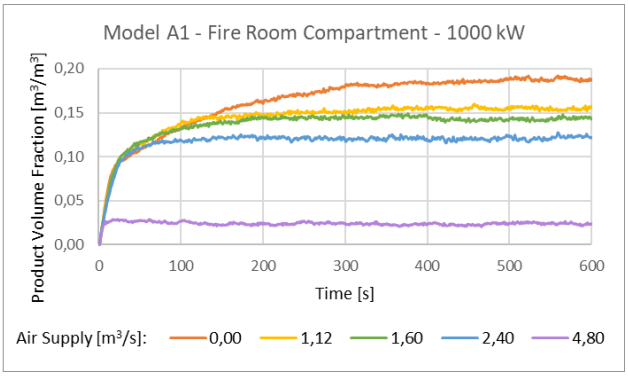
Model A1 - Fire Room Compartment - 1000 kW
Product Volume Fraction [m³/m³]
0,20
0,15
0,10
0,05
0,00
0
100
200
300
400
500
600
Time [s]
Air Supply [m³/s]:
0,00
1,12
1,60
2,40
4,80

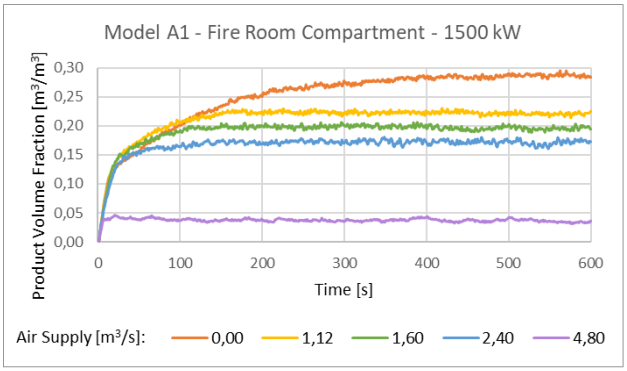
Model A1 - Fire Room Compartment - 1500 kW
Product Volume Fraction [m³/m³]
0,30
0,25
0,20
0,15
0,10
0,05
0,00
0
100
200
300
400
500
600
Time [s]
Air Supply [m³/s]:
0,00
1,12
1,60
2,40
4,80


Model A1 - Fire Room Compartment - 2000 kW
Product Volume Fraction [m³/m³]
0,40
0,35
0,30
0,25
0,20
0,15
0,10
0,05
0,00
0
200
400
600
800
1000
1200
Time [s]
Air Supply [m³/s]:
0,00
1,12
1,60
2,40
4,80

A.1.2. Model A2

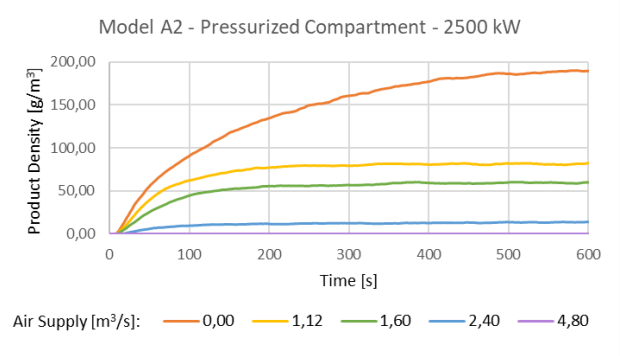
Model A2 - Pressurized Compartment - 2500 kW
Product Density [g/m³]
200,00
150,00
100,00
50,00
0,00
0
100
200
300
400
500
600
Time [s]
Air Supply [m³/s]:
0,00
1,12
1,60
2,40
4,80

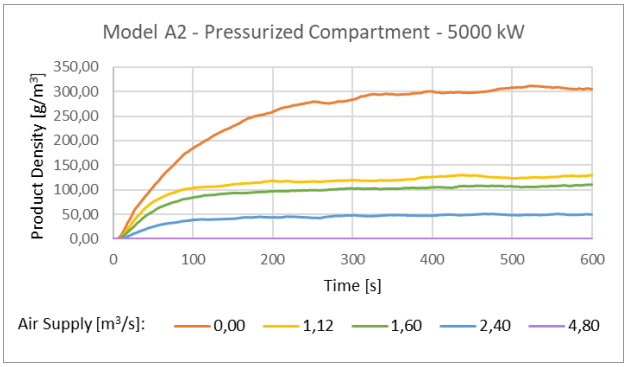
Model A2 - Pressurized Compartment - 5000 kW
Product Density [g/m³]
350,00
300,00
250,00
200,00
150,00
100,00
50,00
0,00
0
100
200
300
400
500
600
Time [s]
Air Supply [m³/s]:
0,00
1,12
1,60
2,40
4,80

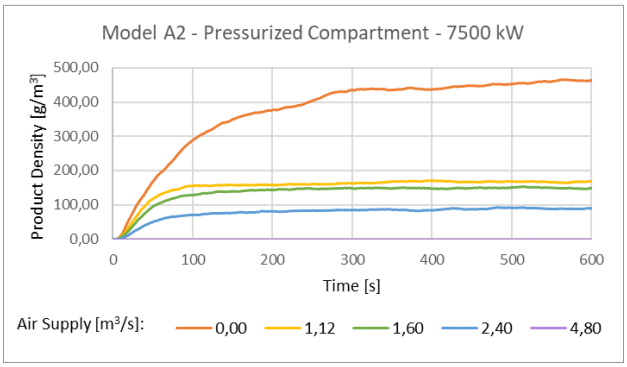
Model A2 - Pressurized Compartment - 7500 kW
Product Density [g/m³]
500,00
400,00
300,00
200,00
100,00
0,00
0
100
200
300
400
500
600
Time [s]
Air Supply [m³/s]:
0,00
1,12
1,60
2,40
4,80

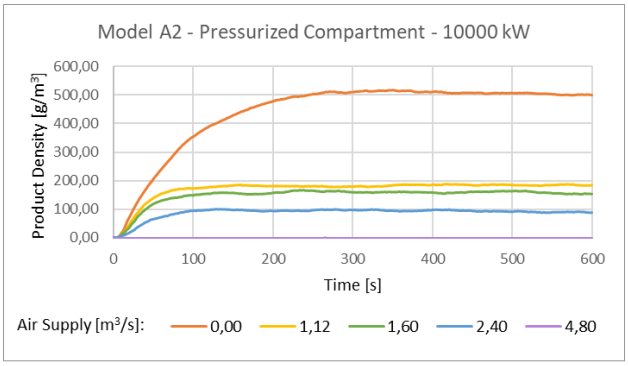
Model A2 - Pressurized Compartment - 10000 kW
Product Density [g/m³]
600,00
500,00
400,00
300,00
200,00
100,00
0,00
0
100
200
300
400
500
600
Time [s]
Air Supply [m³/s]:
0,00
1,12
1,60
2,40
4,80

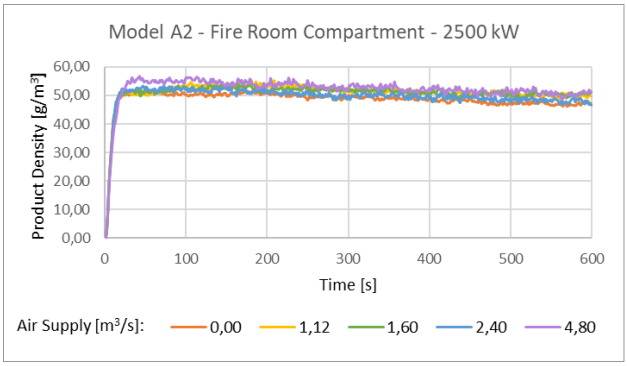
Model A2 - Fire Room Compartment - 2500 kW
Product Density [g/m³]
60,00
50,00
40,00
30,00
20,00
10,00
0,00
0
100
200
300
400
500
600
Time [s]
Air Supply [m³/s]:
0,00
1,12
1,60
2,40
4,80

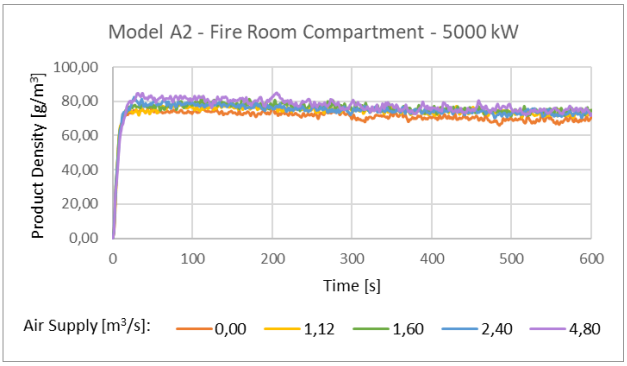
Model A2 - Fire Room Compartment - 5000 kW
Product Density [g/m³]
100,00
80,00
60,00
40,00
20,00
0,00
0
100
200
300
400
500
600
Time [s]
Air Supply [m³/s]:
0,00
1,12
1,60
2,40
4,80

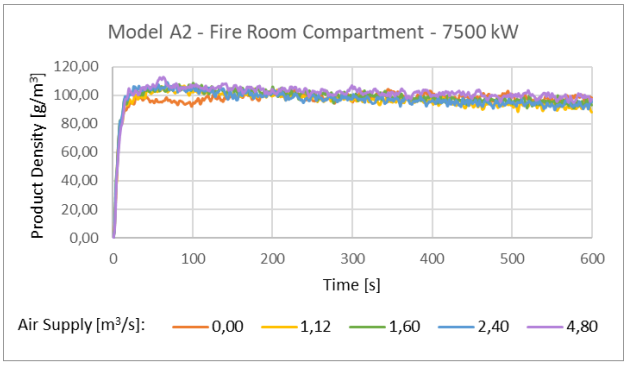
Model A2 - Fire Room Compartment - 7500 kW
Product Density [g/m³]
120,00
100,00
80,00
60,00
40,00
20,00
0,00
0
100
200
300
400
500
600
Time [s]
Air Supply [m³/s]:
0,00
1,12
1,60
2,40
4,80


Model A2 - Fire Room Compartment - 10000 kW
Product Density [g/m³]
160,00
140,00
120,00
100,00
80,00
60,00
40,00
20,00
0,00
0
100
200
300
400
500
600
Time [s]
Air Supply [m³/s]:
0,00
1,12
1,60
2,40
4,80

A.1.3. Model B1

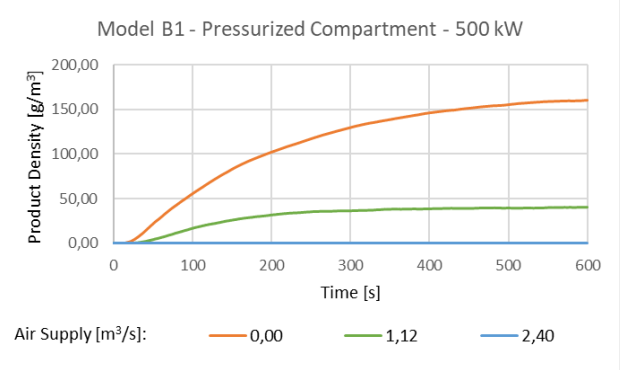
Model B1 - Pressurized Compartment - 500 kW
Product Density [g/m³]
200,00
150,00
100,00
50,00
0,00
0
100
200
300
400
500
600
Time [s]
Air Supply [m³/s]:
0,00
1,12
2,40

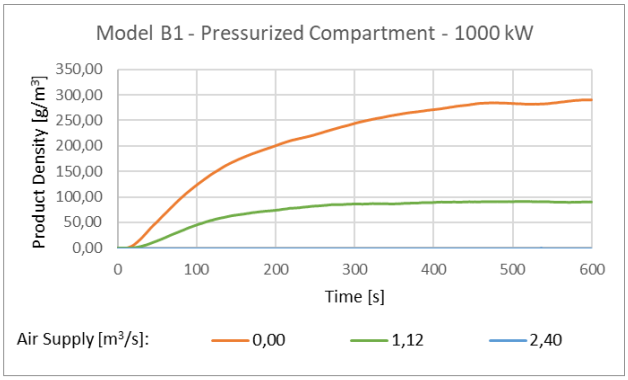
Model B1 - Pressurized Compartment - 1000 kW
Product Density [g/m³]
350,00
300,00
250,00
200,00
150,00
100,00
50,00
0,00
0
100
200
300
400
500
600
Time [s]
Air Supply [m³/s]:
0,00
1,12
2,40

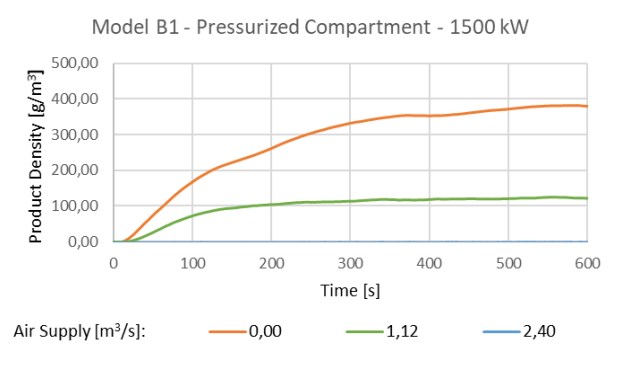
Model B1 - Pressurized Compartment - 1500 kW
Product Density [g/m³]
500,00
400,00
300,00
200,00
100,00
0,00
0
100
200
300
400
500
600
Time [s]
Air Supply [m³/s]:
0,00
1,12
2,40

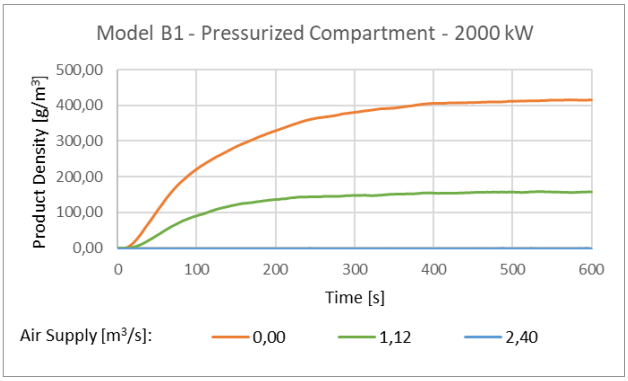
Model B1 - Pressurized Compartment - 2000 kW
Product Density [g/m³]
500,00
400,00
300,00
200,00
100,00
0,00
0
100
200
300
400
500
600
Time [s]
Air Supply [m³/s]:
0,00
1,12
2,40

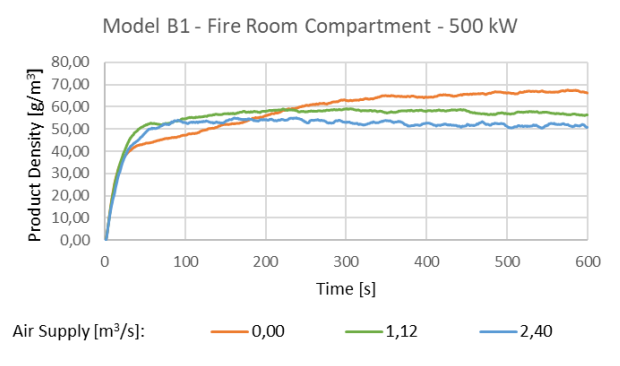
Model B1 - Fire Room Compartment - 500 kW
Product Density [g/m³]
80,00
70,00
60,00
50,00
40,00
30,00
20,00
10,00
0,00
0
100
200
300
400
500
600
Time [s]
Air Supply [m³/s]:
0,00
1,12
2,40


Model B1 - Fire Room Compartment - 1000 kW
Product Density [g/m³]
120,00
100,00
80,00
60,00
40,00
20,00
0,00
0
100
200
300
400
500
600
Time [s]
Air Supply [m³/s]:
0,00
1,12
2,40

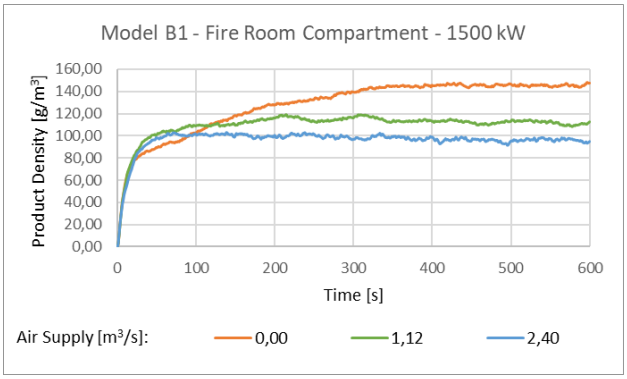
Model B1 - Fire Room Compartment - 1500 kW
Product Density [g/m³]
160,00
140,00
120,00
100,00
80,00
60,00
40,00
20,00
0,00
0
100
200
300
400
500
600
Time [s]
Air Supply [m³/s]:
0,00
1,12
2,40

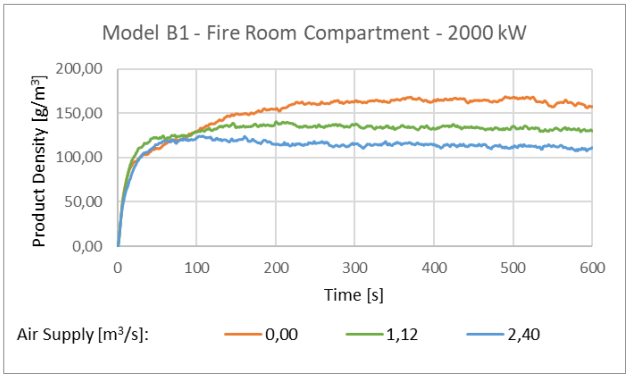
Model B1 - Fire Room Compartment - 2000 kW
Product Density [g/m³]
200,00
150,00
100,00
50,00
0,00
0
100
200
300
400
500
600
Time [s]
Air Supply [m³/s]:
0,00
1,12
2,40

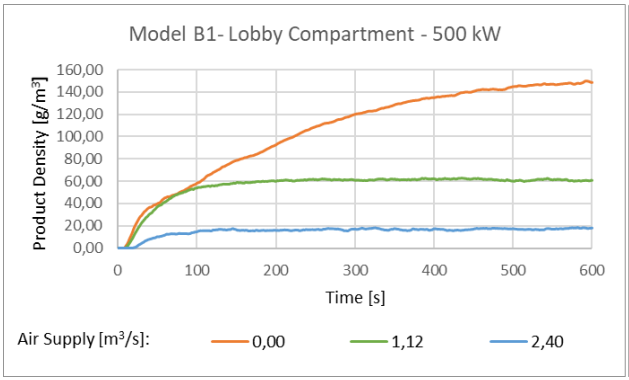
Model B1- Lobby Compartment - 500 kW
Product Density [g/m³]
160,00
140,00
120,00
100,00
80,00
60,00
40,00
20,00
0,00
0
100
200
300
400
500
600
Time [s]
Air Supply [m³/s]:
0,00
1,12
2,40

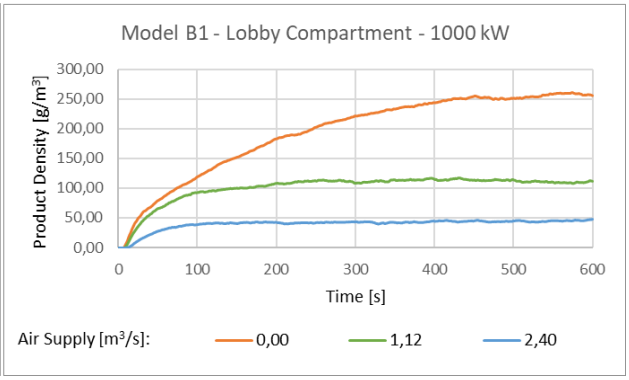
Model B1 - Lobby Compartment - 1000 kW
Product Density [g/m³]
300,00
250,00
200,00
150,00
100,00
50,00
0,00
0
100
200
300
400
500
600
Time [s]
Air Supply [m³/s]:
0,00
1,12
2,40

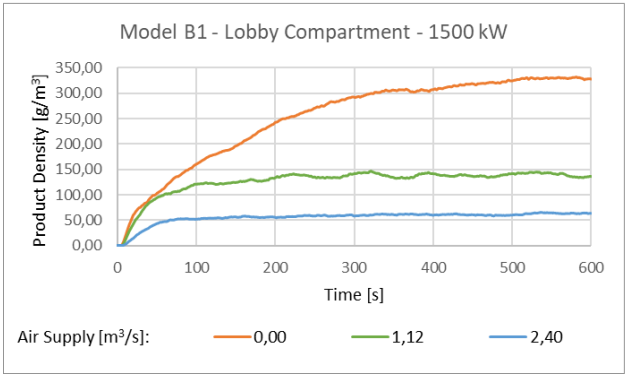
Model B1 - Lobby Compartment - 1500 kW
Product Density [g/m³]
350,00
300,00
250,00
200,00
150,00
100,00
50,00
0,00
0
100
200
300
400
500
600
Time [s]
Air Supply [m³/s]:
0,00
1,12
2,40

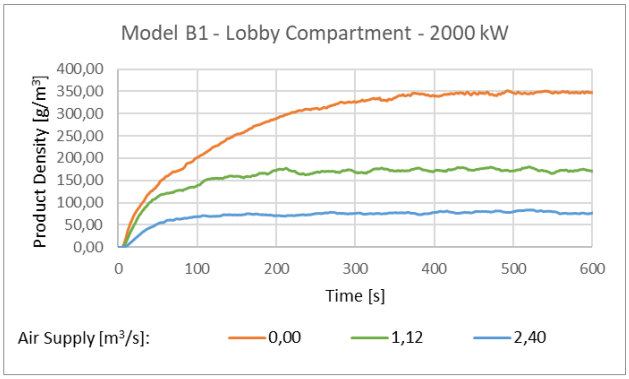
Model B1 - Lobby Compartment - 2000 kW
Product Density [g/m³]
400,00
350,00
300,00
250,00
200,00
150,00
100,00
50,00
0,00
0
100
200
300
400
500
600
Time [s]
Air Supply [m³/s]:
0,00
1,12
2,40

A.1.4. Model B2

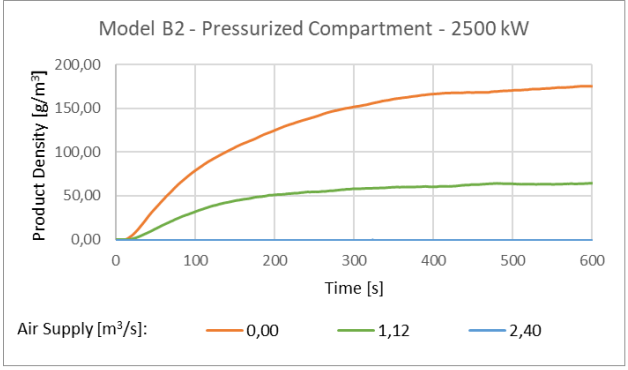
Model B2 - Pressurized Compartment - 2500 kW
Product Density [g/m³]
200,00
150,00
100,00
50,00
0,00
0
100
200
300
400
500
600
Time [s]
Air Supply [m³/s]:
0,00
1,12
2,40

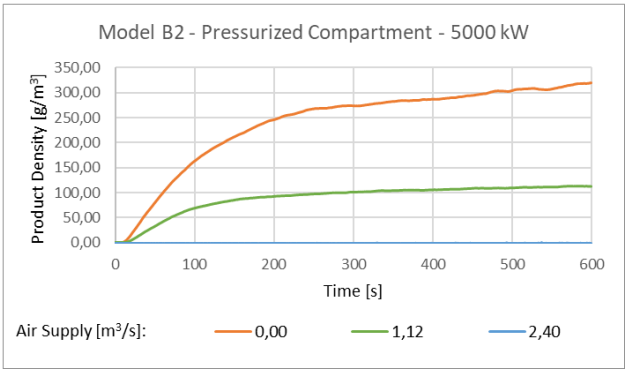
Model B2 - Pressurized Compartment - 5000 kW
Product Density [g/m³]
350,00
300,00
250,00
200,00
150,00
100,00
50,00
0,00
0
100
200
300
400
500
600
Time [s]
Air Supply [m³/s]:
0,00
1,12
2,40

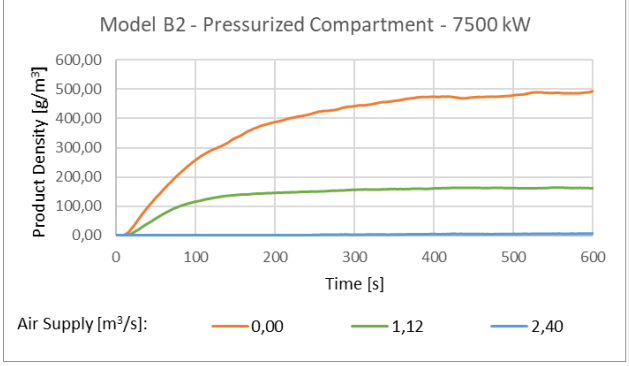
Model B2 - Pressurized Compartment - 7500 kW
Product Density [g/m³]
600,00
500,00
400,00
300,00
200,00
100,00
0,00
0
100
200
300
400
500
600
Time [s]
Air Supply [m³/s]:
0,00
1,12
2,40

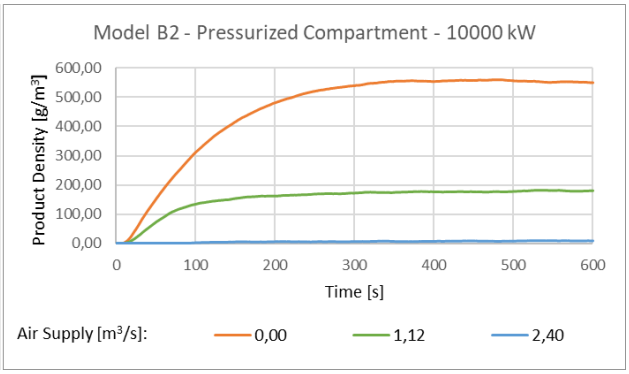
Model B2 - Pressurized Compartment - 10000 kW
Product Density [g/m³]
600,00
500,00
400,00
300,00
200,00
100,00
0,00
0
100
200
300
400
500
600
Time [s]
Air Supply [m³/s]:
0,00
1,12
2,40

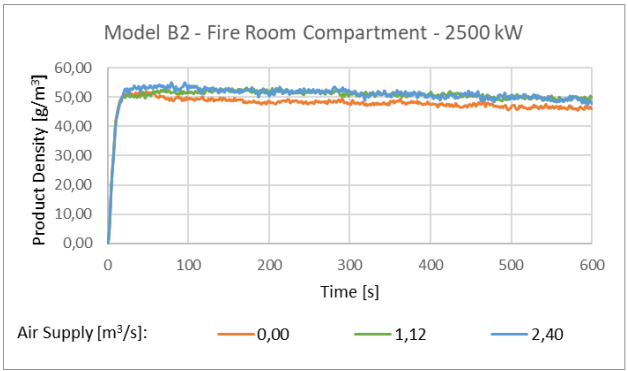
Model B2 - Fire Room Compartment - 2500 kW
Product Density [g/m³]
60,00
50,00
40,00
30,00
20,00
10,00
0,00
0
100
200
300
400
500
600
Time [s]
Air Supply [m³/s]:
0,00
1,12
2,40


Model B2 - Fire Room Compartment - 5000 kW
Product Density [g/m³]
100,00
80,00
60,00
40,00
20,00
0,00
0
100
200
300
400
500
600
Time [s]
Air Supply [m³/s]:
0,00
1,12
2,40

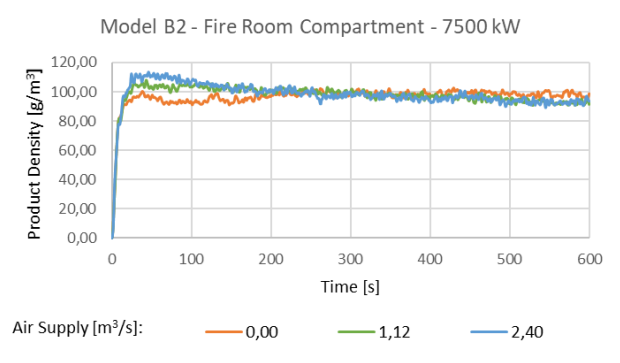
Model B2 - Fire Room Compartment - 7500 kW
Product Density [g/m³]
120,00
100,00
80,00
60,00
40,00
20,00
0,00
0
100
200
300
400
500
600
Time [s]
Air Supply [m³/s]:
0,00
1,12
2,40

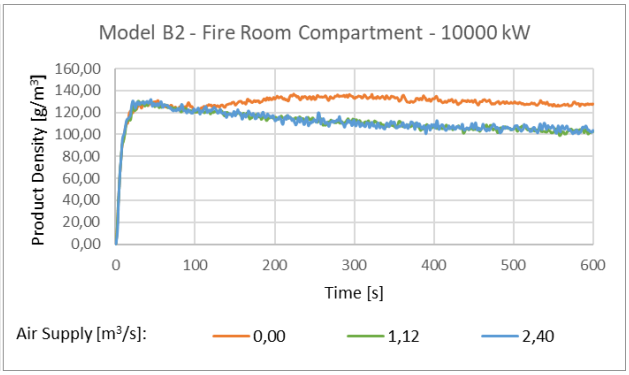
Model B2 - Fire Room Compartment - 10000 kW
Product Density [g/m³]
160,00
140,00
120,00
100,00
80,00
60,00
40,00
20,00
0,00
0
100
200
300
400
500
600
Time [s]
Air Supply [m³/s]:
0,00
1,12
2,40

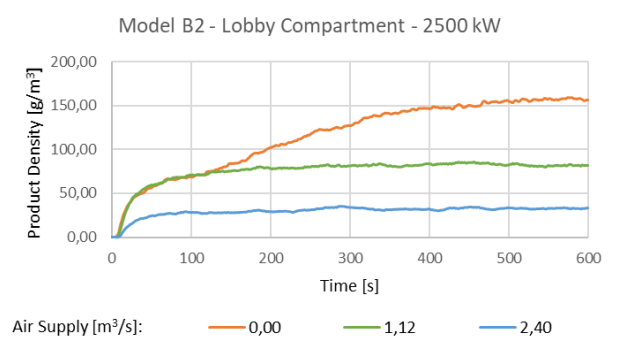
Model B2 - Lobby Compartment - 2500 kW
Product Density [g/m³]
200,00
150,00
100,00
50,00
0,00
0
100
200
300
400
500
600
Time [s]
Air Supply [m³/s]:
0,00
1,12
2,40

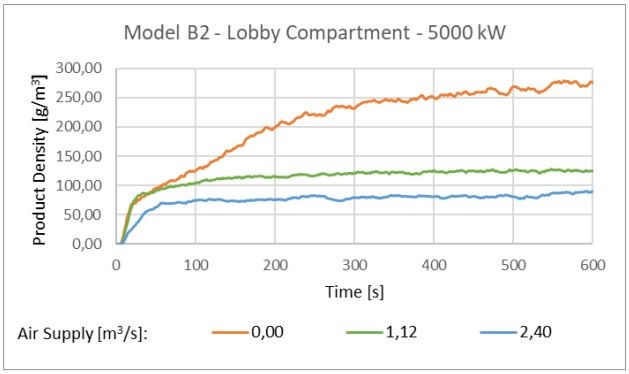
Model B2 - Lobby Compartment - 5000 kW
Product Density [g/m³]
300,00
250,00
200,00
150,00
100,00
50,00
0,00
0
100
200
300
400
500
600
Time [s]
Air Supply [m³/s]:
0,00
1,12
2,40

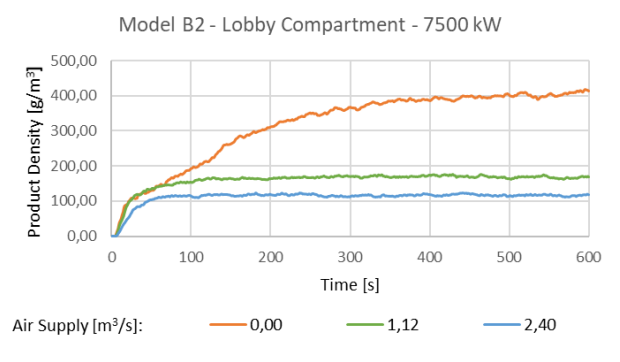
Model B2 - Lobby Compartment - 7500 kW
Product Density [g/m³]
500,00
400,00
300,00
200,00
100,00
0,00
0
100
200
300
400
500
600
Time [s]
Air Supply [m³/s]:
0,00
1,12
2,40

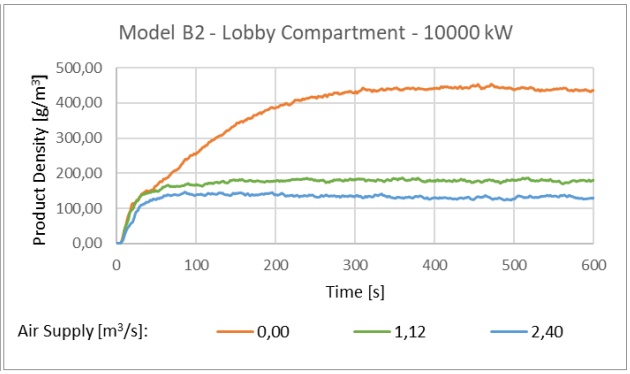
Model B2 - Lobby Compartment - 10000 kW
Product Density [g/m³]
500,00
400,00
300,00
200,00
100,00
0,00
0
100
200
300
400
500
600
Time [s]
Air Supply [m³/s]:
0,00
1,12
2,40

A.1.5. Model C

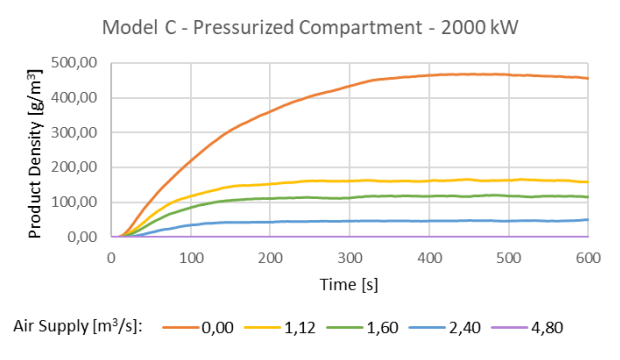

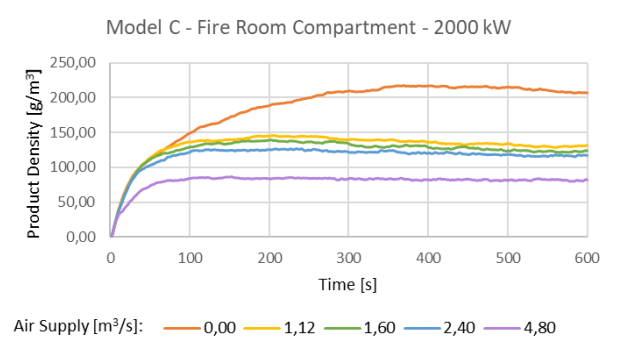

A.1.6. Model D

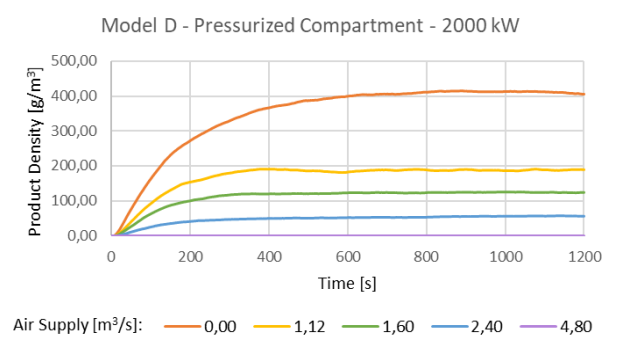

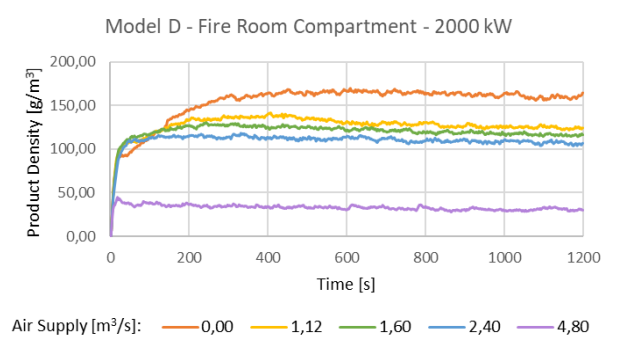

B.1. FDS input files

One FDS input file code per model geometry is presented in this section. This is the same code as used for the mesh sensitivity analysis, which is the smallest HRR and the smallest activated air supply rate. To reuse these codes for other scenarios, the following parameters must be altered:

- HRRPUA, on the `&SURF ID='FIRE'` line
- VOLUME_FLOW, on the `&SURF ID='SUPPLY'` line
- The area of the fire, x1, x2, y1 and y2 coordinates, on the `&OBST ID='Fire'` line

B.1.1. Model A1

```
&HEAD CHID='A1_500_1-12'/
&TIME T_END=600.0/
&DUMP COLUMN_DUMP_LIMIT=.TRUE., DT_RESTART=300.0, DT_SL3D=0.25/

&MESH ID='MESH 1', IJK=48,48,24, XB=0.0,4.8,0.0,4.8,0.0,2.4/
&MESH ID='MESH 2', IJK=62,48,24, XB=4.8,11.0,0.0,4.8,0.0,2.4/

&REAC ID='HoC 20 MJ/kg',
      FUEL='REAC_FUEL',
      C=4.56,
      H=6.56,
      O=2.34,
      N=0.4,
      CO_YIELD=0.1,
      SOOT_YIELD=0.1,
      HEAT_OF_COMBUSTION=2.0E4/

&MATL ID='GYPSUM PLASTER',
      SPECIFIC_HEAT=0.84,
      CONDUCTIVITY=0.48,
      DENSITY=1440.0/
&MATL ID='MINERAL WOOL, PLATES',
      SPECIFIC_HEAT=0.8,
      CONDUCTIVITY=0.041,
      DENSITY=100.0/
```

```
&MATL ID='YELLOW PINE',
      SPECIFIC_HEAT=2.85,
      CONDUCTIVITY=0.14,
      DENSITY=640.0/

&SURF ID='EI 60 WALL',
      RGB=146,202,166,
      BACKING='VOID',
      MATL_ID(1,1)='GYPSUM PLASTER',
      MATL_ID(2,1)='GYPSUM PLASTER',
      MATL_ID(3,1)='MINERAL WOOL, PLATES',
      MATL_ID(4,1)='GYPSUM PLASTER',
      MATL_ID(5,1)='GYPSUM PLASTER',
      MATL_MASS_FRACTION(1,1)=1.0,
      MATL_MASS_FRACTION(2,1)=1.0,
      MATL_MASS_FRACTION(3,1)=1.0,
      MATL_MASS_FRACTION(4,1)=1.0,
      MATL_MASS_FRACTION(5,1)=1.0,
      THICKNESS(1:5)=0.013,0.013,0.12,0.013,0.013/
&SURF ID='EI 60 CEILING',
      BACKING='VOID',
      MATL_ID(1,1)='GYPSUM PLASTER',
      MATL_ID(2,1)='GYPSUM PLASTER',
      MATL_ID(3,1)='MINERAL WOOL, PLATES',
      MATL_ID(4,1)='YELLOW PINE',
      MATL_MASS_FRACTION(1,1)=1.0,
      MATL_MASS_FRACTION(2,1)=1.0,
      MATL_MASS_FRACTION(3,1)=1.0,
      MATL_MASS_FRACTION(4,1)=1.0,
      THICKNESS(1:4)=0.0125,0.0125,0.17,5.0E-3/
&SURF ID='EI 60 FLOOR',
      BACKING='VOID',
      MATL_ID(1,1)='YELLOW PINE',
      MATL_ID(2,1)='MINERAL WOOL, PLATES',
      MATL_ID(3,1)='GYPSUM PLASTER',
```

```
      MATL_ID(4,1)='GYPSUM PLASTER',
      MATL_MASS_FRACTION(1,1)=1.0,
      MATL_MASS_FRACTION(2,1)=1.0,
      MATL_MASS_FRACTION(3,1)=1.0,
      MATL_MASS_FRACTION(4,1)=1.0,
      THICKNESS(1:4)=5.0E-3,0.17,0.0125,0.0125/
&SURF ID='FIRE',
      COLOR='RED',
      HRRPUA=1020.41,
      TMP_FRONT=300.0/
&SURF ID='SUPPLY',
      RGB=26,204,26,
      VOLUME_FLOW=-0.56/

&OBST ID='Fire', XB=7.0,7.7,2.0,2.7,0.0,0.4, SURF_IDS='FIRE','INERT','INERT'/
&OBST ID='Obstruction', XB=4.8,5.0,0.0,2.0,0.0,2.4, SURF_ID='EI 60 WALL'/
&OBST ID='Obstruction', XB=1.2,4.8,1.4,1.6,0.0,2.4, SURF_ID='EI 60 WALL'/
&OBST ID='Supply', XB=4.6,4.8,0.2,1.2,0.8,1.8,
SURF_ID6='SUPPLY','INERT','INERT','INERT','INERT','INERT'/
&OBST ID='Obstruction', XB=4.8,5.0,2.8,4.8,0.0,2.4, SURF_ID='EI 60 WALL'/
&OBST ID='Obstruction', XB=4.8,5.0,2.0,2.8,2.0,2.4, SURF_ID='EI 60 WALL'/
&OBST ID='Obstruction', XB=9.8,10.0,0.0,1.8,0.0,2.4, SURF_ID='EI 60 WALL'/
&OBST ID='Obstruction', XB=9.8,10.0,1.8,3.0,2.0,2.4, SURF_ID='EI 60 WALL'/
&OBST ID='Obstruction', XB=9.8,10.0,3.0,4.8,0.0,2.4, SURF_ID='EI 60 WALL'/
&OBST ID='Supply', XB=4.6,4.8,3.6,4.6,0.8,1.8,
SURF_ID6='SUPPLY','INERT','INERT','INERT','INERT','INERT'/
&OBST ID='Obstruction', XB=1.2,4.8,3.2,3.4,0.0,2.4, SURF_ID='EI 60 WALL'/

&VENT ID='Mesh Vent [XMAX]', SURF_ID='OPEN', XB=11.0,11.0,0.0,4.8,0.0,2.4/
&VENT ID='Mesh Vent [YMAX]', SURF_ID='OPEN', XB=10.0,11.0,4.8,4.8,0.0,2.4/
&VENT ID='Mesh Vent [YMIN]', SURF_ID='OPEN', XB=10.0,11.0,0.0,0.0,0.0,2.4/
&VENT ID='Mesh Vent [ZMAX]', SURF_ID='OPEN', XB=10.0,11.0,0.0,4.8,2.4,2.4/
&VENT ID='Mesh Vent [ZMIN]', SURF_ID='OPEN', XB=10.0,11.0,0.0,4.8,0.0,0.0/
&VENT ID='Mesh Vent [XMIN]', SURF_ID='EI 60 WALL', XB=0.0,0.0,0.0,4.8,0.0,2.4/
&VENT ID='Mesh Vent [YMAX]', SURF_ID='EI 60 WALL', XB=0.0,10.0,4.8,4.8,0.0,2.4/
```

```
&VENT ID='Mesh Vent [YMIN]', SURF_ID='EI 60 WALL', XB=0.0,10.0,0.0,0.0,0.0,2.4/

&VENT ID='Mesh Vent [ZMAX]', SURF_ID='EI 60 CEILING', XB=0.0,10.0,0.0,4.8,2.4,2.4/

&VENT ID='Mesh Vent [ZMIN]', SURF_ID='EI 60 FLOOR', XB=0.0,10.0,0.0,4.8,0.0,0.0/


&SLCF QUANTITY='VELOCITY', VECTOR=.TRUE., PBY=2.4/


&DEVC ID='[Species: PRODUCTS] Density01_MEAN', QUANTITY='DENSITY',
SPEC_ID='PRODUCTS', SPATIAL_STATISTIC='MEAN', XB=0.0,4.8,0.0,4.8,0.0,2.4/

&DEVC ID='[Species: PRODUCTS] Volume Fraction01_MEAN', QUANTITY='VOLUME FRACTION',
SPEC_ID='PRODUCTS', SPATIAL_STATISTIC='MEAN', XB=0.0,4.8,0.0,4.8,0.0,2.4/

&DEVC ID='[Species: CARBON MONOXIDE] Volume Fraction01_MEAN', QUANTITY='VOLUME
FRACTION', SPEC_ID='CARBON MONOXIDE', SPATIAL_STATISTIC='MEAN',
XB=0.0,4.8,0.0,4.8,0.0,2.4/

&DEVC ID='[Species: OXYGEN] Volume Fraction01_MEAN', QUANTITY='VOLUME FRACTION',
SPEC_ID='OXYGEN', SPATIAL_STATISTIC='MEAN', XB=0.0,4.8,0.0,4.8,0.0,2.4/

&DEVC ID='[Species: CARBON DIOXIDE] Volume Fraction01_MEAN', QUANTITY='VOLUME
FRACTION', SPEC_ID='CARBON DIOXIDE', SPATIAL_STATISTIC='MEAN',
XB=0.0,4.8,0.0,4.8,0.0,2.4/


&DEVC ID='[Species: PRODUCTS] Density02_MEAN', QUANTITY='DENSITY',
SPEC_ID='PRODUCTS', SPATIAL_STATISTIC='MEAN', XB=5.0,9.8,0.0,4.8,0.0,2.4/

&DEVC ID='[Species: PRODUCTS] Volume Fraction02_MEAN', QUANTITY='VOLUME FRACTION',
SPEC_ID='PRODUCTS', SPATIAL_STATISTIC='MEAN', XB=5.0,9.8,0.0,4.8,0.0,2.4/

&DEVC ID='[Species: CARBON MONOXIDE] Volume Fraction02_MEAN', QUANTITY='VOLUME
FRACTION', SPEC_ID='CARBON MONOXIDE', SPATIAL_STATISTIC='MEAN',
XB=5.0,9.8,0.0,4.8,0.0,2.4/

&DEVC ID='[Species: OXYGEN] Volume Fraction02_MEAN', QUANTITY='VOLUME FRACTION',
SPEC_ID='OXYGEN', SPATIAL_STATISTIC='MEAN', XB=5.0,9.8,0.0,4.8,0.0,2.4/

&DEVC ID='[Species: CARBON DIOXIDE] Volume Fraction02_MEAN', QUANTITY='VOLUME
FRACTION', SPEC_ID='CARBON DIOXIDE', SPATIAL_STATISTIC='MEAN',
XB=5.0,9.8,0.0,4.8,0.0,2.4/


&TAIL /
```

B.1.2. Model A2

```
&HEAD CHID='A2_2500_1-12'/
&TIME T_END=600.0/
&DUMP COLUMN_DUMP_LIMIT=.TRUE., DT_RESTART=300.0, DT_SL3D=0.25/

&MESH ID='MESH 1', IJK=48,48,24, XB=0.0,4.8,0.0,4.8,0.0,2.4/
&MESH ID='MESH 2', IJK=74,96,24, XB=4.8,12.2,-2.4,7.2,0.0,2.4/

&REAC ID='HoC 20 MJ/kg',
      FUEL='REAC_FUEL',
      C=4.56,
      H=6.56,
      O=2.34,
      N=0.4,
      CO_YIELD=0.1,
      SOOT_YIELD=0.1,
      HEAT_OF_COMBUSTION=2.0E4/

&MATL ID='YELLOW PINE',
      SPECIFIC_HEAT=2.85,
      CONDUCTIVITY=0.14,
      DENSITY=640.0/
&MATL ID='MINERAL WOOL, PLATES',
      SPECIFIC_HEAT=0.8,
      CONDUCTIVITY=0.041,
      DENSITY=100.0/
&MATL ID='GYPSUM PLASTER',
      SPECIFIC_HEAT=0.84,
      CONDUCTIVITY=0.48,
      DENSITY=1440.0/

&SURF ID='EI 60 FLOOR',
      BACKING='VOID',
      MATL_ID(1,1)='YELLOW PINE',
```

```
      MATL_ID(2,1)='MINERAL WOOL, PLATES',
      MATL_ID(3,1)='GYPSUM PLASTER',
      MATL_ID(4,1)='GYPSUM PLASTER',
      MATL_MASS_FRACTION(1,1)=1.0,
      MATL_MASS_FRACTION(2,1)=1.0,
      MATL_MASS_FRACTION(3,1)=1.0,
      MATL_MASS_FRACTION(4,1)=1.0,
      THICKNESS(1:4)=5.0E-3,0.17,0.0125,0.0125/
&SURF ID='EI 60 WALL',
      RGB=146,202,166,
      BACKING='VOID',
      MATL_ID(1,1)='GYPSUM PLASTER',
      MATL_ID(2,1)='GYPSUM PLASTER',
      MATL_ID(3,1)='MINERAL WOOL, PLATES',
      MATL_ID(4,1)='GYPSUM PLASTER',
      MATL_ID(5,1)='GYPSUM PLASTER',
      MATL_MASS_FRACTION(1,1)=1.0,
      MATL_MASS_FRACTION(2,1)=1.0,
      MATL_MASS_FRACTION(3,1)=1.0,
      MATL_MASS_FRACTION(4,1)=1.0,
      MATL_MASS_FRACTION(5,1)=1.0,
      THICKNESS(1:5)=0.013,0.013,0.12,0.013,0.013/
&SURF ID='EI 60 CEILING',
      BACKING='VOID',
      MATL_ID(1,1)='GYPSUM PLASTER',
      MATL_ID(2,1)='GYPSUM PLASTER',
      MATL_ID(3,1)='MINERAL WOOL, PLATES',
      MATL_ID(4,1)='YELLOW PINE',
      MATL_MASS_FRACTION(1,1)=1.0,
      MATL_MASS_FRACTION(2,1)=1.0,
      MATL_MASS_FRACTION(3,1)=1.0,
      MATL_MASS_FRACTION(4,1)=1.0,
      THICKNESS(1:4)=0.0125,0.0125,0.17,5.0E-3/
&SURF ID='FIRE',
      COLOR='RED',
```

```
      HRRPUA=976.57,
      TMP_FRONT=300.0/
&SURF ID='SUPPLY',
      RGB=26,204,26,
      VOLUME_FLOW=-0.56/

&OBST ID='Fire', XB=8.2,9.8,1.6,3.2,0.0,0.4, SURF_IDS='FIRE','INERT','INERT'/
&OBST ID='Obstruction', XB=4.8,5.0,-1.2,2.0,0.0,2.4, SURF_ID='EI 60 WALL'/
&OBST ID='Obstruction', XB=1.2,4.8,1.4,1.6,0.0,2.4, SURF_ID='EI 60 WALL'/
&OBST ID='Supply', XB=4.6,4.8,0.2,1.2,0.8,1.8,
SURF_ID6='SUPPLY','INERT','INERT','INERT','INERT','INERT'/
&OBST ID='Obstruction', XB=4.8,5.0,2.8,6.0,0.0,2.4, SURF_ID='EI 60 WALL'/
&OBST ID='Obstruction', XB=4.8,5.0,2.0,2.8,2.0,2.4, SURF_ID='EI 60 WALL'/
&OBST ID='Supply', XB=4.6,4.8,3.6,4.6,0.8,1.8,
SURF_ID6='SUPPLY','INERT','INERT','INERT','INERT','INERT'/
&OBST ID='Obstruction', XB=1.2,4.8,3.2,3.4,0.0,2.4, SURF_ID='EI 60 WALL'/
&OBST ID='Obstruction', XB=4.8,5.8,6.0,6.2,0.0,2.4, SURF_ID='EI 60 WALL'/
&OBST ID='Obstruction', XB=5.8,7.0,6.0,6.2,2.0,2.4, SURF_ID='EI 60 WALL'/
&OBST ID='Obstruction', XB=10.2,11.4,6.0,6.2,2.0,2.4, SURF_ID='EI 60 WALL'/
&OBST ID='Obstruction', XB=11.4,12.2,6.0,6.2,0.0,2.4, SURF_ID='EI 60 WALL'/
&OBST ID='Obstruction', XB=7.0,10.2,6.0,6.2,0.0,2.4, SURF_ID='EI 60 WALL'/
&OBST ID='Obstruction', XB=4.8,5.8,-1.4,-1.2,0.0,2.4, SURF_ID='EI 60 WALL'/
&OBST ID='Obstruction', XB=5.8,7.0,-1.4,-1.2,2.0,2.4, SURF_ID='EI 60 WALL'/
&OBST ID='Obstruction', XB=7.0,10.2,-1.4,-1.2,0.0,2.4, SURF_ID='EI 60 WALL'/
&OBST ID='Obstruction', XB=10.2,11.4,-1.4,-1.2,2.0,2.4, SURF_ID='EI 60 WALL'/
&OBST ID='Obstruction', XB=11.4,12.2,-1.4,-1.2,0.0,2.4, SURF_ID='EI 60 WALL'/

&VENT ID='Mesh Vent [ZMIN]', SURF_ID='EI 60 FLOOR', XB=0.0,4.8,0.0,4.8,0.0,0.0/
&VENT ID='Mesh Vent [XMIN]', SURF_ID='EI 60 WALL', XB=0.0,0.0,0.0,4.8,0.0,2.4/
&VENT ID='Mesh Vent [YMAX]', SURF_ID='EI 60 WALL', XB=0.0,4.8,4.8,4.8,0.0,2.4/
&VENT ID='Mesh Vent [YMIN]', SURF_ID='EI 60 WALL', XB=0.0,4.8,0.0,0.0,0.0,2.4/
&VENT ID='Mesh Vent [ZMAX]', SURF_ID='EI 60 CEILING', XB=0.0,4.8,0.0,4.8,2.4,2.4/
&VENT ID='Mesh Vent [ZMAX]', SURF_ID='EI 60 CEILING', XB=4.8,12.2,-1.4,6.2,2.4,2.4/
&VENT ID='Mesh Vent [ZMIN]', SURF_ID='EI 60 FLOOR', XB=4.8,12.2,-1.4,6.2,0.0,0.0/
&VENT ID='Mesh Vent [XMIN]', SURF_ID='OPEN', XB=4.8,4.8,-1.4,0.0,0.0,2.4/
```

```
&VENT ID='Mesh Vent [XMIN]', SURF_ID='OPEN', XB=4.8,4.8,4.8,6.2,0.0,2.4/
&VENT ID='Mesh Vent [XMIN]', SURF_ID='EI 60 WALL', XB=12.2,12.2,-1.4,6.2,0.0,2.4/
&VENT ID='Mesh Vent [ZMIN]', SURF_ID='OPEN', XB=4.8,12.2,6.2,7.2,0.0,0.0/
&VENT ID='Mesh Vent [ZMAX]', SURF_ID='OPEN', XB=4.8,12.2,6.2,7.2,2.4,2.4/
&VENT ID='Mesh Vent [XMIN]', SURF_ID='OPEN', XB=4.8,4.8,6.2,7.2,0.0,2.4/
&VENT ID='Mesh Vent [XMIN]', SURF_ID='OPEN', XB=12.2,12.2,6.2,7.2,0.0,2.4/
&VENT ID='Mesh Vent [YMIN]', SURF_ID='OPEN', XB=4.8,12.2,7.2,7.2,0.0,2.4/
&VENT ID='Mesh Vent [ZMIN]', SURF_ID='OPEN', XB=4.8,12.2,-2.4,-1.4,0.0,0.0/
&VENT ID='Mesh Vent [ZMAX]', SURF_ID='OPEN', XB=4.8,12.2,-2.4,-1.4,2.4,2.4/
&VENT ID='Mesh Vent [XMIN]', SURF_ID='OPEN', XB=4.8,4.8,-2.4,-1.4,0.0,2.4/
&VENT ID='Mesh Vent [XMIN]', SURF_ID='OPEN', XB=12.2,12.2,-2.4,-1.4,0.0,2.4/
&VENT ID='Mesh Vent [YMIN]', SURF_ID='OPEN', XB=4.8,12.2,-2.4,-2.4,0.0,2.4/


&DEVC ID='[Species: PRODUCTS] Density01_MEAN', QUANTITY='DENSITY',
SPEC_ID='PRODUCTS', SPATIAL_STATISTIC='MEAN', XB=0.0,4.8,0.0,4.8,0.0,2.4/
&DEVC ID='[Species: PRODUCTS] Density02_MEAN', QUANTITY='DENSITY',
SPEC_ID='PRODUCTS', SPATIAL_STATISTIC='MEAN', XB=5.0,12.2,-1.2,6.0,0.0,2.4/


&TAIL /
```

B.1.3. Model B1

```
&HEAD CHID='B1_500_1-12'/
&TIME T_END=600.0/
&DUMP COLUMN_DUMP_LIMIT=.TRUE., DT_RESTART=300.0, DT_SL3D=0.25/

&MESH ID='MESH 1', IJK=50,48,24, XB=0.0,5.0,0.0,4.8,0.0,2.4/
&MESH ID='MESH 2', IJK=30,20,24, XB=5.0,8.0,1.4,3.4,0.0,2.4/
&MESH ID='MESH 3', IJK=62,48,24, XB=8.0,14.2,0.0,4.8,0.0,2.4/

&REAC ID='HoC 20 MJ/kg',
      FUEL='REAC_FUEL',
      C=4.56,
      H=6.56,
      O=2.34,
      N=0.4,
      CO_YIELD=0.1,
      SOOT_YIELD=0.1,
      HEAT_OF_COMBUSTION=2.0E4/

&MATL ID='GYPSUM PLASTER',
      SPECIFIC_HEAT=0.84,
      CONDUCTIVITY=0.48,
      DENSITY=1440.0/
&MATL ID='MINERAL WOOL, PLATES',
      SPECIFIC_HEAT=0.8,
      CONDUCTIVITY=0.041,
      DENSITY=100.0/
&MATL ID='YELLOW PINE',
      SPECIFIC_HEAT=2.85,
      CONDUCTIVITY=0.14,
      DENSITY=640.0/

&SURF ID='EI 60 WALL',
      RGB=146,202,166,
```

```
      BACKING='VOID',
      MATL_ID(1,1)='GYPSUM PLASTER',
      MATL_ID(2,1)='GYPSUM PLASTER',
      MATL_ID(3,1)='MINERAL WOOL, PLATES',
      MATL_ID(4,1)='GYPSUM PLASTER',
      MATL_ID(5,1)='GYPSUM PLASTER',
      MATL_MASS_FRACTION(1,1)=1.0,
      MATL_MASS_FRACTION(2,1)=1.0,
      MATL_MASS_FRACTION(3,1)=1.0,
      MATL_MASS_FRACTION(4,1)=1.0,
      MATL_MASS_FRACTION(5,1)=1.0,
      THICKNESS(1:5)=0.013,0.013,0.12,0.013,0.013/
&SURF ID='EI 60 CEILING',
      BACKING='VOID',
      MATL_ID(1,1)='GYPSUM PLASTER',
      MATL_ID(2,1)='GYPSUM PLASTER',
      MATL_ID(3,1)='MINERAL WOOL, PLATES',
      MATL_ID(4,1)='YELLOW PINE',
      MATL_MASS_FRACTION(1,1)=1.0,
      MATL_MASS_FRACTION(2,1)=1.0,
      MATL_MASS_FRACTION(3,1)=1.0,
      MATL_MASS_FRACTION(4,1)=1.0,
      THICKNESS(1:4)=0.0125,0.0125,0.17,5.0E-3/
&SURF ID='EI 60 FLOOR',
      BACKING='VOID',
      MATL_ID(1,1)='YELLOW PINE',
      MATL_ID(2,1)='MINERAL WOOL, PLATES',
      MATL_ID(3,1)='GYPSUM PLASTER',
      MATL_ID(4,1)='GYPSUM PLASTER',
      MATL_MASS_FRACTION(1,1)=1.0,
      MATL_MASS_FRACTION(2,1)=1.0,
      MATL_MASS_FRACTION(3,1)=1.0,
      MATL_MASS_FRACTION(4,1)=1.0,
      THICKNESS(1:4)=5.0E-3,0.17,0.0125,0.0125/
&SURF ID='FIRE',
```

```
      COLOR='RED',
      HRRPUA=1020.41,
      TMP_FRONT=300.0/
&SURF ID='SUPPLY',
      RGB=26,204,26,
      VOLUME_FLOW=-0.56/

&OBST ID='Fire', XB=10.2,10.9,2.0,2.7,0.0,0.4, SURF_IDS='FIRE','INERT','INERT'/
&OBST ID='Obstruction', XB=8.0,8.2,0.0,2.0,0.0,2.4, SURF_ID='EI 60 WALL'/
&OBST ID='Obstruction', XB=1.2,4.8,1.4,1.6,0.0,2.4, SURF_ID='EI 60 WALL'/
&OBST ID='Supply', XB=4.6,4.8,0.2,1.2,0.8,1.8,
SURF_ID6='SUPPLY','INERT','INERT','INERT','INERT','INERT'/
&OBST ID='Obstruction', XB=8.0,8.2,2.8,4.8,0.0,2.4, SURF_ID='EI 60 WALL'/
&OBST ID='Obstruction', XB=8.0,8.2,2.0,2.8,2.0,2.4, SURF_ID='EI 60 WALL'/
&OBST ID='Obstruction', XB=13.0,13.2,0.0,1.8,0.0,2.4, SURF_ID='EI 60 WALL'/
&OBST ID='Obstruction', XB=13.0,13.2,1.8,3.0,2.0,2.4, SURF_ID='EI 60 WALL'/
&OBST ID='Obstruction', XB=13.0,13.2,3.0,4.8,0.0,2.4, SURF_ID='EI 60 WALL'/
&OBST ID='Supply', XB=4.6,4.8,3.6,4.6,0.8,1.8,
SURF_ID6='SUPPLY','INERT','INERT','INERT','INERT','INERT'/
&OBST ID='Obstruction', XB=1.2,4.8,3.2,3.4,0.0,2.4, SURF_ID='EI 60 WALL'/
&OBST ID='Obstruction', XB=4.8,5.0,2.8,4.8,0.0,2.4, SURF_ID='EI 60 WALL'/
&OBST ID='Obstruction', XB=4.8,5.0,2.0,2.8,2.0,2.4, SURF_ID='EI 60 WALL'/
&OBST ID='Obstruction', XB=4.8,5.0,0.0,2.0,0.0,2.4, SURF_ID='EI 60 WALL'/

&VENT ID='Mesh Vent [XMIN]', SURF_ID='OPEN', XB=14.2,14.2,0.0,4.8,0.0,2.4/
&VENT ID='Mesh Vent [YMAX]', SURF_ID='OPEN', XB=13.2,14.2,4.8,4.8,0.0,2.4/
&VENT ID='Mesh Vent [YMIN]', SURF_ID='OPEN', XB=13.2,14.2,0.0,0.0,0.0,2.4/
&VENT ID='Mesh Vent [ZMAX]', SURF_ID='OPEN', XB=13.2,14.2,0.0,4.8,2.4,2.4/
&VENT ID='Mesh Vent [ZMIN]', SURF_ID='OPEN', XB=13.2,14.2,0.0,4.8,0.0,0.0/
&VENT ID='Mesh Vent [XMIN]', SURF_ID='EI 60 WALL', XB=0.0,0.0,0.0,4.8,0.0,2.4/
&VENT ID='Mesh Vent [YMAX]', SURF_ID='EI 60 WALL', XB=0.0,4.8,4.8,4.8,0.0,2.4/
&VENT ID='Mesh Vent [YMIN]', SURF_ID='EI 60 WALL', XB=0.0,4.8,0.0,0.0,0.0,2.4/
&VENT ID='Mesh Vent [ZMAX]', SURF_ID='EI 60 CEILING', XB=0.0,4.8,0.0,4.8,2.4,2.4/
&VENT ID='Mesh Vent [ZMIN]', SURF_ID='EI 60 FLOOR', XB=0.0,4.8,0.0,4.8,0.0,0.0/
&VENT ID='Mesh Vent [YMAX]', SURF_ID='EI 60 WALL', XB=8.0,13.2,4.8,4.8,0.0,2.4/
```

```
&VENT ID='Mesh Vent [YMIN]', SURF_ID='EI 60 WALL', XB=8.0,13.2,0.0,0.0,0.0,2.4/
&VENT ID='Mesh Vent [ZMAX]', SURF_ID='EI 60 CEILING', XB=8.0,13.2,0.0,4.8,2.4,2.4/
&VENT ID='Mesh Vent [ZMIN]', SURF_ID='EI 60 FLOOR', XB=8.0,13.2,0.0,4.8,0.0,0.0/
&VENT ID='Mesh Vent [YMAX]', SURF_ID='EI 60 WALL', XB=5.0,8.0,3.4,3.4,0.0,2.4/
&VENT ID='Mesh Vent [YMIN]', SURF_ID='EI 60 WALL', XB=5.0,8.0,1.4,1.4,0.0,2.4/
&VENT ID='Mesh Vent [ZMAX]', SURF_ID='EI 60 CEILING', XB=5.0,8.0,1.4,3.4,2.4,2.4/
&VENT ID='Mesh Vent [ZMIN]', SURF_ID='EI 60 FLOOR', XB=5.0,8.0,1.4,3.4,0.0,0.0/
&VENT ID='Mesh Vent [XMAX]', SURF_ID='OPEN', XB=5.0,5.0,0.0,1.4,0.0,2.4/
&VENT ID='Mesh Vent [XMAX]', SURF_ID='OPEN', XB=5.0,5.0,3.4,4.8,0.0,2.4/
&VENT ID='Mesh Vent [XMAX]', SURF_ID='OPEN', XB=8.0,8.0,0.0,1.4,0.0,2.4/
&VENT ID='Mesh Vent [XMAX]', SURF_ID='OPEN', XB=8.0,8.0,3.4,4.8,0.0,2.4/


&DEVC ID='[Species: PRODUCTS] Density01_MEAN', QUANTITY='DENSITY',
SPEC_ID='PRODUCTS', SPATIAL_STATISTIC='MEAN', XB=0.0,4.8,0.0,4.8,0.0,2.4/
&DEVC ID='[Species: PRODUCTS] Density02_MEAN', QUANTITY='DENSITY',
SPEC_ID='PRODUCTS', SPATIAL_STATISTIC='MEAN', XB=5.0,8.0,1.4,3.4,0.0,2.4/
&DEVC ID='[Species: PRODUCTS] Density03_MEAN', QUANTITY='DENSITY',
SPEC_ID='PRODUCTS', SPATIAL_STATISTIC='MEAN', XB=8.2,13.0,0.0,4.8,0.0,2.4/


&TAIL /
```

B.1.4. Model B2

```
&HEAD CHID='B2_2500_1-12'/
&TIME T_END=600.0/
&DUMP COLUMN_DUMP_LIMIT=.TRUE., DT_RESTART=300.0, DT_SL3D=0.25/

&MESH ID='MESH 1', IJK=50,48,24, XB=0.0,5.0,0.0,4.8,0.0,2.4/
&MESH ID='MESH 2', IJK=30,20,24, XB=5.0,8.0,1.4,3.4,0.0,2.4/
&MESH ID='MESH 3', IJK=74,96,24, XB=8.0,15.4,-2.4,7.2,0.0,2.4/

&REAC ID='HoC 20 MJ/kg',
      FUEL='REAC_FUEL',
      C=4.56,
      H=6.56,
      O=2.34,
      N=0.4,
      CO_YIELD=0.1,
      SOOT_YIELD=0.1,
      HEAT_OF_COMBUSTION=2.0E4/

&MATL ID='YELLOW PINE',
      SPECIFIC_HEAT=2.85,
      CONDUCTIVITY=0.14,
      DENSITY=640.0/
&MATL ID='MINERAL WOOL, PLATES',
      SPECIFIC_HEAT=0.8,
      CONDUCTIVITY=0.041,
      DENSITY=100.0/
&MATL ID='GYPSUM PLASTER',
      SPECIFIC_HEAT=0.84,
      CONDUCTIVITY=0.48,
      DENSITY=1440.0/

&SURF ID='EI 60 FLOOR',
      BACKING='VOID',
```

```
      MATL_ID(1,1)='YELLOW PINE',
      MATL_ID(2,1)='MINERAL WOOL, PLATES',
      MATL_ID(3,1)='GYPSUM PLASTER',
      MATL_ID(4,1)='GYPSUM PLASTER',
      MATL_MASS_FRACTION(1,1)=1.0,
      MATL_MASS_FRACTION(2,1)=1.0,
      MATL_MASS_FRACTION(3,1)=1.0,
      MATL_MASS_FRACTION(4,1)=1.0,
      THICKNESS(1:4)=5.0E-3,0.17,0.0125,0.0125/
&SURF ID='EI 60 WALL',
      RGB=146,202,166,
      BACKING='VOID',
      MATL_ID(1,1)='GYPSUM PLASTER',
      MATL_ID(2,1)='GYPSUM PLASTER',
      MATL_ID(3,1)='MINERAL WOOL, PLATES',
      MATL_ID(4,1)='GYPSUM PLASTER',
      MATL_ID(5,1)='GYPSUM PLASTER',
      MATL_MASS_FRACTION(1,1)=1.0,
      MATL_MASS_FRACTION(2,1)=1.0,
      MATL_MASS_FRACTION(3,1)=1.0,
      MATL_MASS_FRACTION(4,1)=1.0,
      MATL_MASS_FRACTION(5,1)=1.0,
      THICKNESS(1:5)=0.013,0.013,0.12,0.013,0.013/
&SURF ID='EI 60 CEILING',
      BACKING='VOID',
      MATL_ID(1,1)='GYPSUM PLASTER',
      MATL_ID(2,1)='GYPSUM PLASTER',
      MATL_ID(3,1)='MINERAL WOOL, PLATES',
      MATL_ID(4,1)='YELLOW PINE',
      MATL_MASS_FRACTION(1,1)=1.0,
      MATL_MASS_FRACTION(2,1)=1.0,
      MATL_MASS_FRACTION(3,1)=1.0,
      MATL_MASS_FRACTION(4,1)=1.0,
      THICKNESS(1:4)=0.0125,0.0125,0.17,5.0E-3/
&SURF ID='FIRE',
```

```
      COLOR='RED',
      HRRPUA=976.57,
      TMP_FRONT=300.0/
&SURF ID='SUPPLY',
      RGB=26,204,26,
      VOLUME_FLOW=-0.56/

&OBST ID='Fire', XB=11.4,13.0,1.6,3.2,0.0,0.4, SURF_IDS='FIRE','INERT','INERT'/
&OBST ID='Obstruction', XB=8.0,8.2,-1.2,2.0,0.0,2.4, SURF_ID='EI 60 WALL'/
&OBST ID='Obstruction', XB=1.2,4.8,1.4,1.6,0.0,2.4, SURF_ID='EI 60 WALL'/
&OBST ID='Supply', XB=4.6,4.8,0.2,1.2,0.8,1.8,
SURF_ID6='SUPPLY','INERT','INERT','INERT','INERT','INERT'/
&OBST ID='Obstruction', XB=8.0,8.2,2.8,6.0,0.0,2.4, SURF_ID='EI 60 WALL'/
&OBST ID='Obstruction', XB=8.0,8.2,2.0,2.8,2.0,2.4, SURF_ID='EI 60 WALL'/
&OBST ID='Supply', XB=4.6,4.8,3.6,4.6,0.8,1.8,
SURF_ID6='SUPPLY','INERT','INERT','INERT','INERT','INERT'/
&OBST ID='Obstruction', XB=1.2,4.8,3.2,3.4,0.0,2.4, SURF_ID='EI 60 WALL'/
&OBST ID='Obstruction', XB=8.0,9.0,6.0,6.2,0.0,2.4, SURF_ID='EI 60 WALL'/
&OBST ID='Obstruction', XB=9.0,10.2,6.0,6.2,2.0,2.4, SURF_ID='EI 60 WALL'/
&OBST ID='Obstruction', XB=13.4,14.6,6.0,6.2,2.0,2.4, SURF_ID='EI 60 WALL'/
&OBST ID='Obstruction', XB=14.6,15.4,6.0,6.2,0.0,2.4, SURF_ID='EI 60 WALL'/
&OBST ID='Obstruction', XB=10.2,13.4,6.0,6.2,0.0,2.4, SURF_ID='EI 60 WALL'/
&OBST ID='Obstruction', XB=8.0,9.0,-1.4,-1.2,0.0,2.4, SURF_ID='EI 60 WALL'/
&OBST ID='Obstruction', XB=9.0,10.2,-1.4,-1.2,2.0,2.4, SURF_ID='EI 60 WALL'/
&OBST ID='Obstruction', XB=10.2,13.4,-1.4,-1.2,0.0,2.4, SURF_ID='EI 60 WALL'/
&OBST ID='Obstruction', XB=13.4,14.6,-1.4,-1.2,2.0,2.4, SURF_ID='EI 60 WALL'/
&OBST ID='Obstruction', XB=14.6,15.4,-1.4,-1.2,0.0,2.4, SURF_ID='EI 60 WALL'/
&OBST ID='Obstruction', XB=4.8,5.0,0.0,2.0,0.0,2.4, SURF_ID='EI 60 WALL'/
&OBST ID='Obstruction', XB=4.8,5.0,2.0,2.8,2.0,2.4, SURF_ID='EI 60 WALL'/
&OBST ID='Obstruction', XB=4.8,5.0,2.8,4.8,0.0,2.4, SURF_ID='EI 60 WALL'/

&VENT ID='Mesh Vent [ZMIN]', SURF_ID='EI 60 FLOOR', XB=0.0,5.0,0.0,4.8,0.0,0.0/
&VENT ID='Mesh Vent [XMIN]', SURF_ID='EI 60 WALL', XB=0.0,0.0,0.0,4.8,0.0,2.4/
&VENT ID='Mesh Vent [YMAX]', SURF_ID='EI 60 WALL', XB=0.0,5.0,4.8,4.8,0.0,2.4/
&VENT ID='Mesh Vent [YMIN]', SURF_ID='EI 60 WALL', XB=0.0,5.0,0.0,0.0,0.0,2.4/
```

```
&VENT ID='Mesh Vent [ZMAX]', SURF_ID='EI 60 CEILING', XB=0.0,5.0,0.0,4.8,2.4,2.4/
&VENT ID='Mesh Vent [XMIN]', SURF_ID='OPEN', XB=5.0,5.0,0.0,1.4,0.0,2.4/
&VENT ID='Mesh Vent [XMIN]', SURF_ID='OPEN', XB=5.0,5.0,3.4,4.8,0.0,2.4/
&VENT ID='Mesh Vent [ZMAX]', SURF_ID='EI 60 CEILING', XB=8.0,15.4,-1.4,6.2,2.4,2.4/
&VENT ID='Mesh Vent [ZMIN]', SURF_ID='EI 60 FLOOR', XB=8.0,15.4,-1.4,6.2,0.0,0.0/
&VENT ID='Mesh Vent [XMIN]', SURF_ID='OPEN', XB=8.0,8.0,-1.4,1.4,0.0,2.4/
&VENT ID='Mesh Vent [XMIN]', SURF_ID='OPEN', XB=8.0,8.0,3.4,6.2,0.0,2.4/
&VENT ID='Mesh Vent [XMIN]', SURF_ID='EI 60 WALL', XB=15.4,15.4,-1.4,6.2,0.0,2.4/
&VENT ID='Mesh Vent [ZMIN]', SURF_ID='OPEN', XB=8.0,15.4,6.2,7.2,0.0,0.0/
&VENT ID='Mesh Vent [ZMAX]', SURF_ID='OPEN', XB=8.0,15.4,6.2,7.2,2.4,2.4/
&VENT ID='Mesh Vent [XMIN]', SURF_ID='OPEN', XB=8.0,8.0,6.2,7.2,0.0,2.4/
&VENT ID='Mesh Vent [XMIN]', SURF_ID='OPEN', XB=15.4,15.4,6.2,7.2,0.0,2.4/
&VENT ID='Mesh Vent [YMIN]', SURF_ID='OPEN', XB=8.0,15.4,7.2,7.2,0.0,2.4/
&VENT ID='Mesh Vent [ZMIN]', SURF_ID='OPEN', XB=8.0,15.4,-2.4,-1.4,0.0,0.0/
&VENT ID='Mesh Vent [ZMAX]', SURF_ID='OPEN', XB=8.0,15.4,-2.4,-1.4,2.4,2.4/
&VENT ID='Mesh Vent [XMIN]', SURF_ID='OPEN', XB=8.0,8.0,-2.4,-1.4,0.0,2.4/
&VENT ID='Mesh Vent [XMIN]', SURF_ID='OPEN', XB=15.4,15.4,-2.4,-1.4,0.0,2.4/
&VENT ID='Mesh Vent [YMIN]', SURF_ID='OPEN', XB=8.0,15.4,-2.4,-2.4,0.0,2.4/
&VENT ID='Mesh Vent [ZMAX]', SURF_ID='EI 60 CEILING', XB=5.0,8.0,1.4,3.4,2.4,2.4/
&VENT ID='Mesh Vent [YMIN]', SURF_ID='EI 60 WALL', XB=5.0,8.0,1.4,1.4,0.0,2.4/
&VENT ID='Mesh Vent [YMAX]', SURF_ID='EI 60 WALL', XB=5.0,8.0,3.4,3.4,0.0,2.4/
&VENT ID='Mesh Vent [ZMIN]', SURF_ID='EI 60 FLOOR', XB=5.0,8.0,1.4,3.4,0.0,0.0/


&DEVC ID='[Species: PRODUCTS] Density01_MEAN', QUANTITY='DENSITY',
SPEC_ID='PRODUCTS', SPATIAL_STATISTIC='MEAN', XB=0.0,4.8,0.0,4.8,0.0,2.4/
&DEVC ID='[Species: PRODUCTS] Density02_MEAN', QUANTITY='DENSITY',
SPEC_ID='PRODUCTS', SPATIAL_STATISTIC='MEAN', XB=5.0,8.0,1.4,3.4,0.0,2.4/
&DEVC ID='[Species: PRODUCTS] Density03_MEAN', QUANTITY='DENSITY',
SPEC_ID='PRODUCTS', SPATIAL_STATISTIC='MEAN', XB=8.2,15.4,-1.2,6.0,0.0,2.4/


&TAIL /
```

B.1.5. Model C

```
&HEAD CHID='C_2000_1-12'/

&TIME T_END=600.0/

&DUMP COLUMN_DUMP_LIMIT=.TRUE., DT_RESTART=300.0, DT_SL3D=0.25/


&MESH ID='MESH 1', IJK=48,48,24, XB=0.0,4.8,0.0,4.8,0.0,2.4/

&MESH ID='MESH 2', IJK=86,72,24, XB=4.8,13.4,-1.2,6.0,0.0,2.4/


&REAC ID='HoC 20 MJ/kg',
      FUEL='REAC_FUEL',
      C=4.56,
      H=6.56,
      O=2.34,
      N=0.4,
      CO_YIELD=0.1,
      SOOT_YIELD=0.1,
      HEAT_OF_COMBUSTION=2.0E4/


&MATL ID='YELLOW PINE',
      SPECIFIC_HEAT=2.85,
      CONDUCTIVITY=0.14,
      DENSITY=640.0/
&MATL ID='MINERAL WOOL, PLATES',
      SPECIFIC_HEAT=0.8,
      CONDUCTIVITY=0.041,
      DENSITY=100.0/
&MATL ID='GYPSUM PLASTER',
      SPECIFIC_HEAT=0.84,
```

```
      CONDUCTIVITY=0.48,
      DENSITY=1440.0/

&SURF ID='EI 60 FLOOR',
      BACKING='VOID',
      MATL_ID(1,1)='YELLOW PINE',
      MATL_ID(2,1)='MINERAL WOOL, PLATES',
      MATL_ID(3,1)='GYPSUM PLASTER',
      MATL_ID(4,1)='GYPSUM PLASTER',
      MATL_MASS_FRACTION(1,1)=1.0,
      MATL_MASS_FRACTION(2,1)=1.0,
      MATL_MASS_FRACTION(3,1)=1.0,
      MATL_MASS_FRACTION(4,1)=1.0,
      THICKNESS(1:4)=5.0E-3,0.17,0.0125,0.0125/
&SURF ID='EI 60 WALL',
      RGB=146,202,166,
      BACKING='VOID',
      MATL_ID(1,1)='GYPSUM PLASTER',
      MATL_ID(2,1)='GYPSUM PLASTER',
      MATL_ID(3,1)='MINERAL WOOL, PLATES',
      MATL_ID(4,1)='GYPSUM PLASTER',
      MATL_ID(5,1)='GYPSUM PLASTER',
      MATL_MASS_FRACTION(1,1)=1.0,
      MATL_MASS_FRACTION(2,1)=1.0,
      MATL_MASS_FRACTION(3,1)=1.0,
      MATL_MASS_FRACTION(4,1)=1.0,
      MATL_MASS_FRACTION(5,1)=1.0,
      THICKNESS(1:5)=0.013,0.013,0.12,0.013,0.013/
```

```
&SURF ID='EI 60 CEILING',
      BACKING='VOID',
      MATL_ID(1,1)='GYPSUM PLASTER',
      MATL_ID(2,1)='GYPSUM PLASTER',
      MATL_ID(3,1)='MINERAL WOOL, PLATES',
      MATL_ID(4,1)='YELLOW PINE',
      MATL_MASS_FRACTION(1,1)=1.0,
      MATL_MASS_FRACTION(2,1)=1.0,
      MATL_MASS_FRACTION(3,1)=1.0,
      MATL_MASS_FRACTION(4,1)=1.0,
      THICKNESS(1:4)=0.0125,0.0125,0.17,5.0E-3/
&SURF ID='FIRE',
      COLOR='RED',
      HRRPUA=1020.41,
      TMP_FRONT=300.0/
&SURF ID='SUPPLY',
      RGB=26,204,26,
      VOLUME_FLOW=-0.56/


&OBST ID='Fire', XB=7.9,9.3,1.7,3.1,0.0,0.4, SURF_IDS='FIRE','INERT','INERT'/
&OBST ID='Obstruction', XB=4.8,5.0,-1.2,2.0,0.0,2.4, SURF_ID='EI 60 WALL'/
&OBST ID='Obstruction', XB=1.2,4.8,1.4,1.6,0.0,2.4, SURF_ID='EI 60 WALL'/
&OBST ID='Supply', XB=4.6,4.8,0.2,1.2,0.8,1.8,
SURF_ID6='SUPPLY','INERT','INERT','INERT','INERT','INERT'/
&OBST ID='Obstruction', XB=4.8,5.0,2.8,6.0,0.0,2.4, SURF_ID='EI 60 WALL'/
&OBST ID='Obstruction', XB=4.8,5.0,2.0,2.8,2.0,2.4, SURF_ID='EI 60 WALL'/
&OBST ID='Supply', XB=4.6,4.8,3.6,4.6,0.8,1.8,
SURF_ID6='SUPPLY','INERT','INERT','INERT','INERT','INERT'/
&OBST ID='Obstruction', XB=1.2,4.8,3.2,3.4,0.0,2.4, SURF_ID='EI 60 WALL'/
```

```
&OBST ID='Obstruction', XB=12.2,12.4,3.0,6.0,0.0,2.4, SURF_ID='EI 60 WALL'/

&OBST ID='Obstruction', XB=12.2,12.4,1.8,3.0,2.0,2.4, SURF_ID='EI 60 WALL'/

&OBST ID='Obstruction', XB=12.2,12.4,-1.2,1.8,0.0,2.4, SURF_ID='EI 60 WALL'/


&VENT ID='Mesh Vent [ZMIN]', SURF_ID='EI 60 FLOOR', XB=0.0,4.8,0.0,4.8,0.0,0.0/

&VENT ID='Mesh Vent [XMIN]', SURF_ID='EI 60 WALL', XB=0.0,0.0,0.0,4.8,0.0,2.4/

&VENT ID='Mesh Vent [YMAX]', SURF_ID='EI 60 WALL', XB=0.0,4.8,4.8,4.8,0.0,2.4/

&VENT ID='Mesh Vent [YMIN]', SURF_ID='EI 60 WALL', XB=0.0,4.8,0.0,0.0,0.0,2.4/

&VENT ID='Mesh Vent [ZMAX]', SURF_ID='EI 60 CEILING', XB=0.0,4.8,0.0,4.8,2.4,2.4/

&VENT ID='Mesh Vent [ZMAX]', SURF_ID='EI 60 CEILING', XB=4.8,12.2,-1.2,6.0,2.4,2.4/

&VENT ID='Mesh Vent [ZMIN]', SURF_ID='EI 60 FLOOR', XB=4.8,12.4,-1.2,6.0,0.0,0.0/

&VENT ID='Mesh Vent [XMIN]', SURF_ID='OPEN', XB=4.8,4.8,-1.2,0.0,0.0,2.4/

&VENT ID='Mesh Vent [YMAX]', SURF_ID='EI 60 WALL', XB=4.8,12.4,6.0,6.0,0.0,2.4/

&VENT ID='Mesh Vent [YMAX]', SURF_ID='EI 60 WALL', XB=4.8,12.4,-1.2,-1.2,0.0,2.4/

&VENT ID='Mesh Vent [XMIN]', SURF_ID='OPEN', XB=4.8,4.8,4.8,6.0,0.0,2.4/

&VENT ID='Mesh Vent [XMIN]', SURF_ID='OPEN', XB=13.4,13.4,-1.2,6.0,0.0,2.4/

&VENT ID='Mesh Vent [YMIN]', SURF_ID='OPEN', XB=12.4,13.4,6.0,6.0,0.0,2.4/

&VENT ID='Mesh Vent [ZMIN]', SURF_ID='OPEN', XB=12.4,13.4,-1.2,6.0,0.0,0.0/

&VENT ID='Mesh Vent [ZMAX]', SURF_ID='OPEN', XB=12.4,13.4,-1.2,6.0,2.4,2.4/

&VENT ID='Mesh Vent [YMIN]', SURF_ID='OPEN', XB=12.4,13.4,-1.2,-1.2,0.0,2.4/


&DEVC ID='[Species: PRODUCTS] Density01_MEAN', QUANTITY='DENSITY',
SPEC_ID='PRODUCTS', SPATIAL_STATISTIC='MEAN', XB=0.0,4.8,0.0,4.8,0.0,2.4/

&DEVC ID='[Species: PRODUCTS] Density02_MEAN', QUANTITY='DENSITY',
SPEC_ID='PRODUCTS', SPATIAL_STATISTIC='MEAN', XB=5.0,12.2,-1.2,6.0,0.0,2.4/


&TAIL /
```

B.1.6. Model D

```
&HEAD CHID='D_2000_1-12'/
&TIME T_END=1200.0/
&DUMP COLUMN_DUMP_LIMIT=.TRUE., DT_RESTART=300.0, DT_SL3D=0.25/

&MESH ID='MESH 1', IJK=74,72,24, XB=-2.4,5.0,-1.2,6.0,0.0,2.4/
&MESH ID='MESH 2', IJK=60,48,24, XB=5.0,11.0,0.0,4.8,0.0,2.4/

&REAC ID='HoC 20 MJ/kg',
      FUEL='REAC_FUEL',
      C=4.56,
      H=6.56,
      O=2.34,
      N=0.4,
      CO_YIELD=0.1,
      SOOT_YIELD=0.1,
      HEAT_OF_COMBUSTION=2.0E4/

&MATL ID='GYPSUM PLASTER',
      SPECIFIC_HEAT=0.84,
      CONDUCTIVITY=0.48,
      DENSITY=1440.0/
&MATL ID='MINERAL WOOL, PLATES',
      SPECIFIC_HEAT=0.8,
      CONDUCTIVITY=0.041,
      DENSITY=100.0/
&MATL ID='YELLOW PINE',
      SPECIFIC_HEAT=2.85,
      CONDUCTIVITY=0.14,
      DENSITY=640.0/

&SURF ID='EI 60 WALL',
      RGB=146,202,166,
      BACKING='VOID',
```

```
      MATL_ID(1,1)='GYPSUM PLASTER',
      MATL_ID(2,1)='GYPSUM PLASTER',
      MATL_ID(3,1)='MINERAL WOOL, PLATES',
      MATL_ID(4,1)='GYPSUM PLASTER',
      MATL_ID(5,1)='GYPSUM PLASTER',
      MATL_MASS_FRACTION(1,1)=1.0,
      MATL_MASS_FRACTION(2,1)=1.0,
      MATL_MASS_FRACTION(3,1)=1.0,
      MATL_MASS_FRACTION(4,1)=1.0,
      MATL_MASS_FRACTION(5,1)=1.0,
      THICKNESS(1:5)=0.013,0.013,0.12,0.013,0.013/
&SURF ID='EI 60 CEILING',
      BACKING='VOID',
      MATL_ID(1,1)='GYPSUM PLASTER',
      MATL_ID(2,1)='GYPSUM PLASTER',
      MATL_ID(3,1)='MINERAL WOOL, PLATES',
      MATL_ID(4,1)='YELLOW PINE',
      MATL_MASS_FRACTION(1,1)=1.0,
      MATL_MASS_FRACTION(2,1)=1.0,
      MATL_MASS_FRACTION(3,1)=1.0,
      MATL_MASS_FRACTION(4,1)=1.0,
      THICKNESS(1:4)=0.0125,0.0125,0.17,5.0E-3/
&SURF ID='EI 60 FLOOR',
      BACKING='VOID',
      MATL_ID(1,1)='YELLOW PINE',
      MATL_ID(2,1)='MINERAL WOOL, PLATES',
      MATL_ID(3,1)='GYPSUM PLASTER',
      MATL_ID(4,1)='GYPSUM PLASTER',
      MATL_MASS_FRACTION(1,1)=1.0,
      MATL_MASS_FRACTION(2,1)=1.0,
      MATL_MASS_FRACTION(3,1)=1.0,
      MATL_MASS_FRACTION(4,1)=1.0,
      THICKNESS(1:4)=5.0E-3,0.17,0.0125,0.0125/
&SURF ID='FIRE',
      COLOR='RED',
```

```
      HRRPUA=1020.41,
      TMP_FRONT=300.0/
&SURF ID='SUPPLY',
      RGB=26,204,26,
      VOLUME_FLOW=-0.56/

&OBST ID='Fire', XB=6.7,8.1,1.7,3.1,0.0,0.4, SURF_IDS='FIRE','INERT','INERT'/
&OBST ID='Obstruction', XB=4.8,5.0,-1.2,2.0,0.0,2.4, SURF_ID='EI 60 WALL'/
&OBST ID='Obstruction', XB=-1.2,4.8,1.4,1.6,0.0,2.4, SURF_ID='EI 60 WALL'/
&OBST ID='Supply', XB=4.6,4.8,-0.4,0.6,0.8,1.8,
SURF_ID6='SUPPLY','INERT','INERT','INERT','INERT','INERT'/
&OBST ID='Obstruction', XB=4.8,5.0,2.8,6.0,0.0,2.4, SURF_ID='EI 60 WALL'/
&OBST ID='Obstruction', XB=4.8,5.0,2.0,2.8,2.0,2.4, SURF_ID='EI 60 WALL'/
&OBST ID='Obstruction', XB=9.8,10.0,0.0,1.8,0.0,2.4, SURF_ID='EI 60 WALL'/
&OBST ID='Obstruction', XB=9.8,10.0,1.8,3.0,2.0,2.4, SURF_ID='EI 60 WALL'/
&OBST ID='Obstruction', XB=9.8,10.0,3.0,4.8,0.0,2.4, SURF_ID='EI 60 WALL'/
&OBST ID='Supply', XB=4.6,4.8,4.2,5.2,0.8,1.8,
SURF_ID6='SUPPLY','INERT','INERT','INERT','INERT','INERT'/
&OBST ID='Obstruction', XB=-1.2,4.8,3.2,3.4,0.0,2.4, SURF_ID='EI 60 WALL'/

&VENT ID='Mesh Vent [XMAX]', SURF_ID='OPEN', XB=11.0,11.0,0.0,4.8,0.0,2.4/
&VENT ID='Mesh Vent [YMAX]', SURF_ID='OPEN', XB=10.0,11.0,4.8,4.8,0.0,2.4/
&VENT ID='Mesh Vent [ZMAX]', SURF_ID='OPEN', XB=10.0,11.0,0.0,4.8,2.4,2.4/
&VENT ID='Mesh Vent [ZMIN]', SURF_ID='OPEN', XB=10.0,11.0,0.0,4.8,0.0,0.0/
&VENT ID='Mesh Vent [YMIN]', SURF_ID='OPEN', XB=10.0,11.0,0.0,0.0,0.0,2.4/
&VENT ID='Mesh Vent [YMAX]', SURF_ID='EI 60 WALL', XB=5.0,10.0,4.8,4.8,0.0,2.4/
&VENT ID='Mesh Vent [YMIN]', SURF_ID='EI 60 WALL', XB=5.0,10.0,0.0,0.0,0.0,2.4/
&VENT ID='Mesh Vent [ZMAX]', SURF_ID='EI 60 CEILING', XB=5.0,10.0,0.0,4.8,2.4,2.4/
&VENT ID='Mesh Vent [ZMIN]', SURF_ID='EI 60 FLOOR', XB=5.0,10.0,0.0,4.8,0.0,0.0/
&VENT ID='Mesh Vent [XMIN]', SURF_ID='EI 60 WALL', XB=-2.4,-2.4,-1.2,6.0,0.0,2.4/
&VENT ID='Mesh Vent [ZMIN]', SURF_ID='EI 60 FLOOR', XB=-2.4,5.0,-1.2,6.0,0.0,0.0/
&VENT ID='Mesh Vent [ZMAX]', SURF_ID='EI 60 CEILING', XB=-2.4,5.0,-1.2,6.0,2.4,2.4/
&VENT ID='Mesh Vent [YMIN]', SURF_ID='EI 60 WALL', XB=-2.4,5.0,-1.2,-1.2,0.0,2.4/
&VENT ID='Mesh Vent [YMAX]', SURF_ID='EI 60 WALL', XB=-2.4,5.0,6.0,6.0,0.0,2.4/
&VENT ID='Mesh Vent [XMIN]', SURF_ID='OPEN', XB=5.0,5.0,4.8,6.0,0.0,2.4/
```

```
&VENT ID='Mesh Vent [XMIN]', SURF_ID='OPEN', XB=5.0,5.0,-1.2,0.0,0.0,2.4/


&DEVC ID='[Species: PRODUCTS] Density01_MEAN', QUANTITY='DENSITY',
SPEC_ID='PRODUCTS', SPATIAL_STATISTIC='MEAN', XB=-2.4,4.8,-1.2,6.0,0.0,2.4/

&DEVC ID='[Species: PRODUCTS] Density02_MEAN', QUANTITY='DENSITY',
SPEC_ID='PRODUCTS', SPATIAL_STATISTIC='MEAN', XB=5.0,9.8,0.0,4.8,0.0,2.4/


&TAIL /
```